

Outer Dowsing Offshore Wind

Environmental Statement

Appendix 7.1 Physical Processes Technical Baseline

Volume 3

Date: May 2024

Document Reference: 6.3.7.1

Pursuant to APFP Regulation: 5(2)(a)

Rev: 2.0

Company:	Outer Dowsing Offshore Wind	Asset:	Whole Asset			
Project:	Whole Wind Farm	Sub Project/Package:	Whole Asset			
Document Title or Description:	Physical Processes Technical Baseline					
Internal Document Number:	PP1-ODOW-DEV-CS-REP-0162-02	3 rd Party Doc No (If applicable):	N/A			
Outer Dowsing Offshore Wind accepts no liability for the accuracy or completeness of the information in this document nor for any loss or damage arising from the use of such information.						
Rev No.	Date	Status / Reason for Issue	Author	Checked by	Reviewed by	Approved by
V1.0	March 2024	Final	GoBe	GoBe	Shepherd and Wedderburn	ODOW
V2.0	May 2024	Updated Annexes	GoBe	GoBe	ODOW	ODOW

Table of Contents

Acronyms & Terminology	6
Abbreviations / Acronyms.....	6
Terminology	7
Reference Documentation.....	10
7 Marine Processes Technical Baseline	11
7.1 Introduction.....	11
7.2 Purpose.....	11
7.3 Scope and Methodology	12
7.3.1 Study Area.....	12
7.3.2 Data Sources	12
7.4 Baseline Environment	17
7.4.1 Metocean	17
7.4.2 Seabed.....	33
7.4.3 Morphology.....	60
7.5 Future Baseline Environment.....	77
7.6 Designated Sites and Protected Species	77
7.7 References.....	80
7.8 Annex A	85
7.9 Annex B - DETERMINATION OF MARINE PROCESSES REALISTIC WORST-CASE	94
7.10 Annex C - Assessment of spoil mounds.....	95

Table of Tables

Table 7.1 Key sources of information for marine processes	13
Table 7.2 Approximate location and water depth of three model points from MetOceanWorks (2021b; 2021c; 2021d), shown on Figure 7.1	17
Table 7.3 Annual total significant wave height statistics for three model points across the array area	18
Table 7.4 Seasonal wave characteristics from 20 th April 2022 to 20 th April 2023, from data recorded at the SWLB (see Figure 7.1).....	19
Table 7.5 Wave characteristics across three model points in the array area	19
Table 7.6 Annual omni-directional extreme total wave heights and associated parameters for three model points across the array area	23

Table 7.7 Tidal water level descriptors relative to MSL (m) at three locations around the array area	26
Table 7.8 Tidal height harmonic analysis results at the SWLB (location identified on Figure 7.1), relative to LAT (m).....	27
Table 7.9 Extreme water levels in the centre of the array area (MetOceanWorks, 2021b)	32
Table 7.10 Summary of particle size analysis across the array area (GEOxyz, 2022a)	46
Table 7.11 Summary of particle size analysis across the offshore ECC (GEOxyz, 2022b)	47
Table 7.12 Summary of estimated potential sediment mobility across the study area	49
Table 7.13 Estimated potential sediment mobility within the array area calculated from depth-averaged tidal currents	51
Table 7.14 Near-surface and near-bed turbidity values recorded at the SWLB (located in water depths of 22.9m (LAT)).....	52
Table 7.15 Estimated longshore sediment transport rates at Anderby Creek (HR Wallingford <i>et al.</i> , 2002)	57
Table 7.16 Particle size characteristics of dune sediments collected from dune sites at the Landfall area (Saye and Pye, 2004).....	72
Table 7.17 Estimated potential sediment mobility across the study area from modelled tidal currents	85

Table of Plates

Plate 7.1 Array Area annual wave rose for Hm0 and direction at the three model points (from left to right: West, Central, and East, as shown on Figure 7.1) (MetOceanWorks, 2021b; 2021c; 2021d)...	22
Plate 7.2 Wave rose of significant wave height and direction around the Landfall site (ABPmer, 2018)	25
Plate 7.3 Annual rose plot of modelled surface and near bed current speed and direction in the centre of the array area (MetOceanWorks, 2021b)	31
Plate 7.4 Bathymetric profiles across the Project array area, from Cathie (2021)	45
Plate 7.5 Time-series of near-bed turbidity (orange) against current velocity and significant wave height taken from the SWLB from April to August 2022	54
Plate 7.6 Time-series of near-bed turbidity (orange) against current velocity and significant wave height taken from the SWLB from November 2022 to May 2023	55
Plate 8.7 Bathymetric and gradient profile along the offshore ECC at the Inner Dowsing (Sand Bank 1) and North Ridge (Sand Bank 2) sandbanks, as labelled in Figure 8.15. Data from Project Cable Burial Risk Assessment (CBRA).....	65
Plate 7.8 Aerial photograph of the beach at transect L048 (see Figure 7.16), showing outfall and wet sand with channels running out to sea on the lower beach. Photo from 26 May 2012 (Environment Agency, 2013a). Transect is located in the northern half of the offshore ECC.	68
Plate 7.9 Aerial photography of the beach approximately at transect L048 (see Figure 7.16), showing outfall and wet sand with channels running out to sea on the lower beach (APEM, 2023). Transect is located in the northern half of the offshore ECC.	68

Plate 7.10 Difference in the beach profile at transect L049 (see Figure 7.17) over the last three surveys compared to the beach in June 2011. Lowering is shown in red (Environment Agency, 2013a)	71
Plate 7.11 Difference plots between LiDAR data across the dune and beach frontage between 2016 and 2020, with transect locations shown in Figure 7.20. MHWS and MLWS are indicated by the blue and red dots, respectively.....	76

Table of Figures

Figure 7.1 Marine Physical Processes Study Area	16
Figure 7.2 Winter Wave Height (ABPmer <i>et al.</i> , 2008).....	20
Figure 7.3 Mean Spring Tidal Range (ABPmer <i>et al.</i> , 2008).....	29
Figure 7.4 Maximum Modelled Depth-Averaged Spring Tidal Current Speeds and Spring Tidal Ellipses (MetOCeanWorks, 2021)	30
Figure 7.5 Flamborough Front Location	37
Figure 7.6 Bedrock Lithology	38
Figure 7.7 Quaternary Lithology Summary.....	39
Figure 7.8 Quaternary Deposit Thickness.....	40
Figure 7.9 Exposure of pre-Holocene geology at or near seabed in Inner Silver Pit and associated glacial outwash feature (Tappin <i>et al.</i> , 2011)	41
Figure 7.10 Bathymetry of the Study Area within a Regional Context.....	43
Figure 7.11 Surficial Seabed Sediments (Folk, 1954).....	44
Figure 7.12 Bedload Sediment Pathways (adapted from Kenyon and Cooper, 2005).....	58
Figure 7.13 Average Suspended Particulate Matter (Cefas, 2016)	59
Figure 7.14 Major Sandbanks within the Study Area	62
Figure 7.15 Morphology of Array Area, Offshore ECC and at Landfall.....	63
Figure 7.16 Beach Elevation Change from Surveys at 25m Intervals between 2011 and 2010 (Pre and Post Nourishment Activities) at Wolla Bank.....	69
Figure 7.17 Beach Elevation Change between 2013 and 2011 between Moggs Eye and Wolla Bank.....	70
Figure 7.18 Elevation Change from Coastal LiDAR Data between 2018 and 2016 at the Landfall location	73
Figure 7.19 Elevation Change from Coastal LiDAR Data between 2020 and 2018 at the Landfall location	74
Figure 7.20 Elevation Change from Coastal LiDAR Data between 2020 and 2016 at the Landfall location	75
Figure 7.21 Designated Sites of relevance to Marine Physical Processes	79

Acronyms & Terminology

Abbreviations / Acronyms

Abbreviation / Acronym	Description
AfL	Agreement for Lease
ANS	Artificial Nesting Structure
AWAC	Acoustic Wave and Current profiler
BEIS	Department for Business, Energy & Industrial Strategy (now the Department for Energy Security and Net Zero (DESNZ))
BGS	British Geological Survey
Cefas	Centre for Environment, Fisheries and Aquaculture Science
DCO	Development Consent Order
DECC	Department of Energy & Climate Change, now the Department for Energy Security and Net Zero (DESNZ)
DESNZ	Department for Energy Security and Net Zero, formerly Department of Business, Energy and Industrial Strategy (BEIS), which was previously Department of Energy & Climate Change (DECC)
DTI	Department of Trade and Industry
ECC	Export Cable Corridor
EIA	Environmental Impact Assessment
EMODnet	European Marine Observation and Data Network
ES	Environmental Statement
ETWL	Extreme Total Water Level
GT R4 Ltd	The Applicant. The special project vehicle created in partnership between Corio Generation (a wholly owned Green Investment Group portfolio company), Gulf Energy Development and TotalEnergies
HADA	Humber Aggregate Dredging Association
HAT	Highest Astronomical Tide
HPMA	Highly Protected Marine Area
JNCC	Joint Nature Conservation Committee
LAT	Lowest Astronomical Tide
LiDAR	Light Detection and Ranging
MAREA	Marine Aggregate Regional Environmental Assessment
MBES	Multi-Beam Echo Sounder
MHWS	Mean High Water Springs
MLWS	Mean Low Water Springs
MSL	Mean Sea Level
NNRCMP	National Network of Regional Coastal Monitoring Programmes
NSIP	Nationally Significant Infrastructure Project
NTSLF	National Tidal and Sea Level Facility
NCERM2	National Coastal Erosion Risk Mapping
OD	Ordnance Datum
ODN	Ordnance Datum Newlyn
ORCP	Offshore Reactive Compensation Station
OSS	Offshore Substation
OWF	Offshore Wind Farm
OWFL	Offshore Wind Farm Limited

Abbreviation / Acronym	Description
PEIR	Preliminary Environmental Information Report
PSA	Particle Size Analysis
RCP	Representative Concentration Pathway
SAC	Special Area of Conservation
SBP	Sub-bottom Profiler
SNSSTS	Southern North Sea Sediment Transport Study
SPM	Suspended Particulate Matter
SSS	Side Scan Sonar
SSSI	Site of Special Scientific Interest
SWAN	Simulating Waves Nearshore
SWLB	Seawatch Wind Lidar Buoy
TCE	The Crown Estate
TKOWFL	Triton Knoll Offshore Wind Farm Limited
UHRS	Ultra High Resolution Seismic
UKCP18	UK Climate Projections 2018
WTG	Wind Turbine Generator
ZoI	Zone of Influence

Terminology

Term	Definition
Agreement for Lease (AfL) array area	The area of the seabed awarded to GT R4 Ltd. through an Agreement for Lease (AfL) for the development of an offshore windfarm, as part of The Crown Estate's Offshore Wind Leasing Round 4.
Array area	The area offshore within which the generating station (including wind turbine generators (WTG) and inter array cables), offshore accommodation platforms, offshore transformer substations and associated cabling will be positioned.
Baseline	The status of the environment at the time of assessment without the development in place.
Cumulative effects	The combined effect of the Project acting additively with the effects of other developments, on the same single receptor/resource.
Cumulative impact	Impacts that result from changes caused by other past, present or reasonably foreseeable actions together with the Project.
Development Consent Order (DCO)	An order made under the Planning Act 2008 granting development consent for a Nationally Significant Infrastructure Project (NSIP).
Effect	Term used to express the consequence of an impact. The significance of an effect is determined by correlating the magnitude of an impact with the sensitivity of a receptor, in accordance with defined significance criteria.
Environmental Impact Assessment (EIA)	A statutory process by which certain planned projects must be assessed before a formal decision to proceed can be made. It involves the collection and consideration of environmental information, which fulfils the assessment requirements of the EIA Regulations, including the publication of an Environmental Statement (ES).
EIA Regulations	Infrastructure Planning (Environmental Impact Assessment) Regulations 2017.

Term	Definition
Environmental Statement (ES)	The suite of documents that detail the processes and results of the EIA.
Impact	An impact to the receiving environment is defined as any change to its baseline condition, either adverse or beneficial.
Intertidal	The area between Mean High Water Springs (MHWS) and Mean Low Water Springs (MLWS).
Landfall	The location at the land-sea interface where the offshore export cables and fibre optic cables will come ashore.
Maximum Design Scenario	The project design parameters, or a combination of project design parameters that are likely to result in the greatest potential for change in relation to each impact assessed.
Mitigation	Mitigation measures are commitments made by the Project to reduce and/or eliminate the potential for significant effects to arise as a result of the Project. Mitigation measures can be embedded (part of the project design) or secondarily added to reduce impacts in the case of potentially significant effects.
Offshore Export Cable Corridor (Offshore ECC)	The Offshore Export Cable Corridor (Offshore ECC) is the area within the Order Limits within which the export cables running from the array to Landfall will be situated.
Offshore Reactive Compensation Station (ORCP)	A structure attached to the seabed by means of a foundation, with one or more decks and a helicopter platform (including bird deterrents) housing electrical reactors and switchgear for the purpose of the efficient transfer of power in the course of HVAC transmission by providing reactive compensation.
Offshore Substation (OSS)	A structure attached to the seabed by means of a foundation, with one or more decks and a helicopter platform (including bird deterrents), containing— (a) electrical equipment required to switch, transform, convert electricity generated at the wind turbine generators to a higher voltage and provide reactive power compensation; and (b) housing accommodation, storage, workshop auxiliary equipment, radar and facilities for operating, maintaining and controlling the substation or wind turbine generators.
Order Limits	The area subject to the application for development consent, The limits shown on the works plans within which the Project may be carried out.
Receptor	A distinct part of the environment on which effects could occur and can be the subject of specific assessments. Examples of receptors include species (or groups) of animals or plants, people (often categorised further such as 'residential' or those using areas for amenity or recreation), watercourses etc.
The Applicant	GT R4 Ltd. The Applicant making the application for a DCO. The Applicant is GT R4 Limited (a joint venture between Corio Generation, TotalEnergies and Gulf Energy Development (GULF)), trading as Outer Dowsing Offshore Wind. The Project is being developed by Corio Generation (a wholly owned Green Investment Group portfolio company), TotalEnergies and GULF.
The Planning Inspectorate	The Planning Inspectorate. The agency responsible for operating the planning process for Nationally Significant Infrastructure Projects (NSIPs).
The Project	Outer Dowsing Offshore Wind, an offshore wind generating station together with associated onshore and offshore infrastructure.

Term	Definition
Wind Turbine Generator (WTG)	A structure comprising a tower, rotor with three blades connected at the hub, nacelle and ancillary electrical and other equipment which may include J-tube(s), transition piece, access and rest platforms, access ladders, boat access systems, corrosion protection systems, fenders and maintenance equipment, helicopter landing facilities and other associated equipment, fixed to a foundation.

Reference Documentation

Document Number	Title
6.1.3	Project Description

7 Marine Processes Technical Baseline

7.1 Introduction

1. This technical report provides a detailed baseline description of Marine Processes in relation to the Outer Dowsing Offshore Wind (“the Project”). Specifically, this report considers Marine Processes seaward of Mean High Water Springs (MHWS), which for the purposes of both this technical report and the subsequent Offshore Environmental Impact Assessment (EIA) Report, include the following elements:
 - Morphology, including bathymetry, geology, surficial sediments and seabed form;
 - Hydrodynamics, including tidal and non-tidal influences, and waves; and
 - Sediment transport, including bedload, littoral and suspended sediment transport.
2. GT R4 Limited (trading as Outer Dowsing Offshore Wind) hereafter referred to as the ‘Applicant’, is proposing to develop the Project. The Project will be located approximately 54km from the Lincolnshire coastline in the southern North Sea. The Project will include both offshore and onshore infrastructure including an offshore generating station (windfarm), export cables to Landfall, Offshore Reactive Compensation Platforms (ORCP), onshore cables, connection to the electricity transmission network, ancillary and associated development and areas for the delivery of up to two Artificial Nesting Structures (ANS) and the creation of a biogenic reef (if these compensation measures are deemed to be required by the Secretary of State) (see Volume 1, Chapter 3: Project Description for full details (document reference 6.1.3)).
3. This baseline description sets out the ‘conceptual understanding’ of the marine and coastal system in which the Project is located and describes how the processes operating within this system link together and evolve in response to applied natural and anthropogenic forces. This understanding underpins the assessments of potential impacts resulting from the Project (Volume 1, Chapter 7: Marine Processes (document reference 6.1.7)).

7.2 Purpose

4. The primary purpose of this report is to provide a contemporary and comprehensive analysis of site-specific and regional Marine Processes data within the study area. This Environmental Statement (ES) document has been produced following the completion of pre-application consultation, to be submitted alongside the application to The Planning Inspectorate for a Development Consent Order (DCO).
5. The remainder of this report is structured in the following way:
 - Definition of the study area;
 - Outline of the data sources used to inform the characterisation;
 - A review of the baseline (existing) conditions of the study area; and
 - Identification of Designated Sites of relevance to Marine Processes.

6. This document will accompany document reference 6.1.7 and should be read in conjunction with Volume 3, Appendix 7.2: Marine Processes Modelling Report (document reference 6.3.7.2).

7.3 Scope and Methodology

7.3.1 Study Area

7. The baseline description of the Marine Processes environment provides a regional (far-field) overview prior to focusing on the study area. This document recognises the different types of project activities and marine processes present within the study area. As such descriptions are provided for the following sub-areas:
 - Offshore array (including Wind Turbine Generators (WTGs), Offshore Substations (OSSs), offshore accommodation platforms, inter-array cables and interlink cables);
 - The Offshore Export Cable Corridor (Offshore ECC) (including export cables and Offshore Reactive Compensations Stations (ORCPs));
 - Landfall; and
 - Compensation areas, including areas for Artificial Nesting Structures (ANS) and biogenic reef creation (Figure 7.1).
8. The characterisation within this document has been carried out on the basis of the Agreement for Lease (AfL) array area, with any relevant changes for the array area as refined for the purposes of the DCO application identified within this document as required.
9. Of note is that the offshore ECC includes the transition from offshore to nearshore marine process environmental conditions.
10. A presentation of the study area is given in Figure 7.1. These areas include buffer zones to represent a potential “Zone of Influence (ZoI)” for impacts that might be created within the main areas of activity. The buffer zones are scaled to conservatively represent the equivalent distance of tidal excursion on a mean spring tide and comprise a distance of between, approximately, 10km and 15km.

7.3.2 Data Sources

11. The following Project specific surveys have been used to characterise the seabed and oceanographic conditions within the array and within the offshore ECC:
 - Geophysical survey: carried out with an Ultra High Resolution Seismic (UHRS), Multi-Beam Echo Sounder (MBES), Side Scan Sonar (SSS), and Sub-bottom Profiler (SBP).
 - Benthic survey: including drop down camera data and grab samples to allow a characterisation of the seabed features and sediment composition. The survey additionally included sediment Particle Size Analysis (PSA) and contaminant analysis using the grab samples.
 - Metocean measurements: including wave, wind and current measurements from a Seawatch Wind Lidar Buoy (SWLB) deployed within the array area. Monthly datasets are provided from April 2022 to April 2023.

- Metocean preliminary design criteria: including modelled wind, wave, and hydrodynamic (currents and water levels) data.
- Desk-based geological and geotechnical survey: including the use of client-issued and publicly available data to establish the likely ground conditions and create a preliminary ground model of the area in order to provide recommendations for future site surveys.

12. Where relevant, survey data from other Offshore Wind Farms (OWFs) and marine industries have been used to support the characterisation of the Marine Process environment. This includes:

- Race Bank OWF (Centrica, 2009) and associated surveys;
- Triton Knoll Offshore Wind Farm (Triton Knoll Offshore Wind Farm Limited (TKOWFL, 2011; 2012; 2014; 2015) and associated surveys; and
- Dudgeon and Sheringham Shoal Extensions (Equinor, 2022) and associated surveys.

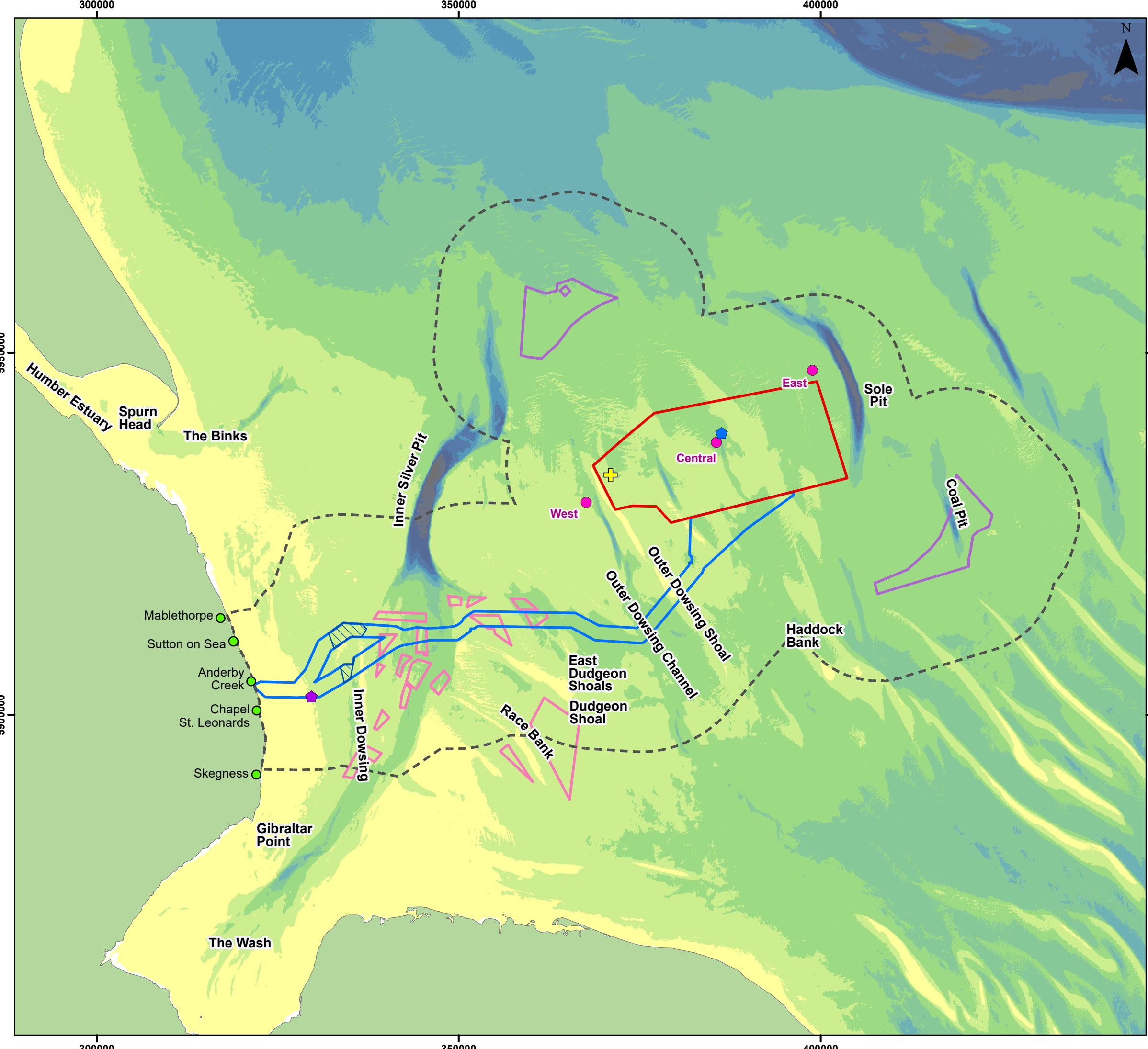
13. The age of data has been taken into account, with caution afforded to datasets older than five years old, although they have been considered within the baseline description where relevant. Comprehensive coverage of the Project specific surveys within both the array area and ECC is such that data from other sources is not heavily relied upon to fill data gaps.

Table 7.1 Key sources of information for marine processes

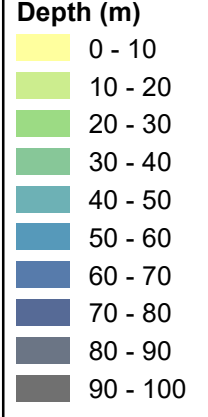
Source	Summary	Spatial Coverage
Generic		
Marine Aggregate Regional Environmental Assessment (MAREA) of the Humber and Outer Wash Region (Humber Aggregate Dredging Association (HADA), 2012)	Regional characterisation of geology, morphology, surficial sediments, coastal processes, and hydrodynamics.	Partial coverage
Triton Knoll Offshore Wind Farm (OWF) Environmental Statement (ES) and associated technical reports (TKOWFL, 2011; 2012; 2014; 2015)	Regional and site-specific characterisation of geology, morphology, surficial sediments, coastal processes and hydrodynamics, including survey and model outputs.	Partial coverage
Race Bank OWF ES and associated technical reports (Centrica, 2009; EMU and Osiris, 2008)	Regional and site-specific characterisation of geology, morphology, surficial sediments, coastal processes and hydrodynamics, including survey and model outputs.	Partial coverage
Dudgeon and Sheringham Shoal Extensions ES and associated technical reports (Equinor, 2022)	Regional and site-specific characterisation of geology, morphology, surficial sediments, coastal processes and	Partial coverage

Source	Summary	Spatial Coverage
	hydrodynamics, including survey and model outputs.	
The Humber Regional Environmental Characterisation Source: Tappin <i>et al.</i> (2011)	Physical processes, bathymetry, morphology and geology off the east coast of England.	Partial coverage
Offshore Energy Strategic Environmental Assessment 3 (OESEA3) Environmental Report (Department of Energy and Climate Change (DECC), 2016)	Regional characterisation of geology, morphology, surficial sediments, coastal processes, and hydrodynamics.	Partial coverage
Metocean Data		
Atlas of UK Marine Renewable Energy Resources. Source: UK Renewables Atlas - ABPmer (www.renewables-atlas.info) (ABPmer <i>et al.</i> , 2008)	Low resolution modelled hindcast wave, wind and hydrodynamic data. Summary data provided only.	Full coverage
SEASTATES Metocean Data and Statistics Interactive Map (ABPmer, 2018) Source: www.seastates.net/	Modelled hindcast wave and hydrodynamic data.	Full coverage
Centre for Environment, Fisheries and Aquaculture Science (Cefas) WaveNet data Source: www.cefas.co.uk/cefas-data-hub/wavenet/	Wave records from point locations, including Chapel Point and Dowsing.	Partial coverage
Project Metocean Design Criteria (MetOceanWorks, 2021a; 2021b; 2021c; 2021d)	Numerical modelling to inform design criteria.	Partial coverage; array area but ECC not included
SWLB Metocean Measurements	Wave, wind and current data from Project array area between April and November 2022.	Partial coverage
National Tidal and Sea Level Facility (NTSLF) Real-time data Source: https://ntslf.org/data/uk-network-real-time	Records of real-time tide gauge data for sites around the UK.	Partial coverage
Morphology and Sediment Transport		
Southern North Sea Sediment Transport Study Phase 2 (SNSSTS II) Source: HR Wallingford <i>et al.</i> (2002)	Information on observed and modelled littoral and seabed sediment transport.	Partial coverage
British Geological Survey (BGS) Offshore GeoIndex Map Source: www.bgs.ac.uk/GeoIndex/offshore.htm	Seabed sediment maps (based on Folk classification) and borehole records from point locations. Data gaps exist in the coastal zone.	Full coverage

Source	Summary	Spatial Coverage
Cefas Suspended Sediment Climatologies around the UK	Monthly and seasonal Suspended Particulate Matter (SPM) maps.	Full coverage
Department of Trade and Industry (DTI) Technical Report: Sandbanks, sand transport and offshore windfarms Source: Kenyon and Cooper (2005)	Detail on offshore and littoral sediment transport, including morphological form and behaviour of offshore sandbanks.	Partial coverage
European Marine Observation and Data Network (EMODnet) Bathymetry Data (EMODnet, 2020)	Interactive bathymetry map.	Full coverage
Anglian Regional Coastal Monitoring Programme and associated reports (Environment Agency, 2011; 2013a; 2013b; 2019a; 2019b; 2021) Source: https://coastalmonitoring.org/anglian/	Monitoring data to inform coastal characteristics and change, including topographic survey data, aerial imagery and oceanographic data.	Partial coverage
Project-specific geophysical survey (Enviros, 2022)	Geophysical survey using UHRS, MBES, SSS, and SBP.	Partial coverage; array area but ECC not included
Project-specific benthic surveys: Benthic Ecology OWF Area Results Report (Vol. 1) (GEOxyz, 2022a) and Benthic Ecology ECC Area Results Report (Vol. 2) (GEOxyz, 2022b)	Benthic sediment grab samples including PSA at locations within the array area and offshore ECC.	Full coverage
Outer Dowsing Desktop Study and Preliminary Ground Model (Cathie, 2021)	Desk-based geological and geotechnical survey to provide recommendations for future site surveys.	Full coverage
National Network of Regional Coastal Monitoring Programmes (NNRCMP) Light Detection and Ranging (LiDAR) data Source: https://www.coastalmonitoring.org/cco/	Aerial photography and LiDAR data around the coast of the UK, showing beach morphology change over time.	Partial coverage
Future Changes		
UK Climate Projections Science Report: UKCP18 Marine report. Source: Palmer <i>et al.</i> (2018)	Sea level rise predictions for coastal locations.	Partial coverage
UK FUTURECOAST Project (Defra, 2002)	Sea level rise predictions for coastal locations and assessments of shoreline behaviour.	Partial coverage



- Legend**
- Array Area
 - Offshore Export Cable Corridor
 - ORCP Area
 - Artificial Nesting Structure Area
 - Biogenic Reef Restoration Area
 - Physical Processes Zone of Influence
 - + Cefas Dowsing WaveNet Site
 - ⬠ Chapel Point Directional Waverider Buoy
 - ⬠ Lidar Buoy SWLB059
 - Metocean Model Data Points



Coordinate System: WGS 1984 UTM Zone 31N
 0 10 20 km
 Scale: 1:500,000
 A3 Page Size

Environmental Statement
 Marine Physical Processes Study Area
 Figure 7.1



Document Path: Z:\GIS\GIS - Projects\0152 Outer Dowsing ELA\GIS\Figures\ES\Physical Processes Technical Report\ODOW_0152_PPTR_Fig7.1_Study Area.mxd

7.4 Baseline Environment

7.4.1 Metocean

14. This section provides an overview of the influences of tidal, non-tidal and wave processes on the study area.

7.4.1.1 Waves

15. Wave-energy is dependent on the friction action of the wind on the sea surface that drives directional sea-surface and storm surge currents. These in turn drive non-directional rotational near-bed currents when wind and swell waves interact with the seabed (Tappin *et al.*, 2011). The wave regime frequently plays an important role in the erosion, transport and deposition of sediments, although its influence on the seabed can be unpredictable due to changes in wind patterns and variation in bathymetry (HADA, 2012b).

16. Prevailing winds within the study area originate predominantly from the south-southwest, although waves from this direction have a notably limited fetch and are unlikely to develop into large waves by the time they reach the array area. The study area is therefore mainly dominated by waves generated within the North Sea basin, with long fetch generated from the northerly and north-easterly sectors (TKOWFL, 2011). In the offshore region wind and swell dominate the character of the waves, and as waves travel into shallower water interaction with the seabed causes shoaling, refraction, and eventually breaking (HADA, 2012b). The wave climate closer to the shore is complex as a result of refraction and sheltering effects associated with sandbanks and the coast, which have a focusing effect on incoming waves (TKOWFL, 2015).

Offshore Array

17. The wave climate within the Project array area has been characterised generally using regional-scale information from the UK Atlas of Marine Renewable Energy Resources (ABPmer *et al.*, 2008), as well as hindcast data from ABPmer's SEASTATES database (ABPmer, 2018). This is supported by data from Project specific metocean design criteria, which used a bespoke Simulating Waves Nearshore (SWAN) model validated against measured regional datasets, including the Centre for Environment, Fisheries and Aquaculture Science (Cefas) Dowsing wave buoy located to the west of the array area (MetOceanWorks, 2021a). Data is provided at three locations, details of which are outlined in Table 7.2 and shown on Figure 7.1. This is further supported by measurements from the Cefas Dowsing wave buoy and Project SLWB, the locations of which are shown on Figure 7.1.

Table 7.2 Approximate location and water depth of three model points from MetOceanWorks (2021b; 2021c; 2021d), shown on Figure 7.1

Location ID	Latitude	Longitude	Mean Sea Level (MSL) Depth (m)
West	53.4964° N	1.0040° E	23
Central	53.5750° N	1.2720° E	23

Location ID	Latitude	Longitude	Mean Sea Level (MSL) Depth (m)
East	53.6672° N	1.4690° E	28

18. Annual mean wave heights within the array area are approximately between 1.37m and 1.46m, decreasing in a shoreward direction. Wave heights are highest during the winter months, as shown on Figure 7.2, ranging between around 1.70m in the west of the array area to 1.95m in the east (ABPmer *et al.*, 2008).
19. Annual total significant wave height¹, or H_{m0} , statistics for each model point (shown on Figure 7.1) are provided in Table 7.3. In the centre of the array area, mean significant wave heights are approximately 1.3m. Both mean and maximum significant wave heights increase with distance offshore, as shown in Figure 7.2, whilst minimum values are generally similar. An analysis of approximately 16 years of measurements from the Cefas Dowsing wave buoy (location shown on Figure 7.1) provides a mean significant wave height of 1.2m, with a peak wave height of 6.5m (Cefas, 2021).

Table 7.3 Annual total significant wave height statistics for three model points across the array area

Model point	Minimum (m)	Mean (m)	Maximum (m)
West	0.1	1.3	6.6
Central	0.1	1.3	7.7
East	0.1	1.4	8.1

20. Data recorded at the SWLB (see Figure 7.1) between April 2022 and April 2023 recorded a mean significant wave height of 1.2m, a peak wave period² of 6.2 seconds, and a maximum wave height³ of 1.8m (Fugro, 2023). Seasonal statistics calculated from this data are presented in Table 7.4, demonstrating that wave heights are highest during winter, with higher peak wave periods, and lowest during summer. These values corroborate those identified within the model data, as well as recorded from the Cefas Dowsing wave buoy. A large proportion of the waves observed on site approach from the north-northeast, with 25% of observations associated with the 0° - 30° directional band, and longest period waves also approaching from this sector. The largest wave heights measured tended to be approaching from the east-southeast and north-northeast. The largest wave height of 8.1m H_{max} was recorded on 18th January 2023 during a northerly event (Fugro, 2023).

¹ Significant wave height, H_{m0} , refers to the approximately the average height of the highest one third of the waves in a defined period, estimated from the wave spectrum as $4\sqrt{m_0}$.

² Spectral peak period, T_p , the period at which most energy is present in the wave spectrum.

³ Maximum wave height, H_{max} , maximum individual wave height occurring within a defined period.

Table 7.4 Seasonal wave characteristics from 20th April 2022 to 20th April 2023, from data recorded at the SWLB (see Figure 7.1)

Season ⁴	Significant Wave Height Spectral (m)	Significant Wave Height Deterministic (m)	Maximum Wave Height (m)	Peak Period Tp (s)
Spring	1.17	1.10	1.73	6.69
Summer	0.78	0.31	1.13	5.34
Autumn	1.36	1.21	1.96	5.79
Winter	1.56	1.51	2.34	7.21

21. A frequency analysis of significant wave heights and directions at each model point in the array area (shown in Figure 7.1) is presented in Plate 7.1. The main characteristics of the wave regime are summarised in Table 7.5 and Table 7.6, using data from MetOceanWorks (2021b; 2021c; 2021d) modelling.

Table 7.5 Wave characteristics across three model points in the array area

Model Point	Prevailing Wave Direction	Most Frequent H _{m0} and Associated Parameters			Highest H _{m0} ⁵ and Associated Parameters		
		H _{m0} (m)	T _p (s)	Direction	H _{m0} (m)	T _p (s)	Direction
West	North (N) (12.9%) and North-northwest (NNW) (11.9%)	0.5 – 1.0 (35.4%)	4 – 6 (15.1%)	N	5.5 – 6.0 (0.03%)	10 – 12 (0.02%)	NNW
Central	N (12.9%) and NNW (10.7%)	0.5 – 1.0 (33.0%)	4 – 6 (16.6%)	N	6.0 – 6.5 (0.02%)	10 – 14 (0.02%)	NNW
East	N (12.0%) and NNW (10.7%)	0.5 – 1.0 (31.6%)	4 – 6 (17.1%)	N	6.5 – 7.0 (0.01%)	12 – 14 (0.01%)	NNW

⁴ Seasons are defined as meteorological, with spring representing March to May, summer representing June to August, autumn representing September to November, and winter representing December to February.

⁵ Values <0.01% have not been considered.

300000

350000

400000

450000

6000000

6000000

5900000

5900000

5850000

5850000

300000

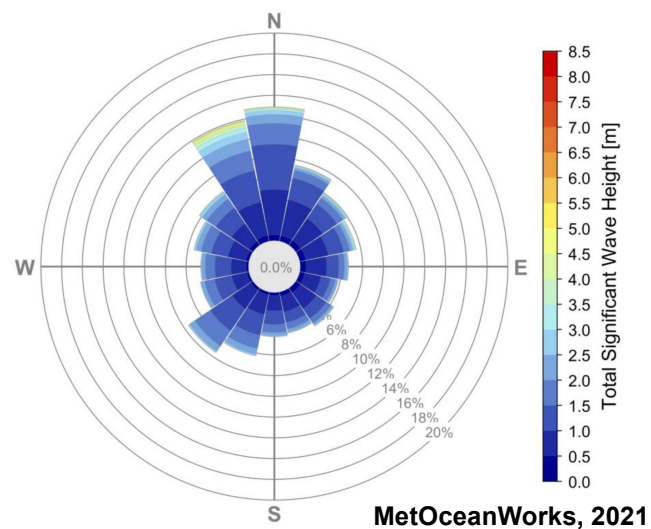
350000

400000

450000

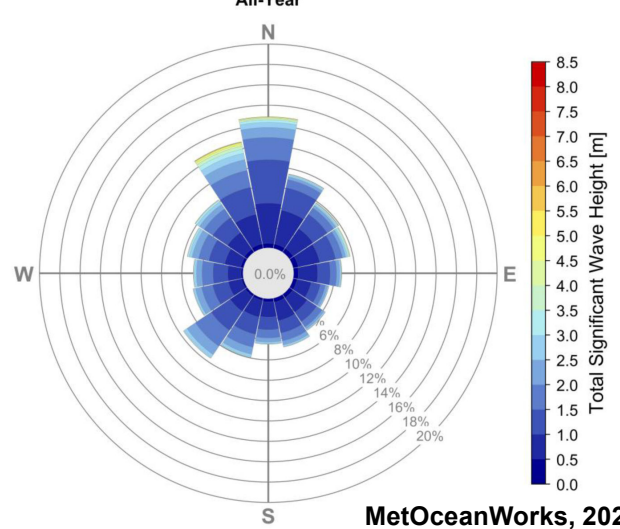
Metoccean Modelling Point (West)

All-Year



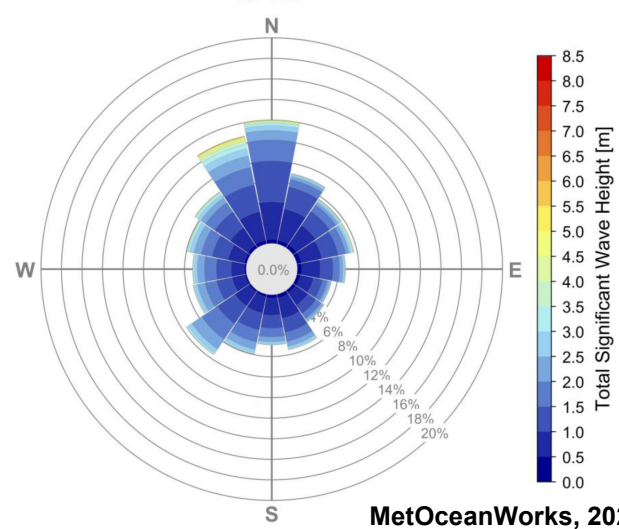
Metoccean Modelling Point (Central)

All-Year



Metoccean Modelling Point (East)

All-Year

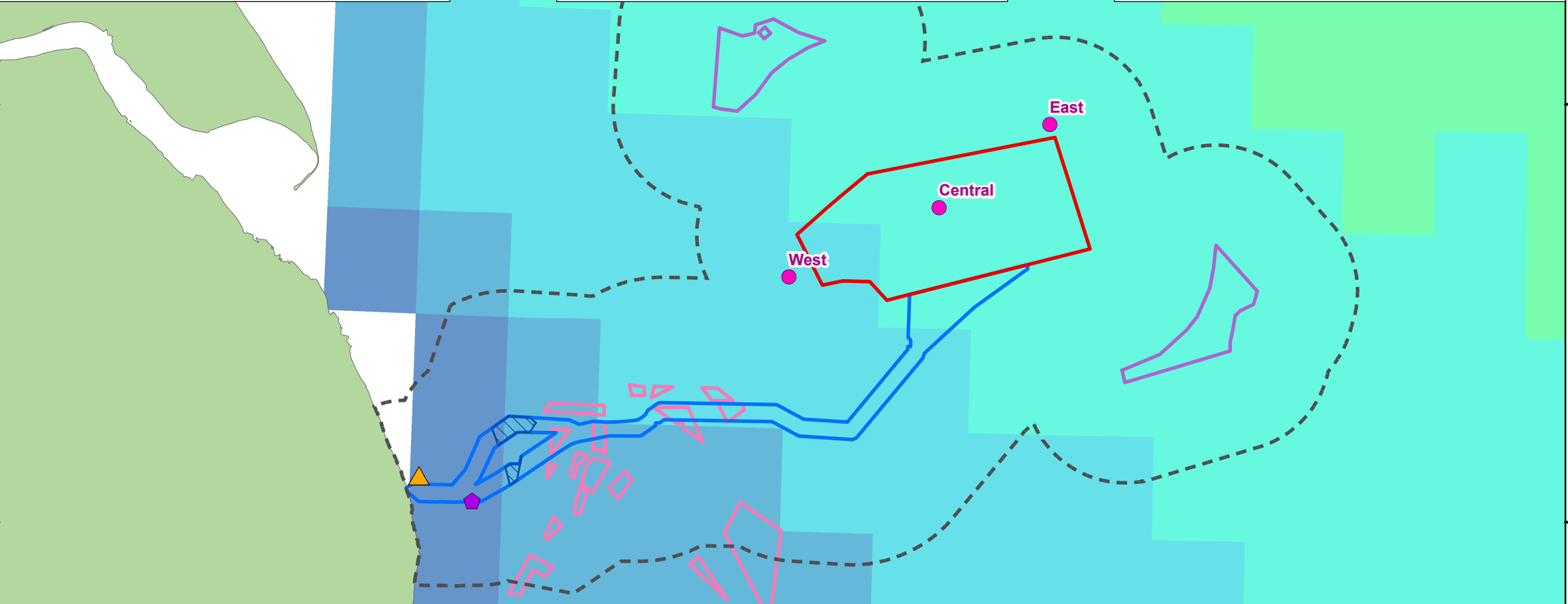


Legend

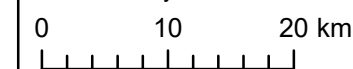
- Array Area
- Offshore Export Cable Corridor
- ORCP Area
- Artificial Nesting Structure Area
- Biogenic Reef Restoration Area
- Physical Processes Zone of Influence
- Chapel Point Directional Waverider Buoy
- Seastates Data (ABPmer, 2018)
- Metoccean Model Data Points

Mean Winter Wave Height (m)

- < 1.25
- 1.25 - 1.5
- 1.5 - 1.75
- 1.75 - 2
- 2 - 2.25
- 2.25 - 2.5



Coordinate System: WGS 1984 UTM Zone 31N



Scale: 1:600,000

A3 Page Size

Environmental Statement

Winter Wave Height (ABPmer *et al.*, 2008)

Figure 7.2



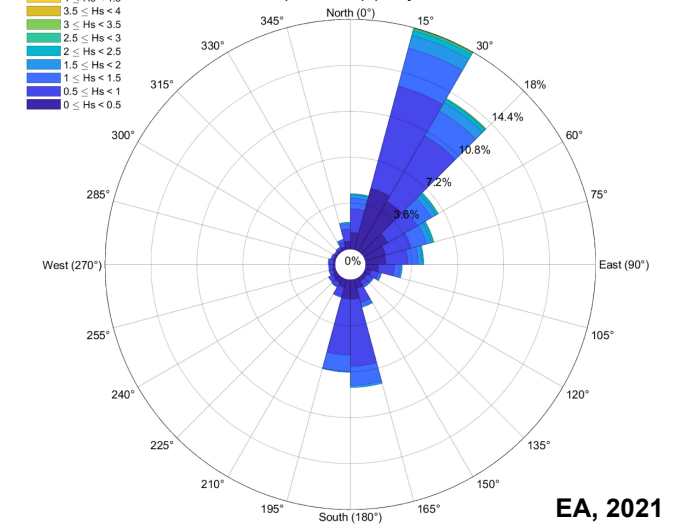
Date: 28/02/2024
 Produced By: BPHB
 Revision: 0.1



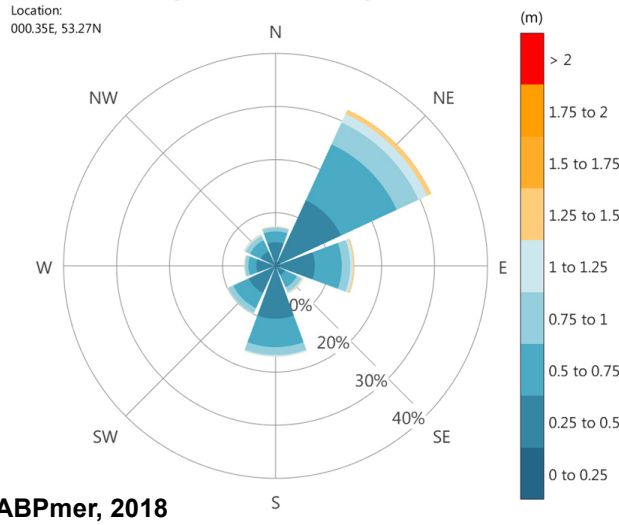
Contains ESRI Basemapping;
 EMDONet 2020 bathymetry

Chapel Point Waverider Buoy

Chapel Point Hs (m) - all years



Seastates Significant Wave Height



Document Path: Z:\GIS\GIS - Projects\0152 Outer Dowsing ELA\GIS\Figures\ES\Physical Processes Technical Report\ODOW_0152_P1-R_Fig7.2_Winter_Wave_Height.mxd

22. Although the wave regime is generally similar across the array area, differences can be identified between the three model points. The main characteristics are as follows:

- In the centre of the array area, the most frequent wave direction is from the north (12.9%) and north-northwest (10.7%), with a smaller fraction from the southwest (7.6%) and north-northeast (7.5%) (as shown in Plate 7.1). This coincides with the longest fetch distances extending out into the northern North Sea, as well as the prevailing wind direction from the southwest. Across the three model points, this pattern is generally similar, although the dominance of the north-northwestern direction is most pronounced in the west of the array area (Table 7.5). Further offshore, there is an increasing proportion of waves from the south-southeast, with a difference of 1.5% over the three model points.
- In the centre of the array area, 33.0% of waves have a significant wave height between 0.5m and 1m, with a further 28.7% between 1.0m and 1.5m. The largest waves arrive from the north-northwest with a significant total wave height of 6.0m to 6.5m, although these comprise just 0.02% of the record (values under 0.01% have been excluded). The most frequent significant wave height is between 0.5m and 1.0m for all model points, although the proportion within this range decreases further offshore, as significant wave heights become generally higher. This is reflected in the highest significant wave heights, which increase from between 5.5m and 6.0m in the west to between 6.5m and 7.0m in the east (Table 7.5).
- The majority of the record (43.8%) in the centre of the array area comprises waves with a peak wave period, or T_p , of between 4 and 6 seconds, and a further 28.4% with a peak wave period between 6 to 8 seconds. The largest peak wave period is between 16 and 18 seconds, which occurs in 0.02% of the record. Across the model points from west to east, peak wave periods generally increase, with the proportion of waves between 6 and 8 seconds increasing from 23.9% in the west to 32.0% in the east.
- For the centre of the array area, significant wave heights are of the order of 5.3m, 6.8m, and 8.3m and maximum wave heights are 9.7m, 12.3m, and 14.9m for return periods of 1, 10, and 100 years, respectively. These are associated with peak wave period values of 11, 12.8, and 14.5 seconds. Both values increase with distance from the shore, as shown in Table 7.6.
- Overall, waves further offshore within the array area are generally higher, with longer peak wave periods and higher extreme total wave heights. This is likely to reflect generally shallowing bathymetry close to the shore, although these changes are minor and the model points are located in broadly similar water depths (Table 7.2). Waves further offshore within the array area occur slightly more from the south-southeast and other directions, with the dominance of the north and north-northwestern directions increasing closer to shore (Plate 7.1). Closer to shore, along the offshore ECC, the waves generally become more oriented from the north and northeast, as outlined in paragraph 24 *et seq.*

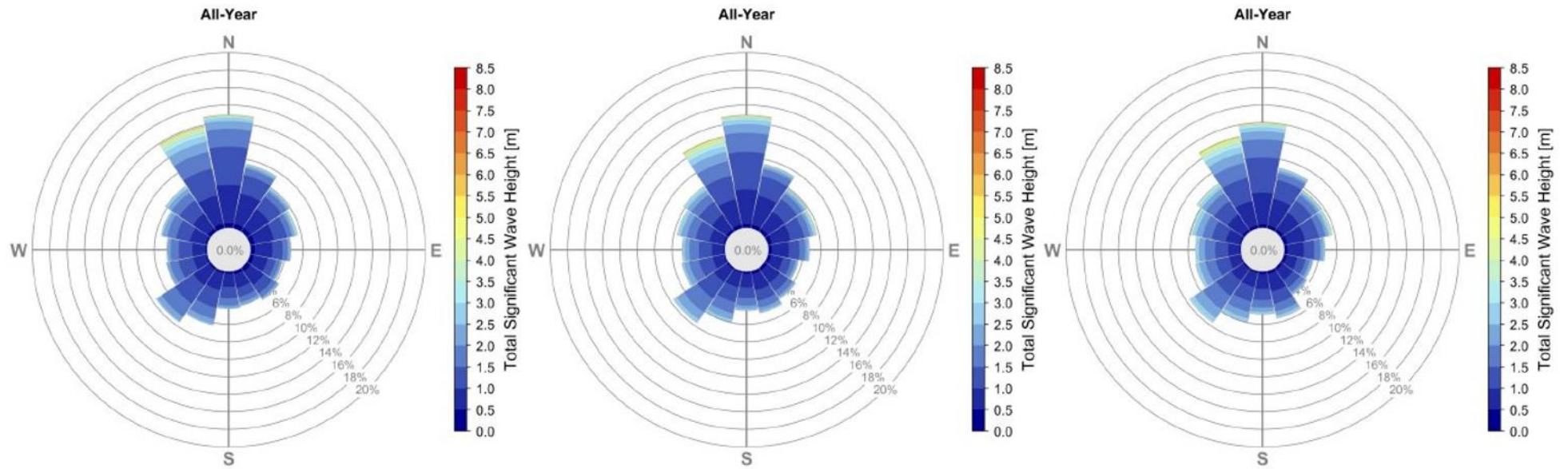


Plate 7.1 Array Area annual wave rose for Hm0 and direction at the three model points (from left to right: West, Central, and East, as shown on Figure 7.1) (MetOceanWorks, 2021b; 2021c; 2021d)

Table 7.6 Annual omni-directional extreme total wave heights and associated parameters for three model points across the array area

Return Period (years)	West		Central			East			
	H_{m0}^6 (m)	T_p (s) ⁷	H_{max}^8 (m)	H_{m0} (m)	T_p (s)	H_{max} (m)	H_{m0} (m)	T_p (s)	H_{max} (m)
1	5.0	11.3	9.5	5.3	11.0	9.7	5.4	10.9	10.1
5	5.8	12.3	10.7	6.3	12.2	11.5	6.5	12.2	11.9
10	6.2	12.7	11.4	6.8	12.8	12.3	7.0	12.8	12.9
50	6.9	13.7	12.7	7.8	14.0	14.1	8.2	14.1	14.9
100	7.2	14.1	13.3	8.3	14.5	14.9	8.7	14.6	15.8
500	7.9	14.9	14.5	9.3	15.6	16.7	9.8	15.9	17.9

Offshore Export Cable Corridor

23. Hindcast data from ABPmer’s SEASTATES database has been used to characterise wave conditions within the Offshore ECC (ABPmer, 2018), along with data from other OWF ES reports and observational wave records from a Directional Waverider Buoy situated off Chapel Saint Leonards, known as the Chapel Point Directional Waverider Buoy.
24. Waves in the most offshore part of the Offshore ECC originate mainly from the north, with smaller components from the southeast and southwest, and can reach over 2m in significant wave height (ABPmer, 2018). Further west along the ECC the wave climate is complex, with refraction and sheltering effects occurring due to the presence of sandbanks, including Inner Dowsing (TKOWFL, 2014). Prevailing waves continue to originate from the north and northeast, with smaller components from the southwest and east (TKOWFL, 2014; ABPmer, 2018). Available records show that the largest waves are observed in more offshore waters, decreasing in a landwards direction. The most frequently observed wave periods are typically between 3 and 4 seconds, generally indicative of locally generated wind waves, corresponding to a significant wave height between 0.5 and 1.0m (TKOWFL, 2014).

⁶ Significant wave height, H_{m0} , refers to the approximately the average height of the highest one third of the waves in a defined period, estimated from the wave spectrum as $4\sqrt{m_0}$.

⁷ Spectral peak period, T_p , the period at which most energy is present in the wave spectrum.

⁸ Maximum wave height, H_{max} , maximum individual wave height occurring within a defined period.

25. Closer to the shore, the wave regime has been characterised using data from the Chapel Point Directional Waverider Buoy, which is located approximately 6.2km offshore and around 1km south of the Offshore ECC. Waves occur most frequently from the north-northeast and northeast, with the largest waves coming from these directions, coinciding with long fetch distances into the North Sea. The annual mean wave height recorded is 0.8m, with wave heights highest during the winter months, and the most common peak wave periods are between 4 and 6 seconds. Significant wave heights have been calculated as 3.3m, 3.9m, and 4.2m for return periods of 1, 10, and 100 years, respectively (Environment Agency, 2021).

Coast

26. The dominant wave direction along the Lincolnshire coast is from the northeast, with the majority of waves having an annual significant wave height between 0 and 1.0m (ABPmer, 2018; Plate 7.2). A nearshore Acoustic Wave and Current profiler (AWAC) deployed at Chapel Point from 2006 to 2009, at an approximate water depth of 5m, logged an overall mean wave height of 0.65m (Environment Agency, 2013b). Modelled wave statistics show little variation in the nearshore wave height over a range of return periods, suggesting that wave shoaling is limited up the coast (TKOWFL, 2012).
27. The wave regime exerts the dominant forcing to littoral transport within the nearshore zone, with the wave direction leading to a generally southward drift of sediments towards the Wash (HR Wallingford *et al.*, 2002; Environment Agency, 2010; 2011). The wave regime only influences offshore sediment transport during extreme events. A 1-year return period significant wave height at the Lincolnshire coast has been modelled as 4.5m (Environment Agency, 2011; TKOWFL, 2012).

Compensation Areas

28. Mean significant wave heights in the ANS areas are of the order of 1.5m throughout the year, with mean winter wave heights of between, approximately, 1.8m to 1.9m (ABPmer *et al.*, 2008). Waves at the northerly ANS area originate primarily from the north, whereas the dominant wave direction at the southerly ANS areas is from the northwest, with a smaller proportion from the north and south (ABPmer, 2018). The wave regime within the biogenic reef creation area is generally similar to that of the offshore ECC, characterised in paragraph 23 *et seq.*, with annual significant wave heights generally between 0.75m (in the nearshore zone) and 1.35m (further offshore), with waves arriving primarily from the north.

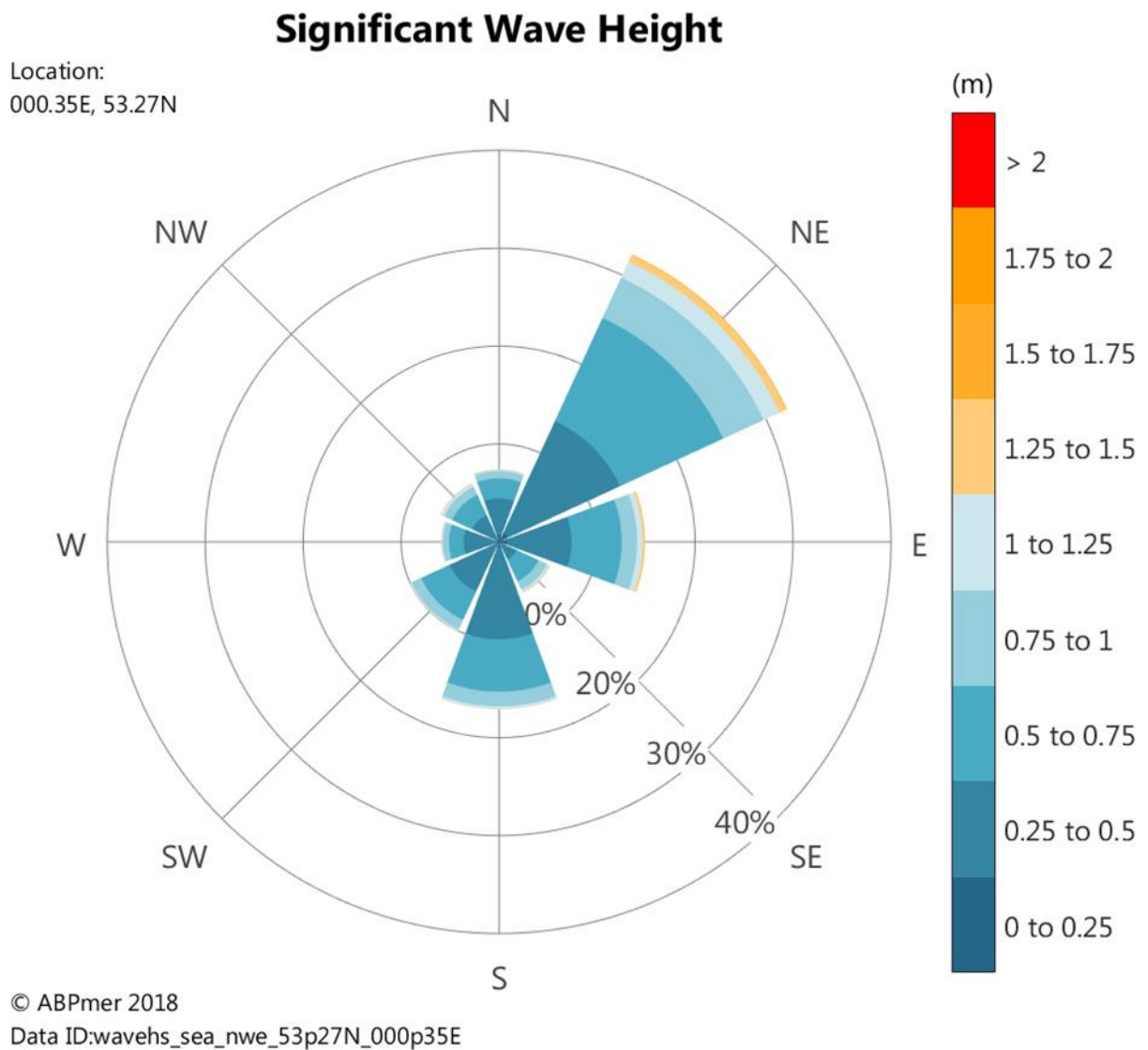


Plate 7.2 Wave rose of significant wave height and direction around the Landfall site (ABPmer, 2018)

7.4.1.2 Tides

29. The tidal regime in the southern North Sea is under the influence of two amphidromic points, at which the tidal range is near zero. These points are located off the west coast of Denmark and between East Anglia and the Netherlands, with the first having the greatest influence at the Project location (Sündermann and Pohlmann, 2011). Tides rotate anti-clockwise around these points, resulting in a semi-diurnal tide flooding to the southeast and ebbing to the northwest (HADA, 2012a; Orsted, 2021). Tidal ranges increase in a shoreward direction with distance from the amphidrome, from approximately 2.5m in the eastern extent of the study area to around 5.5m along the coast (Figure 7.3; ABPmer *et al.*, 2008).

30. Modelled regional tidal ellipses, available from the UK Atlas of Marine Renewable Energy Resources (ABPmer *et al.*, 2008), provide some indication of current flow direction across the site, showing that flows are orientated northwest to southeast in the east of the study area (indicated in Figure 7.4). Towards the west, they become less rectilinear and more rotary, and are mainly oriented north to south to the west of Inner Silver Pit. The influence of bathymetry can also be seen in modelled depth-average spring tidal current speeds shown in Figure 7.4, with faster currents occurring in areas with deeper water channels.

Offshore Array

31. Tidal water levels throughout the array generally increase in range from the northeast to southwest, transitioning from a meso-tidal to macro-tidal⁹ regime. Modelled spring and neap tidal ranges in the centre of the array are 3.62m and 1.76m, respectively. Summary tidal statistics for three locations within the array area are shown in Table 7.7, with locations marked on Figure 7.1 and outlined in Table 7.2 (MetOceanWorks, 2021b; 2021c; 2021d). This is corroborated by tidal height harmonic analysis results from the SWLB buoy (location shown in Figure 7.1), the results of which are shown in Table 7.8. The largest residual, or non-tidal current¹⁰, recorded was 0.86m (both positive and negative). Residual water levels show a seasonal increase over the winter months, often fluctuating over a period of, approximately, 24 hours, which have been interpreted as indicative of coastally trapped waves passing the site (Fugro, 2023).

Table 7.7 Tidal water level descriptors relative to MSL (m) at three locations around the array area

Datum	Description	West	Central	East
MSR	Mean Spring Range	4.14	3.62	3.28
MNR	Mean Neap Range	2.00	1.76	1.58
HAT	Highest Astronomical Tide	2.61	2.33	2.15
MHWS	Mean High Water Springs	2.07	1.81	1.64
MHW	Mean High Water	1.65	1.45	1.32
MHWN	Mean High Water Neaps	1.00	0.88	0.79
MSL	Mean Sea Level	0.00	0.00	0.00
MLWN	Mean Low Water Neaps	-1.00	-0.88	-0.79
MLW	Mean Low Water	-1.62	-1.43	-1.30
MLWS	Mean Low Water Springs	-2.07	-1.81	-1.64
LAT	Lowest Astronomical Tide	-2.72	-2.42	-2.22

⁹ Defined by spring tidal range: micro-tidal, tidal range <2m; meso-tidal, tidal range 2 – 4m; macro-tidal, tidal range >4m.

¹⁰ This may also be described as the departure from the predicted tidal height.

Table 7.8 Tidal height harmonic analysis results at the SWLB (location identified on Figure 7.1), relative to LAT¹¹ (m)

Parameter	Description	Value (Heights Relative to LAT)
MSR	Mean Spring Range	3.50
MNR	Mean Neap Range	1.70
HAT	Highest Astronomical Tide	4.94
MHWS	Mean High Water Springs	4.28
MHWN	Mean High Water Neaps	3.38
MSL	Mean Sea Level	2.53
MLWN	Mean Low Water Neaps	1.68
MLWS	Mean Low Water Springs	0.78
LAT	Lowest Astronomical Tide	0.00

32. Data recorded at the SWLB (see Figure 7.1) between April 2022 and April 2023 recorded mean depth-averaged tidal current speeds of 0.83m/s and 0.41m/s for springs and neap, respectively. The maximum depth-averaged tidal current expected to occur at this location is 1.28m/s during springs, with near-surface total current velocities of up to 1.42m/s observed.
33. Surface and near-bed (1m above bed) current flows have been modelled at three locations across the array area (as shown in Figure 7.1; MetOceanWorks, 2021a). In the centre of the array area, annual mean and 1 in 50-year return period surface current speeds are 0.53m/s and 1.49m/s, respectively, with current speeds showing a generally increasing trend from northeast to southwest. Mean spring peak near-surface currents between 0.50m/s and 0.75m/s have generally been identified as corresponding the presence of sandwaves by Belderson *et al.* (1982). A similar pattern is found in near-bed current speeds, with mean and 1 in 50-year return period speeds of 0.34m/s and 0.95m/s, respectively. (MetOceanWorks, 2021b). A frequency analysis of this data, shown in Plate 7.3, shows that:
- Both surface and near-bed currents flow primarily towards the southeast (21.8%) and northwest (20.3%), with currents flowing towards the northwest being slightly faster;
 - At both depths, there is a smaller current component flowing towards the north-northwest (17.5%) and south-southeast (16.7%). These current speeds are both generally faster than the main current component, with the fastest currents flowing towards the north-northwest; and
 - Current speeds decrease towards the seabed due to frictional drag effects enforced by the seabed.

¹¹ LAT has been identified as being 2.45m below MSL across the Array Area (Enviros, 2022).

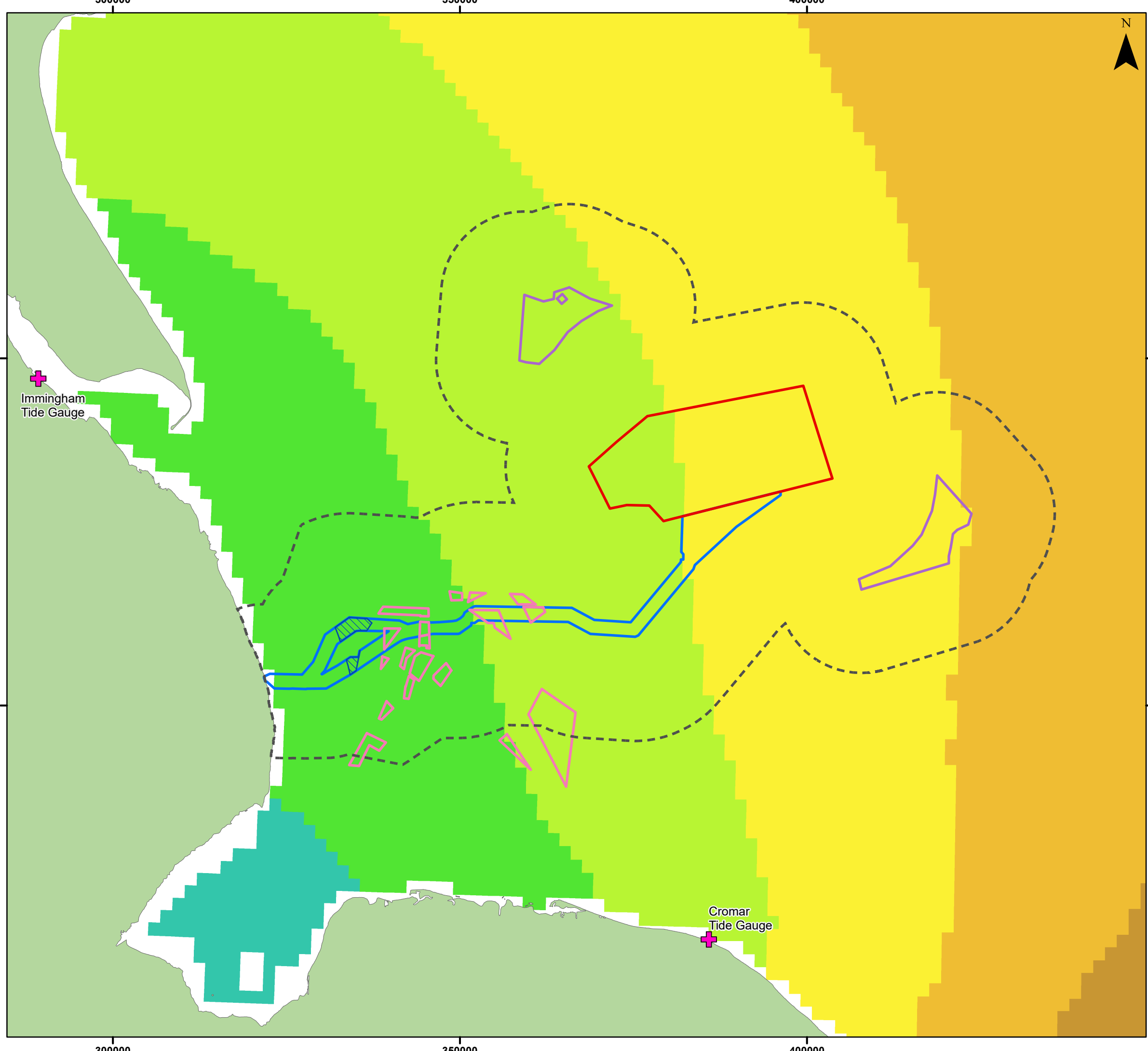
34. Modelled current speeds at other locations within the array area show a similar, if not identical pattern. At the eastern model point (shown on Figure 7.1), the main current component is more dominant, with 29.9% towards to the southeast and 27.4% towards the northwest, and currents towards the south-southeast and north-northwest only 12.2% and 11.8% respectively (MetOceanWorks, 2021c). In contrast, currents at the western model point primarily flow towards the south-southeast (21.2%) and north-northwest (22.2%), with the northwest and southeast components being smaller (MetOceanWorks, 2021d).

Offshore Export Cable Corridor

35. In the eastern half of the ECC, tidal flows are generally oriented to the southeast on the flood tide and northwest on the ebb tide, as in the array area. Closer inshore flows become oriented north to south, with the Inner Silver Pit approximately marking a transition (ABPmer *et al.*, 2008; TKOWFL, 2015; Figure 7.4). Here, tidal flows are oriented towards the south on the flood tide and north on the ebb (TKOWFL, 2015). In close proximity to the coast, tidal flows are oriented closer to the orientation of the coastline (ABPmer *et al.*, 2008; Figure 7.4).
36. Modelled maximum depth-averaged spring tidal current speeds generally increase from east to west along the export cable, from around 1.2m/s to 1.3m/s close to the array area to over 1.4m/s south of Inner Silver Pit before reducing slightly close to the shore, as shown on Figure 7.4. Faster current speeds occur where deeper water channels are present, for example on the flanks of the Outer Dowsing Channel and Sole Pit, where speeds reach over 1.4m/s. This is supported by the literature, with hydrodynamic modelling for the Inner Silver Pit by Pingree and Griffiths (1979) suggesting that current velocities are increased within bathymetric deeps (HADA, 2012a). More benign current speeds, of the order of 0.6m/s to 1.0m/s occur within the northern extents of the Inner Silver Pit, in particular where it is oriented from the northeast to the southwest (Figure 7.4).

Coast

37. The Lincolnshire coast is a macro-tidal environment, with tidal currents generally following the orientation of the coastline with a flood tide to the south and an ebb tide to the north (Environment Agency, 2013b). The mean spring and neap tidal ranges adjacent to the Triton Knoll Landfall area approximately 500m north of the Project Landfall are 5.8m and 2.9m, respectively, and at Skegness the mean spring and neap ranges are 6.1m and 3.0m, respectively (HADA, 2012a; TKOWFL, 2014; Figure 7.3). Peak flow speeds are found to be more than 0.8m/s generally, exceeding 1.0m/s in places (TKOWFL, 2015).



Legend

- Array Area
- Offshore Export Cable Corridor
- ORCP Area
- Artificial Nesting Structure Area
- Biogenic Reef Restoration Area
- Physical Processes Zone of Influence
- + Tide Gauge Location

Mean Spring Tidal Range (m)

- 1.01 - 2
- 2.01 - 3
- 3.01 - 4
- 4.01 - 5
- 5.01 - 6
- 6.01 - 7

Coordinate System: WGS 1984 UTM Zone 31N

0 10 20 km

Scale: 1:525,000

A3 Page Size

Environmental Statement

Mean Spring Tidal Range
(ABPmer *et al.*, 2008)

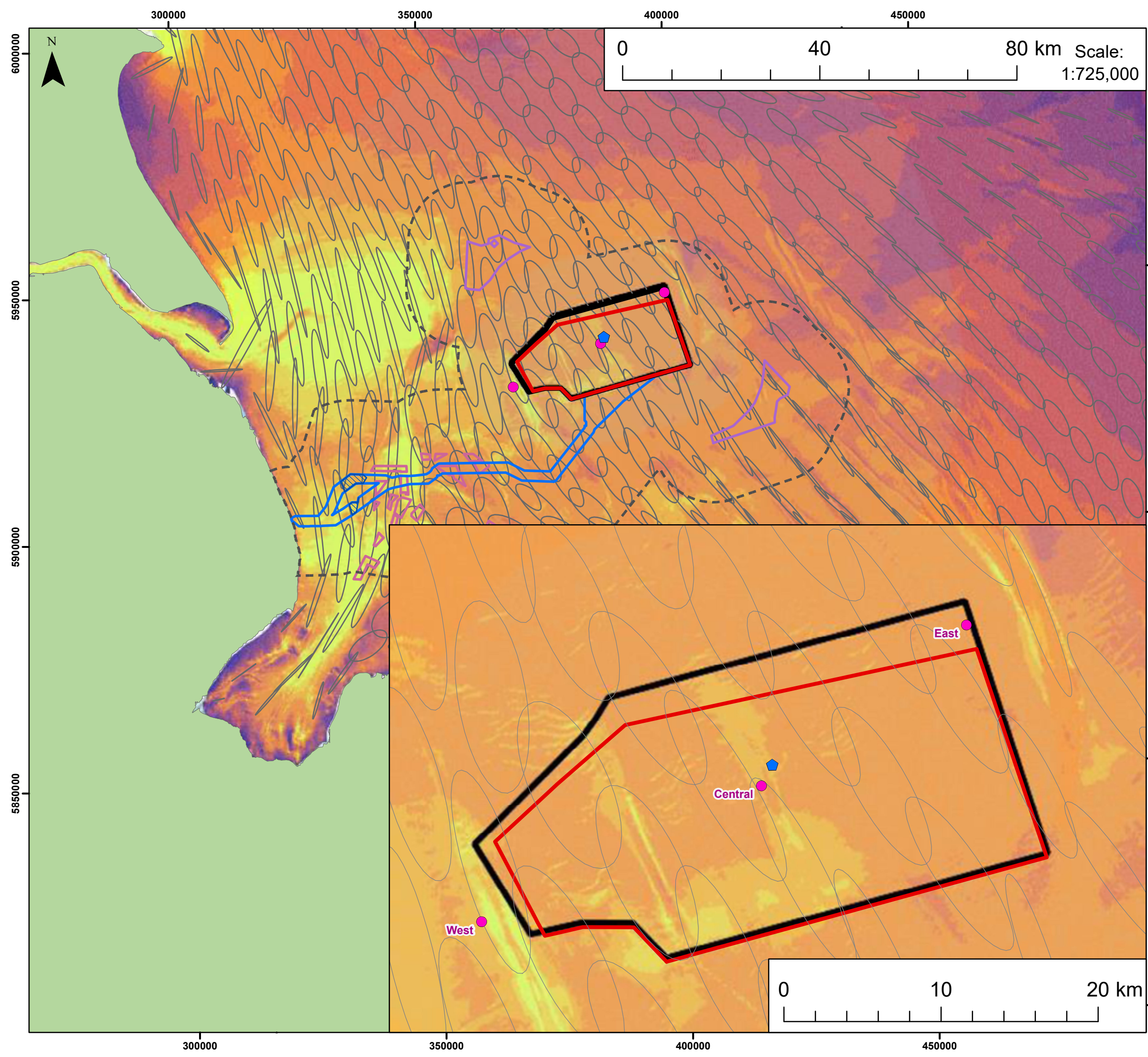
Figure 7.3




Date: 16/02/2024
Produced By: BPHB
Revision: 0.1

Contains ESRI Basemapping;
EMDOnet 2020 bathymetry

Document Path: Z:\GIS\GIS - Projects\0152 Outer Dowsing ELA\GIS\Figures\ES\Physical Processes Technical Report\DOOW_0152_PPTR_Fig7.3_Mean_Spring_Tidal_Range.mxd



Legend

- Array Area
- AfL Array Area
- Offshore Export Cable Corridor
- ORCP Area
- Artificial Nesting Structure Area
- Biogenic Reef Restoration Area
- Physical Processes Zone of Influence
- Metocean Model Data Points
- ◆ Lidar Buoy SWLB059
- Spring Tidal Ellipses

<p>Depth-averaged Current Speed (m/s)</p> <ul style="list-style-type: none"> < 0.1 0.1 - 0.2 0.2 - 0.3 0.3 - 0.4 0.4 - 0.5 0.5 - 0.6 0.6 - 0.7 0.7 - 0.8 0.8 - 0.9 0.9 - 1 1 - 1.2 1.2 - 1.3 1.3 - 1.4 > 1.4 	<p>5900595 5900590 5900585 5900580</p>
--	--

Coordinate System: WGS 1984 UTM Zone 31N

A3 Page Size

Environmental Statement

Maximum Modelled Depth-Averaged Spring Tidal Current Speeds and Spring Tidal Ellipses (MetOceanWorks, 2021)

Figure 7.4




Date: 28/02/2024
Produced By: BPHB
Revision: 0.1

Contains ESRI Basemapping; EMDOnet Geology 2016

Document Path: Z:\GIS\GIS - Projects\0152 Outer Dowsing EIA\GIS\Figures\ES\Physical Processes Technical Report\ODOW_0152_PPT_R_Fig7.4_Depth_MetOceanWorks.mxd

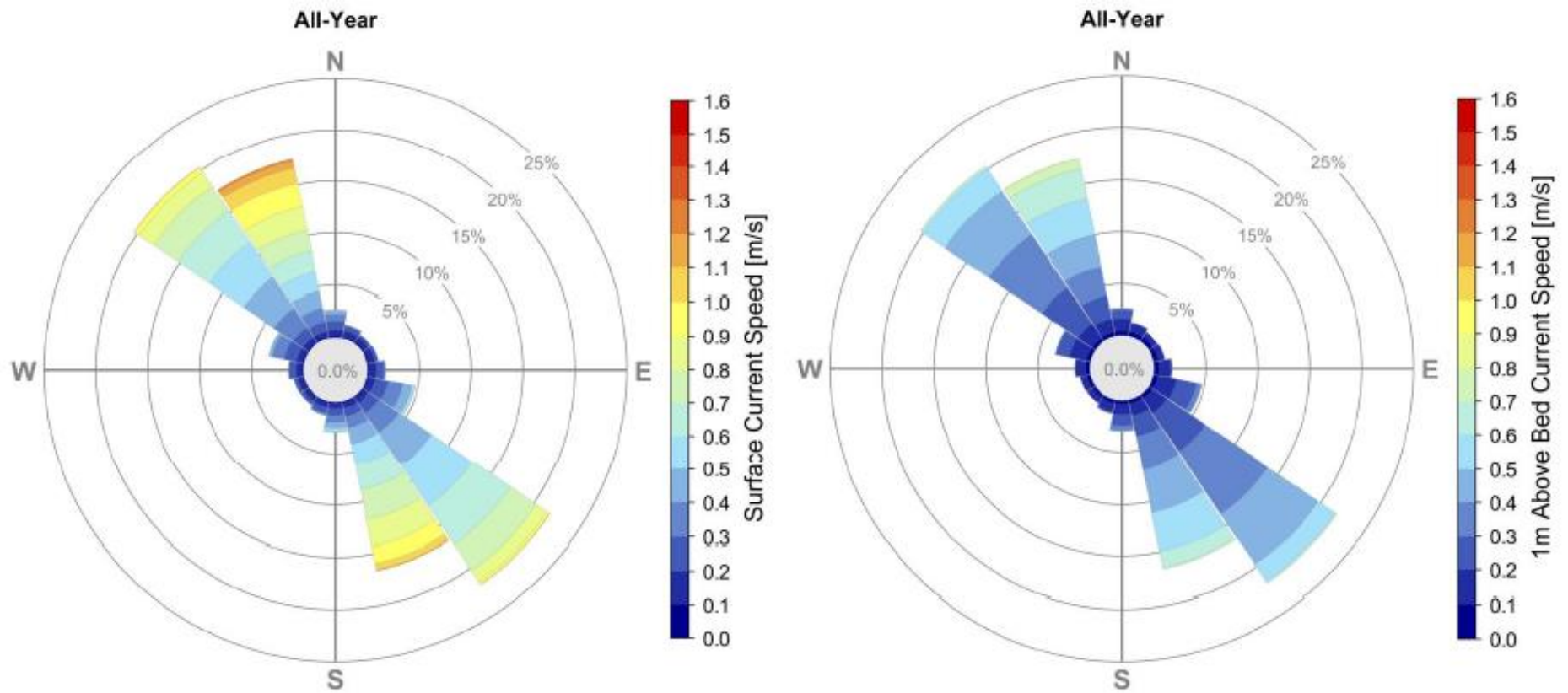


Plate 7.3 Annual rose plot of modelled surface and near bed current speed and direction in the centre of the array area (MetOceanWorks, 2021b)

Compensation Areas

38. Modelled mean tidal ranges for the northern ANS areas are, approximately, 4.1m and 2.1m for spring and neap, respectively. Tidal flows are generally oriented to the south-southeast on the flood tide and north-northwest on the ebb. For the southern ANS area modelled mean tidal ranges are of the order of 3.1m and 1.6m for spring and neap, respectively, with tidal flows oriented southeast to southwest (ABPmer *et al.*, 2008). Modelled maximum depth-averaged spring tidal current speeds are generally between 1.0m/s and 1.2m/s, as indicated in Figure 7.4. Within the biogenic reef creation area, mean spring tidal ranges increase from, approximately, 4.0m in the east to up to 5.7m close to the coast (ABPmer *et al.*, 2008). Current speeds are generally faster and more complex than further offshore, as characterised in paragraph 35.

7.4.1.3 Non-tidal

39. Superimposed upon regular tidal behaviour are various non-tidal influences, which mainly originate from meteorological effects. An example is surges, formed by rapid changes in atmospheric pressure causing the water levels to fluctuate considerably above or below the tidal level. The geometry and location of the North Sea Basin makes it particularly susceptible to large surge events (Flather and Williams, 2000; Environment Agency, 2011).

40. Storm surges in this region are usually external surges, generated by pressure gradients travelling from the deep Atlantic waters onto the shallow continental shelf by strong winds to the north causing an increase in tidal levels. As the resultant water movements propagate into the North Sea they are affected by the Earth's rotation and rapidly decreasing depth causing a storm surge (HADA, 2012a). A notable major storm surge in the region occurred in December 2013, with water levels reaching between 5.0m and 5.5m (Ordnance Datum Newlyn (ODN)¹²) at the Lincolnshire coast (Spencer *et al.*, 2015).

Offshore Array

41. Modelled extreme water levels for the centre of the array area are shown in Table 7.9 (with the location of the modelled point shown in Figure 7.1 and outlined in Table 7.2).

Table 7.9 Extreme water levels in the centre of the array area (MetOceanWorks, 2021b)

Return Period (Years)	Positive Surge (m)	Wave Crest height (m)	Extreme Total Water Level (ETWL) Relative to MSL (m)
1	1.09	6.23	7.68
5	1.41	7.83	9.53
10	1.55	8.62	10.43
50	1.88	10.55	12.64
100	2.01	11.40	13.61
500 ¹³	2.01	14.99	17.16

¹² 0.0m ODN approximates to mean sea level.

¹³ 100-year return period surge used (in the ISO 19902 equation) for return periods of 100 years and greater.

Offshore Export Cable Corridor

42. When surge currents are superimposed on astronomical tidal currents, they can combine to enforce short-term controls on the sediment regime. This is most pronounced in the shallow nearshore environment. In this region peak surge currents are in the range of 0.6m/s to 0.8m/s for a 1 in 50-year surge events, with currents directed towards the east (HR Wallingford *et al.*, 2002; TKOWFL, 2014).

Coast

43. As well as influencing sediment transport, storm surges can result in increased coastal erosion. The Environment Agency has produced a national dataset of “design sea levels” based on analysis of tide gauge data which incorporates the effect of surges. Extreme sea levels at Immingham, within the Humber Estuary, have been calculated as 4.17m, 4.53m, and 4.93m for return periods of 1, 10, and 100 years, respectively, although this will be amplified by the estuary’s morphology. The closest tide gauge to the south of the Landfall site is located at Cromer, on the North Norfolk coast (shown on Figure 7.3), where extreme sea levels have been calculated as 3.07m, 3.48m, 3.93m for 1, 10, and 100-year return periods, respectively (Environment Agency, 2018).

Compensation Areas

44. Modelled extreme water levels resulting from storm surges in the ANS areas are likely to be analogous to those modelled for the array area, provided in paragraph 41. Surge currents within the biogenic reef creation area are likely to be generally similar to those characterised in paragraph 42 and 43.

7.4.1.4 Frontal Systems and Stratification

45. Frontal zones mark boundaries between water masses, including tidally mixed and stratified areas, and are numerous on the European continental shelf (DECC, 2016). The Flamborough Front is a seasonal tidal mixing front which marks the transition between the well-mixed southern North Sea and stratified northern North Sea water bodies (Figure 7.5). This seasonal feature develops during summer months, approximately, 10km offshore from Flamborough Head and generally follows the 50m isobath (Hill *et al.*, 1993). This feature is located, approximately, 24km north of the array area, as shown on Figure 7.5, and is therefore outside the ZoI for the Project.

7.4.2 Seabed

7.4.2.1 Geology

46. As shown in Figure 7.6, the bedrock geology across the west of the study area is composed of Upper Cretaceous fine-grained limestones of the Chalk Group, with Late Triassic to Late Jurassic limestone, mudstones, and sandstones in the east. These include the Lias, West Sole and Humber groups (BGS, 1995; HADA, 2012a). Bedrock exposures are present within bathymetric deeps including the Sole Pit and Inner Silver Pit, outlined further in subsequent sections (Tappin *et al.*, 2011; Cathie, 2021).

47. The bedrock geology is overlain by Quaternary sediments, including both early Pleistocene deltaic sediments as well as later Pleistocene sediments deposited during alternating glacial and interglacial conditions. Of the deltaic sediments, only the Winterton Shoal and Yarmouth Roads formation are exposed at seabed, mainly along the flanks of deep channels such as the Sole Pit (as shown on Figure 7.7). Later glacial and interglacial deposits include (in order of decreasing age): the Swarte Bank, Egmond Ground and Sand Hole, Bolders Bank and Botney Cut formations, shown on Figure 7.7. The Bolders Bank Formation, a glacial till (clay, sand and gravel debris deposited from ice sheets), is present throughout the majority of the study area and is exposed at the seabed in the Inner Silver Pit.
48. These deposits are overlain by a generally thin veneer of Holocene marine sediments. This layer rarely exceeds 5m, except for areas with tidal sandbanks and large sandwaves (Tappin *et al.*, 2011). In areas overlying the Bolders Bank Formation this layer is generally less than 1 to 2m thick (Cathie, 2021). The Quaternary sediment thickness varies throughout the study area between <5m to more than 50m, with the greatest thicknesses observed to the east of the array area and on either side of the Inner Silver Pit (shown on Figure 7.8).

Offshore Array

49. The western half of the Project array area is underlain by Cretaceous Chalk, with Lias, West Sole and Humber groups present in the east (Figure 7.6). The depth of sediment cover overlying the bedrock is spatially variable, with BGS datasets suggesting Quaternary sediment thicknesses generally between 5m to 20m in the western part of the array area and increasing towards the east, with the thickest deposits, between 30 and 50m, in the middle of the array area and on the eastern edge (Figure 7.8; Cathie, 2021). The chalk bedrock to the west of the array area will therefore be located approximately between 5m and 30m below the seabed (BGS, 2022). Possible chalk layers were interpreted on Project-specific geophysical data as occurring between approximately 5m and 35m below the seabed, although limited penetration on the seismic data within the western part of the array area does not allow for a more comprehensive characterisation (Enviros, 2022).
50. These Quaternary sediments comprise Pleistocene deposits as well as a layer of Holocene marine sediments. A desk-based study by Cathie (2021) concluded that Holocene sediment cover, Bolders Bank Formation, and Swarte Bank Formations are expected within the top 100m below seabed of the array area (Figure 7.7). The Bolders Bank Formation is described as firm to stiff, slightly gravelly clay with pockets of sand and gravel, occasional sandy horizons and some boulders (TKOWFL, 2014; Cathie, 2021). Due to the firm to stiff clay content, the widespread presence of Bolders Bank Formation under Holocene sediments could limit the development of deeper scour (> 5m) (Orsted, 2021). The Swarte Bank Formation is a valley infill deposit composed of chalky till, glacio-lacustrine mud and marine clay, and marine interglacial sediments (Tappin *et al.*, 2011).

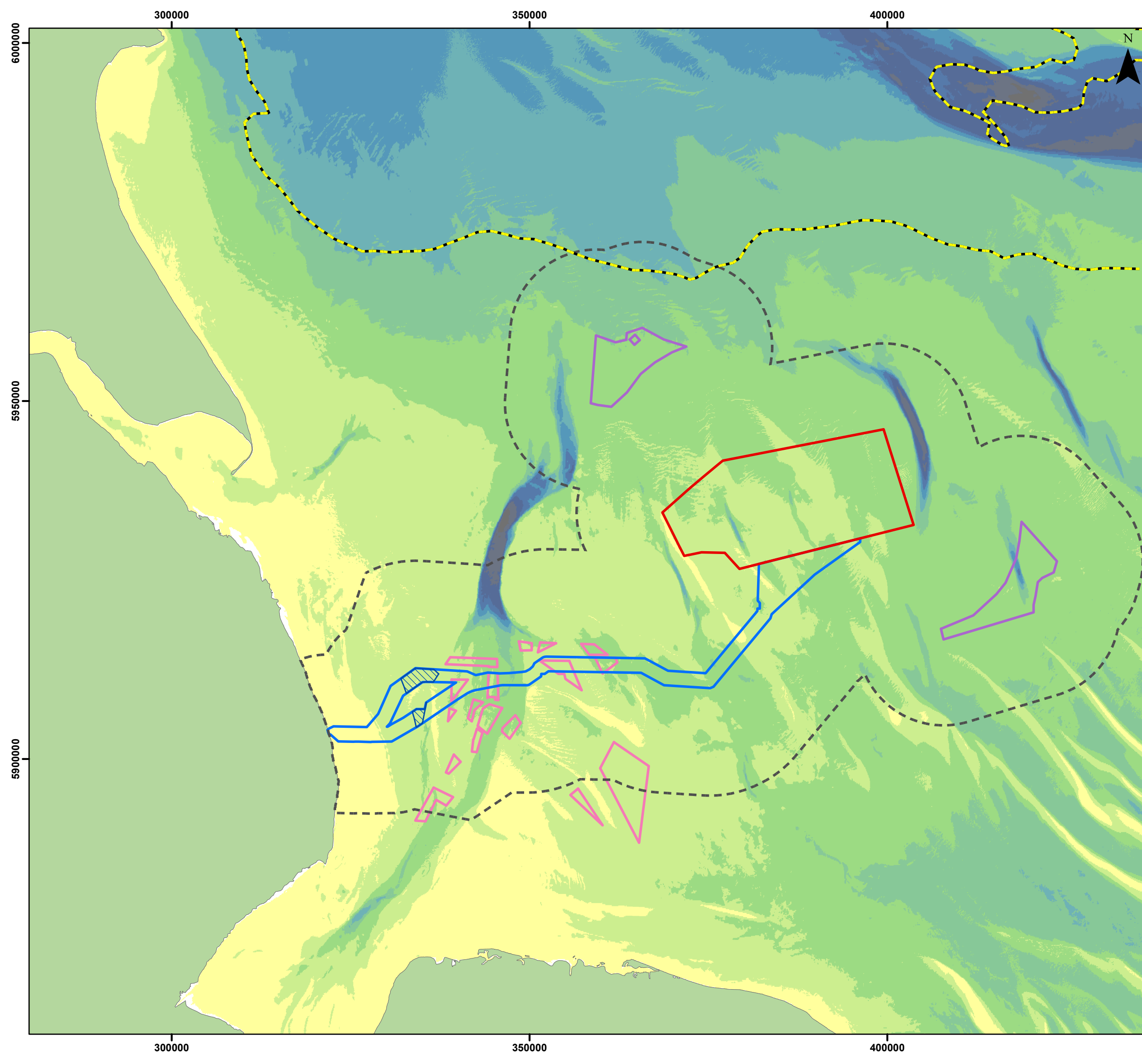
Offshore Export Cable Corridor

51. The Offshore ECC is characterised mainly by Pleistocene deposits present above Cretaceous Chalk bedrock, overlain in turn by a veneer of Holocene sediments of variable thickness. As outlined above, Pleistocene deposits across the area include a complex sequence of Egmond Ground and Swarte Bank formations, extensively incised by channelling and infilling with Botney Cut Formations and overlain in much of the region by Bolders Bank Formation (Tappin *et al.*, 2011; Equinor, 2022). The thicknesses of these, as well as the overlying Holocene sediments, vary across the ECC, and a combination of geophysical investigations have been used to characterise specific areas (EMU and Osiris, 2008; Centrica, 2009; Tappin *et al.*, 2011; TKOWFL, 2011; Dove *et al.*, 2017; Equinor, 2022). These datasets corroborate the evidence collected from Project-specific geophysical investigations carried out along the Offshore ECC (GEOxyz, 2022c).
52. Seismic stratigraphy information is presented in Dove *et al.* (2017) of a profile extending south from just west of the Project array area, crossing the offshore ECC approximately one third of the way west along its length. At the approximate location of the offshore ECC, the seabed geology comprises of thick Holocene sediments of over 10m in some areas, representing a local sandbank feature, underlain by a combination of Bolders Bank, Sand Hole, and Egmond Ground formations approximately 15m to 20m thick (Dove *et al.*, 2017). Assuming a cable burial depth of up to 5m, the offshore ECC at this point along the route would be located primarily in mixed Holocene sands and gravels.
53. Geotechnical investigations at the Race Bank OWF array area, combined with BGS information, were interpreted as a sequence of surficial sands overlying the Bolders Bank Formation, which in turn overlies a layer of mixed Egmond Ground and Swarte Bank deposits. The superficial Holocene sands range in thickness, with a maximum of 18m within the Race Bank feature. However, in the far northwest of the Race Bank array area, which is closest to the Project Offshore ECC, there is no layer of superficial sands, with the Bolders Bank Formation extending approximately 10m to 15m below the seabed (EMU and Osiris, 2008). This supports regional-scale information from Tappin *et al.* (2011), which identifies a generally thin veneer of Holocene sediments apart from areas with large sandbank and sandwave features. This suggests that areas of the offshore ECC will have a very thin or non-existent Holocene sediment layer, particularly across areas of flat bathymetry. A full consideration of cable installation and protection options is provided in document reference 6.1.3 with impacts on Marine Process receptors assessed in document reference 6.1.7.
54. Further west, to the south of the Inner Silver Pit, the Quaternary sediment thickness is generally less than 5m, as shown in Figure 7.8. Chalk bedrock, as well as Bolders Bank till, is exposed in the Inner Silver Pit and its associated glacial outwash feature to the south, shown in Figure 7.9. These outcrops either have no surficial sediment cover or it is thin (less than one metre) (Tappin *et al.*, 2011). Upper chalk units recovered in geotechnical investigations carried out for the Triton Knoll ECC, to the north of the Project ECC, were almost all classified as either weak or very weak and of low to medium density (TKOWFL, 2011).

55. This characterisation corroborates that from Project-specific geophysical investigations, which identified relatively compacted Late Cretaceous bedrock overlain by a Quaternary succession of Pleistocene and Holocene sediments, with a number of mobile sand units interpreted as Upper Holocene. The Holocene sand deposits are seen throughout the length of the Offshore ECC, and range in size from sand ripples to major sandbanks. A prominent high-amplitude reflector can be seen on the SBP data, which is thought to represent a glacial unconformity, separating more compacted Late Cretaceous chalk bedrock from overlying Quaternary sediments. The depth of this unconformity (therefore representing the depth of chalk bedrock) is found at a maximum of, approximately, 20m below the seabed along the Offshore ECC, and is very shallow further west, outcropping to the south of Inner Silver Pit as inferred from lacking reflectors on the SBP data (GEOxyz. 2022c).

Coast

56. The onshore bedrock geology is composed of Burnham Chalk, overlain by marine sand deposits. Historical boreholes (1994) from the intertidal area at the Landfall site contain medium density, slightly silty sandy gravel and silty, fine sandy clay shallow marine deposits to a depth of approximately 9m. Beyond this depth, sand and gravel with stiffer clay and chalk begin to occur with occasional boulders, with no evidence of bedrock within the first 12m (BGS, 2022).



- Legend**
- Array Area
 - Offshore Export Cable Corridor
 - ORCP Area
 - Artificial Nesting Structure Area
 - Biogenic Reef Restoration Area
 - Physical Processes Zone of Influence
 - Location of Flamborough Front - July 2018

- Depth (m)**
- 0 - 10
 - 10 - 20
 - 20 - 30
 - 30 - 40
 - 40 - 50
 - 50 - 60
 - 60 - 70
 - 70 - 80
 - 80 - 90
 - 90 - 100

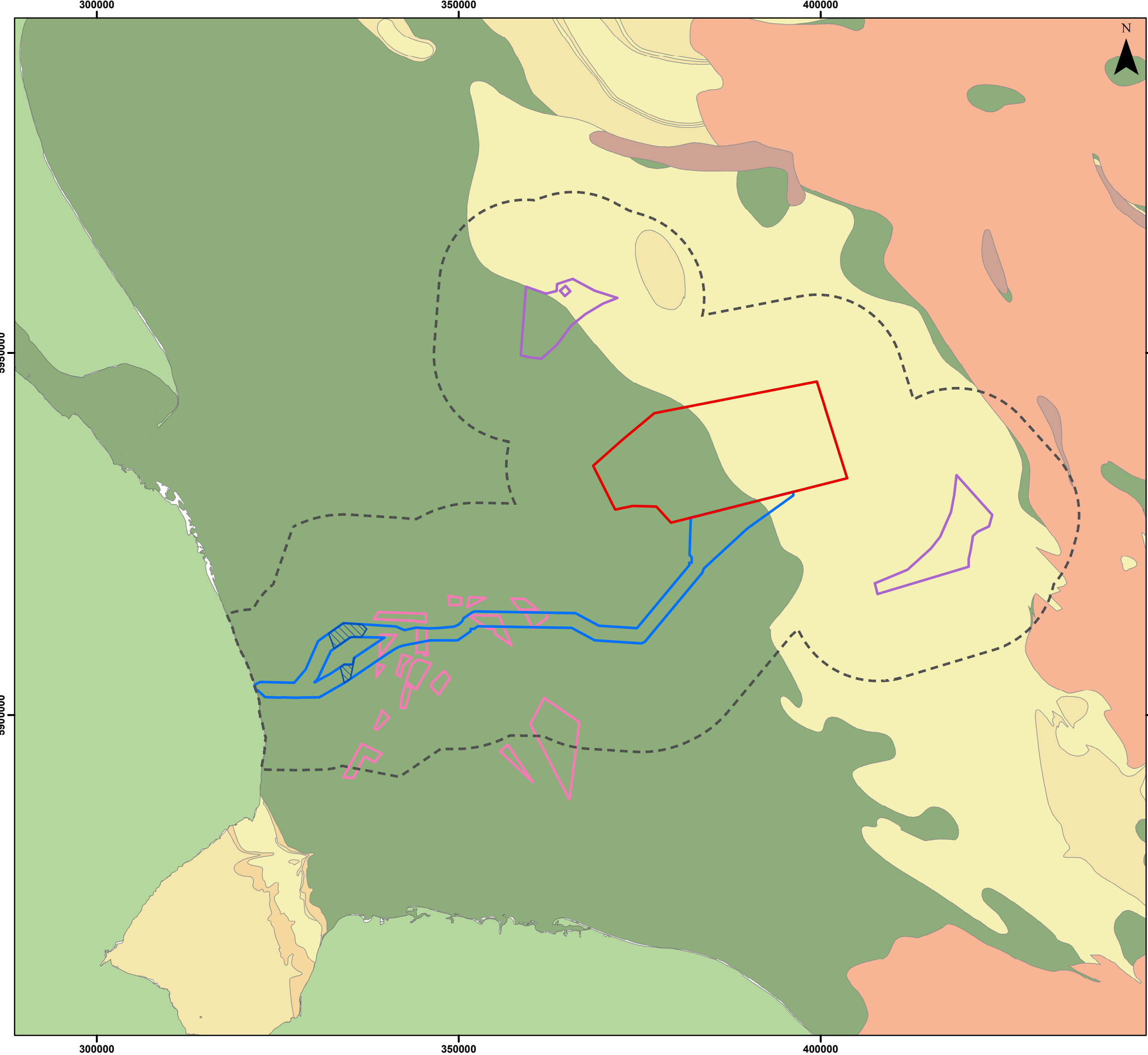


Coordinate System: WGS 1984 UTM Zone 31N
 0 10 20 km
 Scale: 1:500,000 A3 Page Size

Environmental Statement
 Flamborough Front Location
 Figure 7.5



Document Path: Z:\GIS\GIS - Projects\0152 Outer Dowsing EIA\GIS\Figures\ES\Physical Processes Technical Report\ODOW_0152_PPTR_Fig7.5_Flamborough_Front.mxd



Legend

- Array Area
- Offshore Export Cable Corridor
- ORCP Area
- Artificial Nesting Structure Area
- Biogenic Reef Restoration Area
- Physical Processes Zone of Influence

Bedrock Summary Lithologies (BGS)

- Chalk
- Mesozoic interbedded
- Mesozoic mudstones
- Mesozoic sandstones and limestones
- Palaeozoic sedimentary
- Tertiary interbedded



Coordinate System: WGS 1984 UTM Zone 31N

0 10 20 km

Scale: 1:500,000

A3 Page Size

Environmental Statement

Bedrock Lithology

Figure 7.6



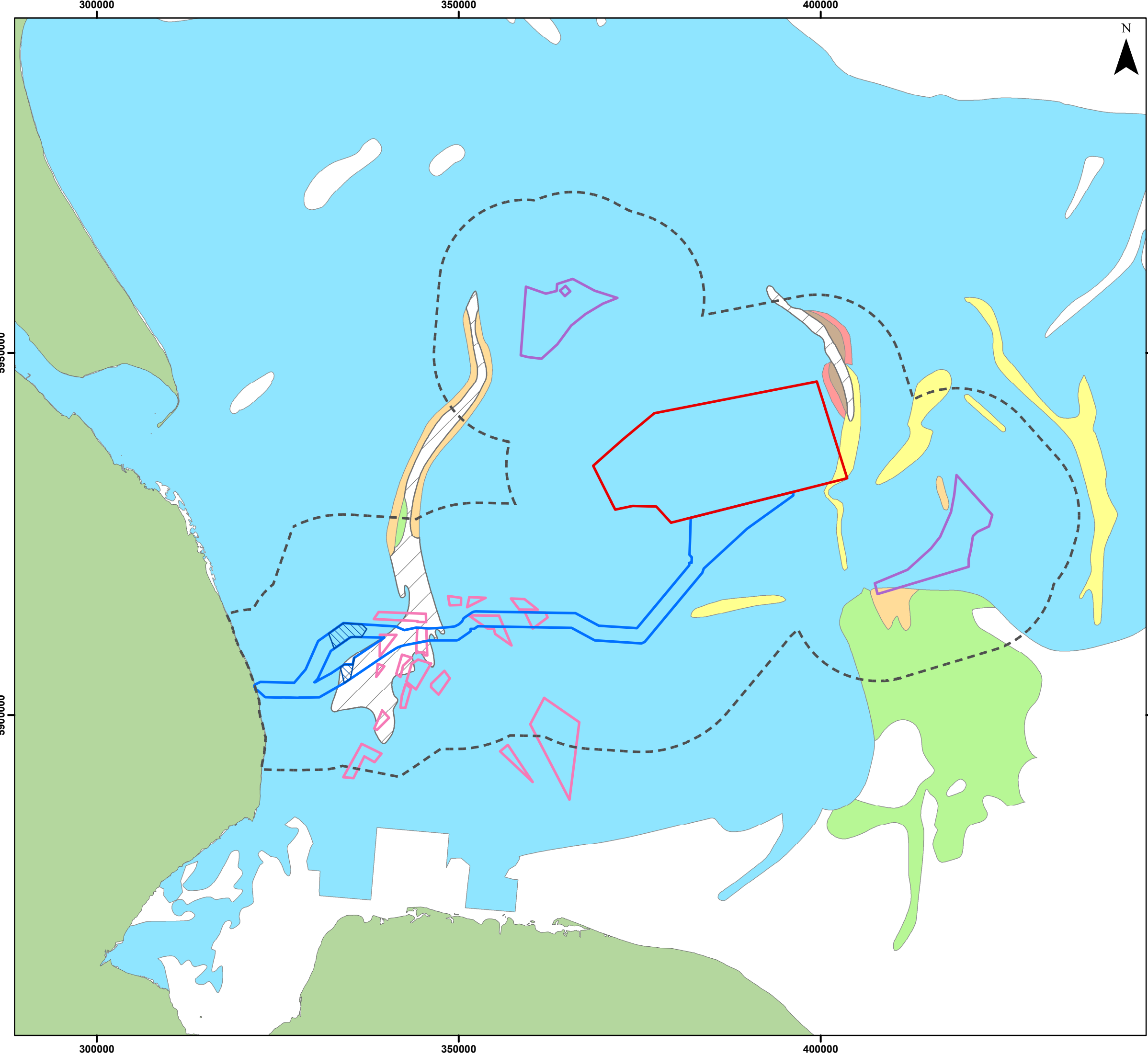
OUTER DOWSING
OFFSHORE WIND



Date: 16/02/2024
Produced By: BPHB
Revision: 0.1

Contains ESRI Basemapping;
EMDOnet 2020 bathymetry

Document Path: Z:\GIS\GIS - Projects\0152 Outer Dowsing EIA\GIS\Figures\ES\Physical Processes Technical Report\ODOW_0152_PPTR_Fig7.6_Bedrock_Lithology.mxd



Legend

- Array Area
- Offshore Export Cable Corridor
- ORCP Area
- Artificial Nesting Structure Area
- Physical Processes Zone of Influence

Quaternary Deposits Summary Lithologies (BGS)

- Botney Cut Formation
- Bolders Bank Formation
- Egmond Ground and Sand Hole Formations
- Swarte Bank Formation
- Yarmouth Roads Formation (Deltaic)
- Winterton Shoal Formation (Deltaic)
- Undivided Mesozoic

Quaternary Geology (Cameron *et al.*, 1986; Tappin, 1991)



Coordinate System: WGS 1984 UTM Zone 31N

0 10 20 km

Scale: 1:500,000

A3 Page Size

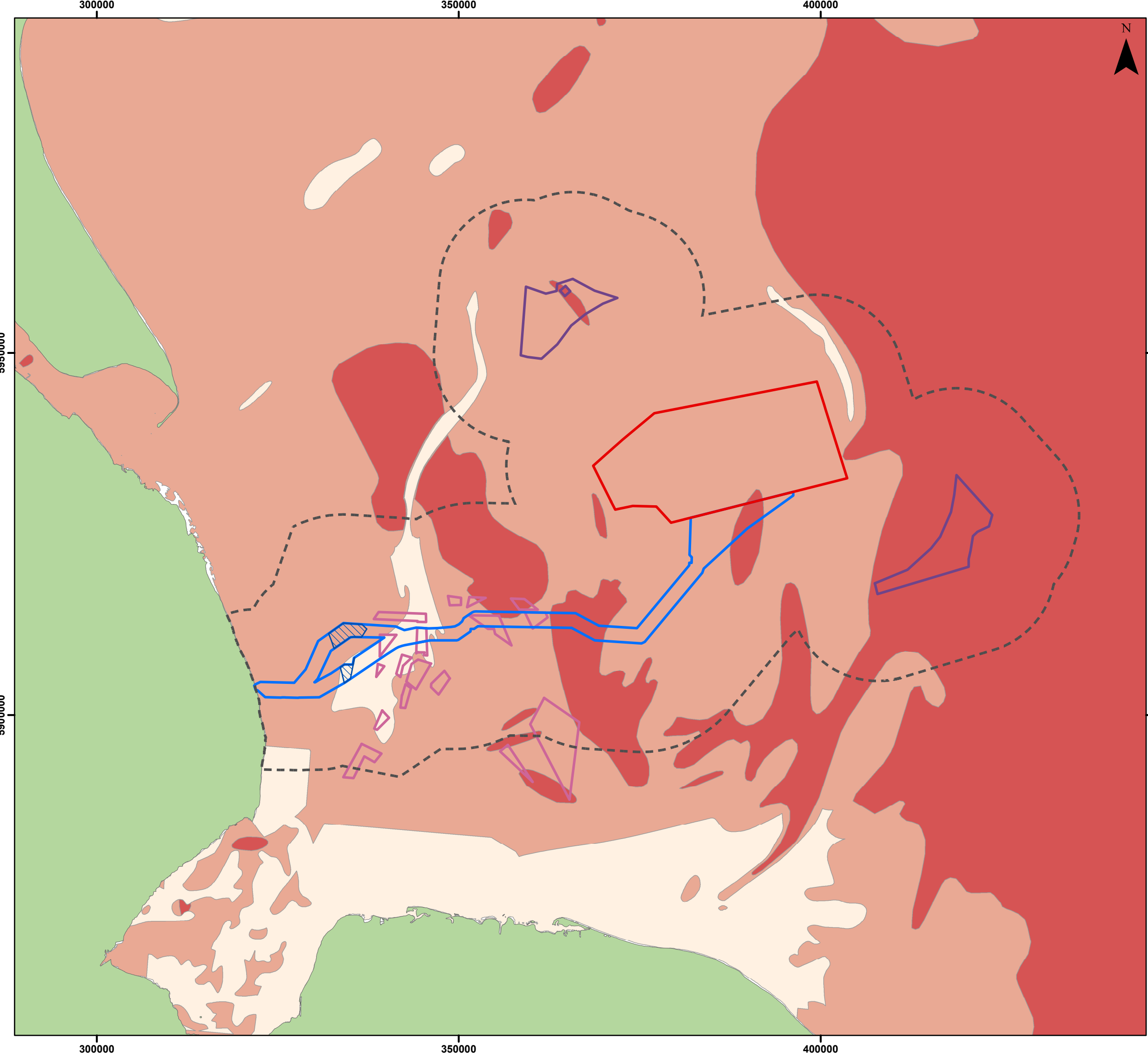
Environmental Statement

Quaternary Lithology Summary

Figure 7.7



Document Path: Z:\GIS\GIS - Projects\0152 Outer Dowsing ELA\GIS\Figures\ES\Physical Processes Technical Report\ODOW_0152_PPTTR_Fig7.7 Quaternary Lithology Summary.mxd

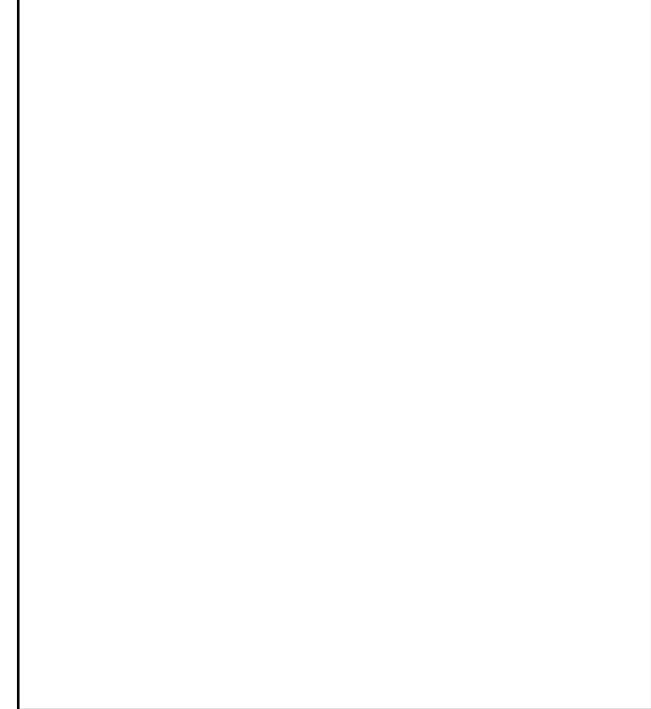


Legend

- Array Area
- Offshore Export Cable Corridor
- ORCP Area
- Artificial Nesting Structure Area
- Biogenic Reef Restoration Area
- Physical Processes Zone of Influence

Quaternary Deposit Thickness (BGS)

- < 5m
- 5m - 50m
- > 50m



Coordinate System: WGS 1984 UTM Zone 31N

0 10 20 km

Scale: 1:500,000

A3 Page Size

Environmental Statement

Quaternary Deposit Thickness

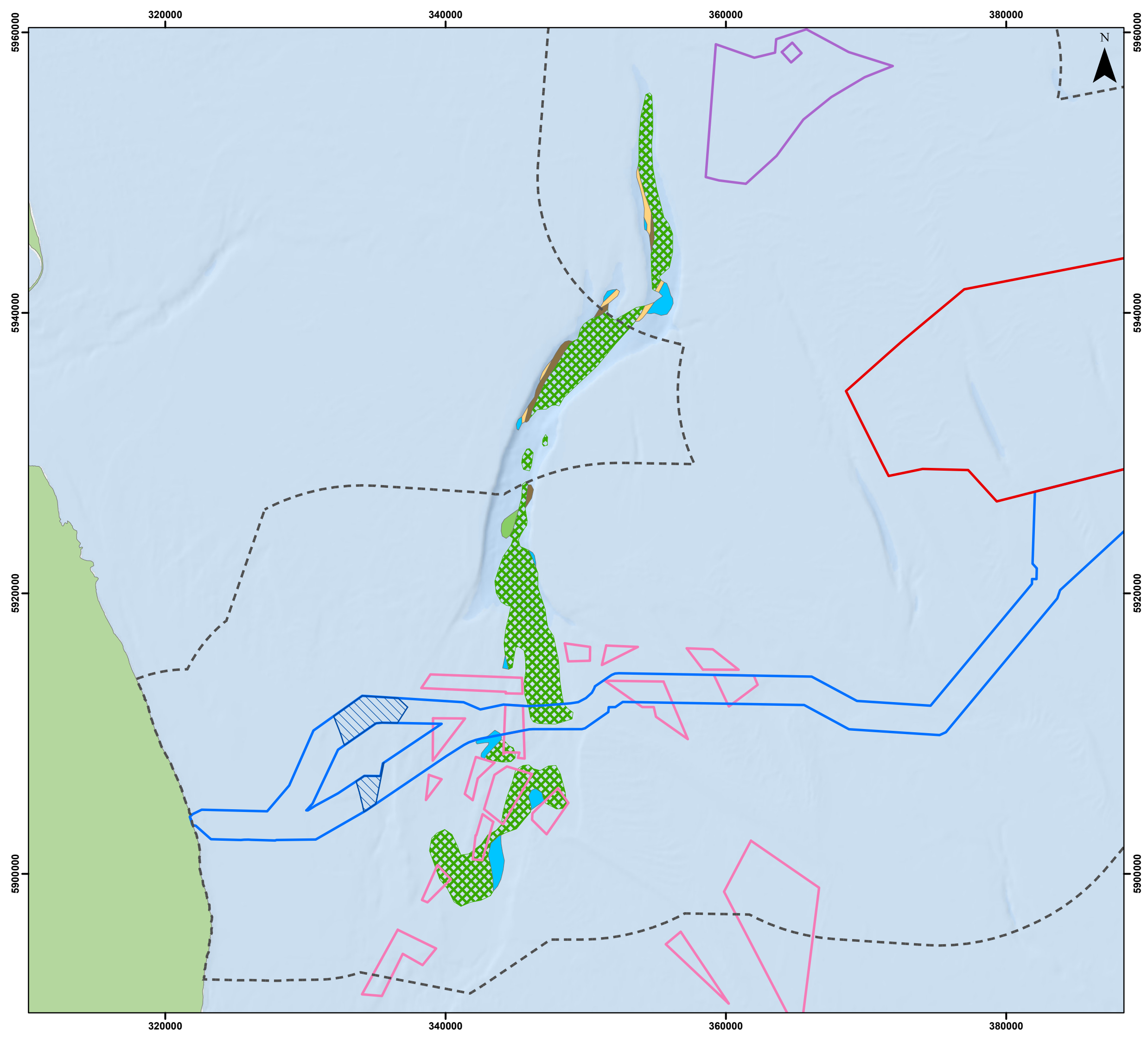
Figure 7.8



Date: 16/02/2024
 Produced By: BPHB
 Revision: 0.1

Contains ESRI Basemapping; EMDOnet 2020 bathymetry

Document Path: Z:\GIS\GIS - Projects\0152 Outer Dowsing EIA\GIS\Figures\ES\Physical Processes Technical Report\ODOW_0152_PPTR_Fig7.8_Quaternary_Deposits_Thickness.mxd



Legend

- Array Area
- Offshore Export Cable Corridor
- ORCP Area
- Artificial Nesting Structure Area
- Biogenic Reef Restoration Area
- Physical Processes Zone of Influence

Pre-Holocene Geology at/near Seabed (Tappin, 2011)

- Mesozoic - Chalk Group - Early to Late Cret.
- Quaternary - Bolders Bank Formation
- Quaternary - Egmond Ground Formation
- Quaternary - Sand Hole Formation
- Quaternary - Swarte Bank Formation



Coordinate System: WGS 1984 UTM Zone 31N
 0 5 10 km
 Scale: 1:250,000 A3 Page Size

Environmental Statement

Exposure of Pre-Holocene Geology at or Near Seabed in Inner Silver Pit and Associated Glacial Outwash Feature (Tappin *et al.*, 2011)
 Figure 7.9

Date: 16/02/2024
 Produced By: BPHB
 Revision: 0.1

Contains ESRI Basemapping; Esri, Garmin, GEBCO, NOAA NGDC, and other contributorsEMDNet 2020

Document Path: Z:\GIS\GIS - Projects\0152 Outer Dowsing EIA\GIS\Figures\ES\Physical Processes Technical Report\ODOW_0152_PPT-R_FIG7.9_Preholocene_Geology.mxd

Compensation Areas

57. The northern ANS area is located in an area of Cretaceous chalk bedrock overlain by Quaternary sediments between, approximately, 5m and 50m in thickness, which are in turn overlain by a veneer of Holocene sediments. The southern ANS area overlies Late Triassic to Late Jurassic bedrock, similar to the eastern half of the Project array area (Figure 7.6), overlain by a generally thicker (>50m) layer of Quaternary glacial and valley infill sediments (Figure 7.8). The biogenic reef creation area can be characterised using the information provided in paragraph 51 *et seq.*, with Cretaceous chalk close to the seabed surface in some areas as indicated on Figure 7.9.

7.4.2.2 Seabed

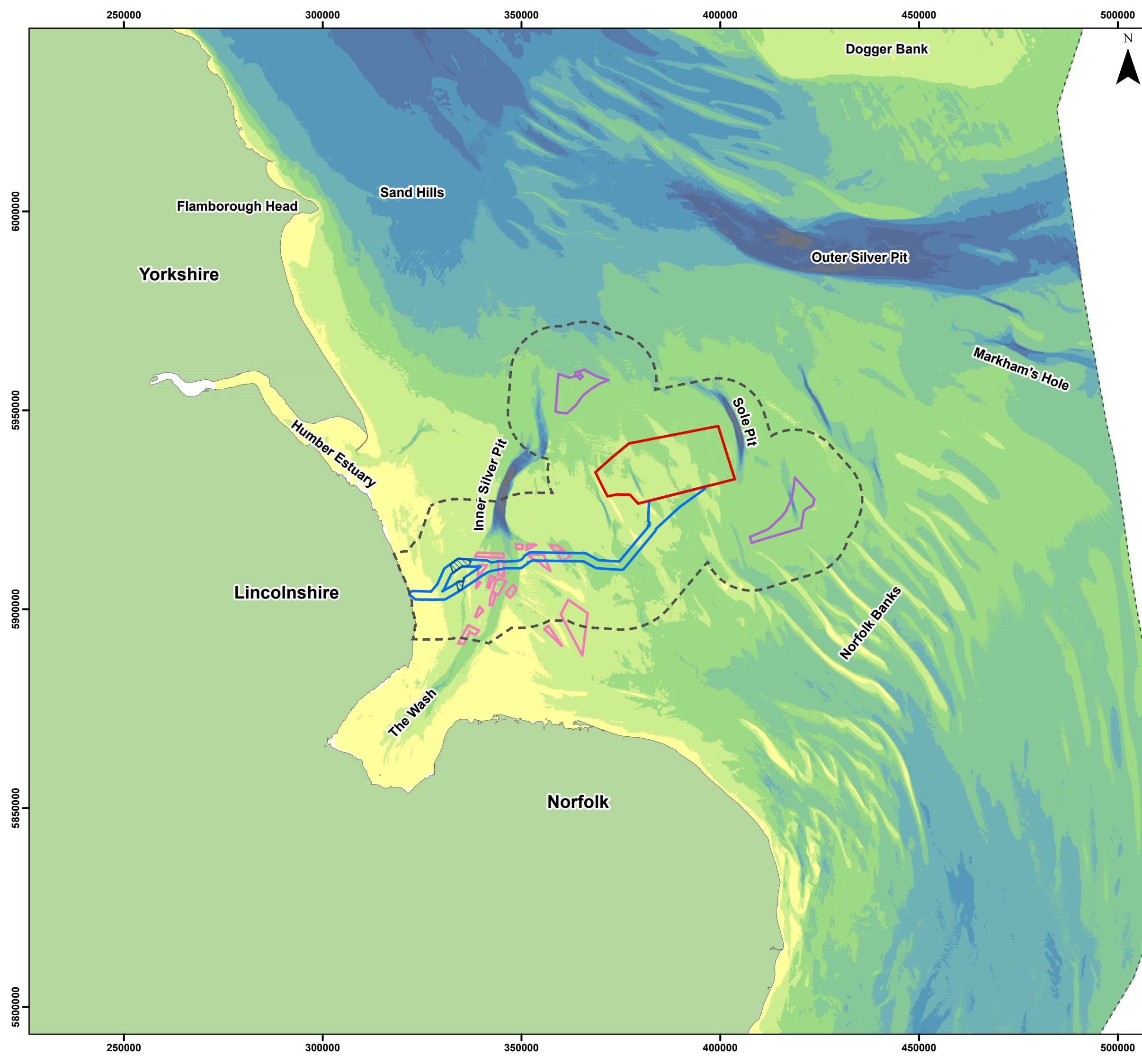
58. Water depths across the region vary widely, from 0m to 94.6m depth (Lowest Astronomical Tide (LAT)), with an average depth of 15.5m. The region is characterised by generally flat bathymetry punctuated by a number of large-scale glacial landforms (shown on Figure 7.10), for which information is provided in Paragraph 92 *et seq.*, as well as a number of large sandbanks. These features lead to the large variation in water depth across the study area (Cathie, 2021).

59. As outlined previously, Holocene sediment forms a thin veneer over Pleistocene or older deposits, rarely exceeding 5m thickness apart from in areas of sandbanks (Cameron *et al.*, 1992; Tappin *et al.* 2011). The majority of these sediments are derived from the reworking of Quaternary deposits, with limited contribution from modern fluvial sources. As shown on Figure 7.11, the region is characterised by a mix of mainly sand and gravel, with a higher proportion of sand to the east (Tappin *et al.*, 2011; BGS, 2022). The distribution of sediments is strongly influenced by the underlying geology and bathymetry, particularly the presence of landforms such as Inner Silver Pit (TKOWFL, 2014).

60. Gravel rich sediments (gravel, sandy gravel, and muddy sand gravel) dominate the western part of the study area forming large-scale bathymetric features that reflect pre-existing glacial, fluvio-glacial, fluvial and coastal processes. Elsewhere the gravel layer is mostly less than a few tens of cm thick and overlies Bolders Bank Formation till or chalk bedrock (near the coast) (HADA, 2012a). The presence of muddy sediments is typically restricted to within bathymetric deeps such as Inner Silver Pit, as well as at localised areas in shallower water depths (DECC, 2016), with the offshore ECC crossing through an area of muddy sandy gravel located to the south of the Inner Silver Pit, as shown on Figure 7.11.

Offshore Array

61. Water depths in the array area range from 6.1m to 43.5m, with over 90% between 15m and 25m (LAT). Several bathymetric lows are present in the centre and west of the array area (see Figure 7.1, reaching a maximum depth of 25m below the seabed (45m from sea level). A series of sandbanks and sandwave features are present in the north of the array area, with amplitudes of 10m to 12m and 2m to 3m, respectively. Variations in water depth across the array area correspond with these features, about which further information is provided in paragraph 94 *et seq.* Four bathymetric profiles across the array area are shown in Plate 7.4 on which the bathymetric lows and sandbank features are clearly visible (Cathie, 2021).



Legend

- Array Area
- Offshore Export Cable Corridor
- ORCP Area
- Artificial Nesting Structure Area
- Biogenic Reef Restoration Area
- Physical Processes Zone of Influence

Depth (m)

- 0 - 10
- 10 - 20
- 20 - 30
- 30 - 40
- 40 - 50
- 50 - 60
- 60 - 70
- 70 - 80
- 80 - 90
- 90 - 100



Coordinate System: WGS 1984 UTM Zone 31N

0 25 50 km

Scale: 1:900,000 A3 Page Size

Environmental Statement

Bathymetry of the Study Area within a Regional Context

Figure 7.10

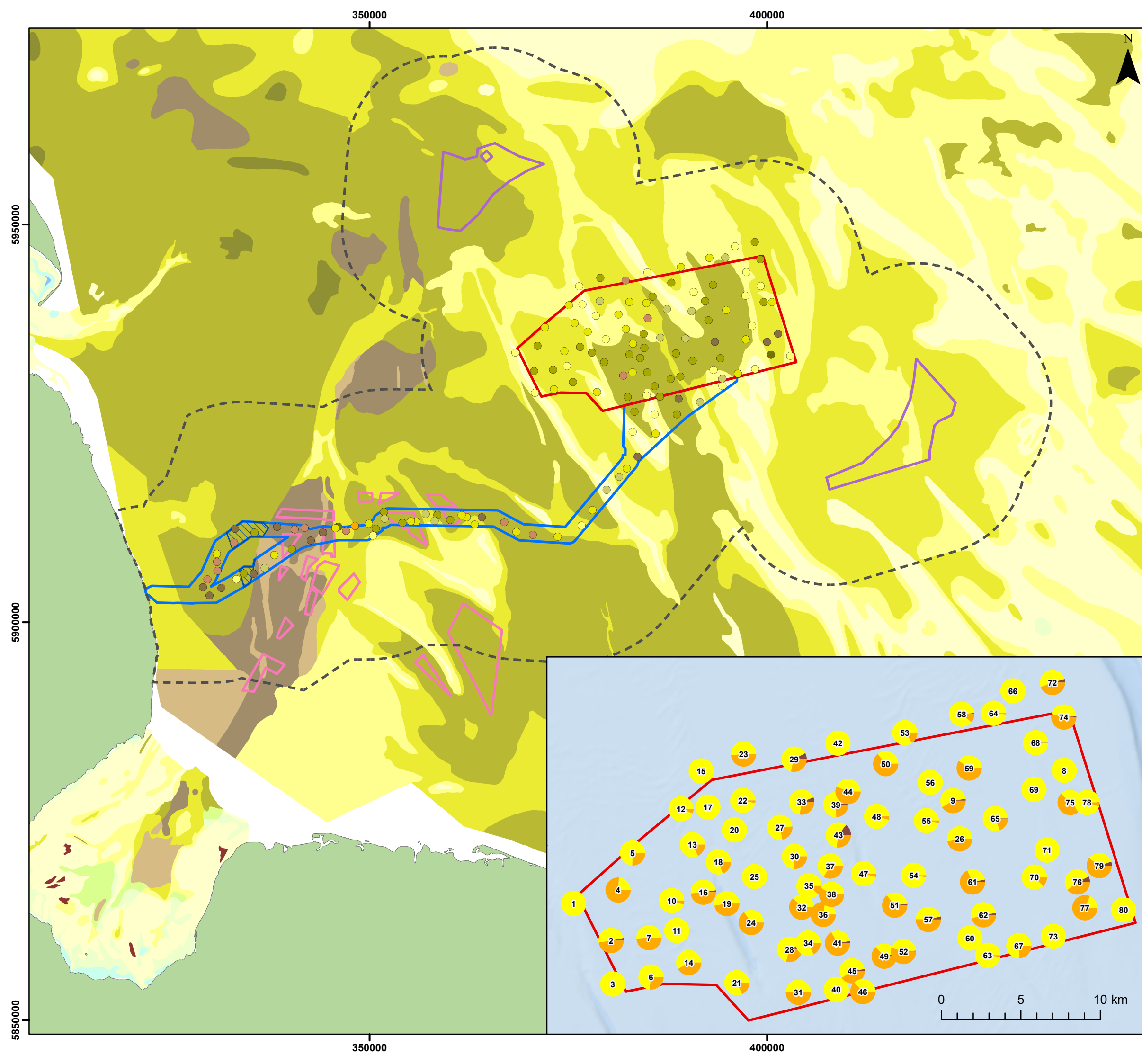


Date: 16/02/2024
 Produced By: BPHB
 Revision: 0.1

Contains ESRI Basemapping;
 EMDOnet 2020 bathymetry

GoBe

Document Path: Z:\GIS\GIS - Projects\0152 Outer Dowsing EIA\GIS\Figures\ES\Physical Processes Technical Report\ODOW_0152_PPTR_Fig7_10 Bathymetry_Regional.mxd



Legend

- Array Area
- Offshore Export Cable Corridor
- ORCP Area
- Artificial Nesting Structure Area
- Biogenic Reef Restoration Area
- Physical Processes Zone of Influence

Seabed Sediments (FOLK)

- 1.1.1 Mud
- 1.1.2 (gravelly) Mud
- 1.2.1 sandy Mud
- 1.3.1 muddy Sand
- 1.3.2 (gravelly) muddy Sand
- 2.1.1 Sand
- 2.1.2 (gravelly) Sand
- 3.1.1 gravelly Sand
- 3.2.1 sandy Gravel
- 3.3.1 Gravel
- 4.1.1 gravelly Mud
- 4.3.1 gravelly muddy Sand
- 4.4.1 muddy sandy Gravel
- 5. Rock and Boulders

Benthic Samples - Folk Class (GEOxyz, August / November 2022)

- Sand
- Slightly Gravelly Sand
- Slightly Gravelly Muddy Sand
- Gravelly Sand
- Sandy Gravel
- Muddy Sandy Gravel
- Gravelly Muddy Sand
- Gravel

Sediment composition (%)

- Fines
- Sand
- Gravel



Coordinate System: WGS 1984 UTM Zone 31N
 0 10 20 km
 Scale: 1:450,000 A3 Page Size

Environmental Statement
 Surficial Seabed Sediments (Folk, 1954)
 Figure 7.11

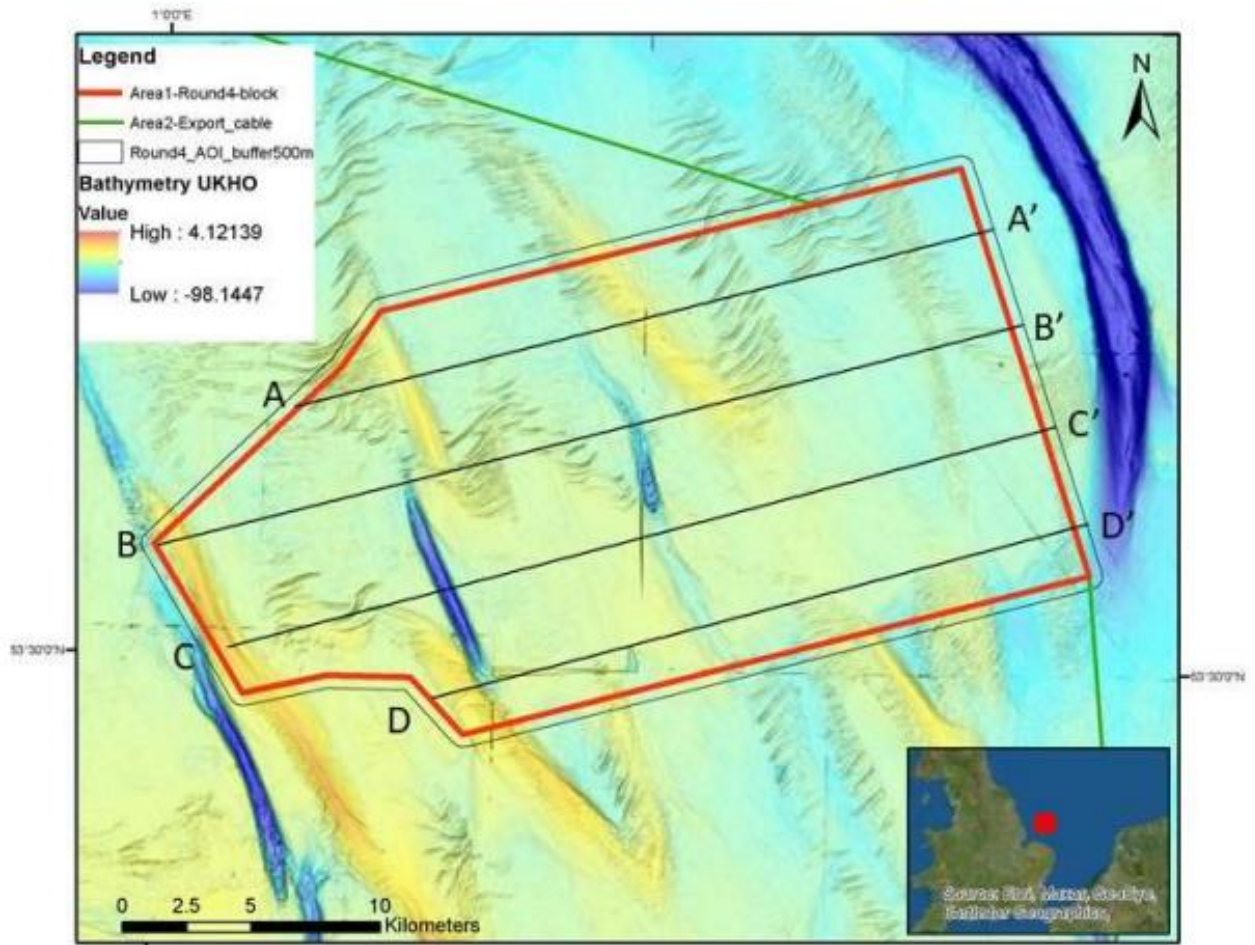




Date: 16/02/2024
 Produced By: BPHB
 Revision: 0.1

Contains ESRI Basemapping;
 Esri, Garmin, GEBCO, NOAA
 NGDC, and other
 contributorsEMDOnet Geology

Document Path: Z:\GIS\GIS - Projects\0152 Outer Dowsing EIA\GIS\Figures\ES\Physical Processes Technical Report\00W_0152_PPT-R_Fig7_11_Sebded_Sediments.mxd



Graphic Profile A-A'



Graphic Profile B-B'



Graphic Profile C-C'



Graphic Profile D-D'

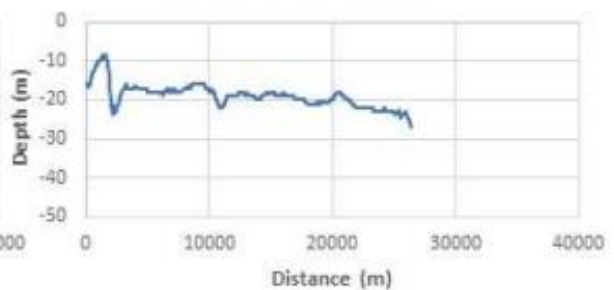


Plate 7.4 Bathymetric profiles across the Project array area, from Cathie (2021)

62. Particle size analysis has been carried out across the array area (in addition to the offshore ECC, see paragraph 64) as part of the Project benthic ecology characterisation, details of which are shown in Figure 7.11 and outlined in Table 7.10 (GEOxyz, 2022a). The results of this analysis indicate a variable sediment type across the array area with a general sand dominance, lower proportion of gravel and minimal proportion of fines. The overall mean sediment size across the array area is 1.3mm, with the sand fraction generally classified as medium and coarse sand. The proportion of sand increased at shallower depths associated with sandbank features, although a high sand content was found in high proportions at one sample point located within a seabed canyon, reflecting the general dominance of sand across the array area. The proportion of fines was generally low, with a slightly higher content observed at deeper sample points. A significant correlation was found between the sorting coefficient and depth, indicating that sediments within the deeper areas of the survey were generally more variable than sediments sampled from sandbank crests (GEOxyz, 2022a). This is likely to be a result of sediment transport processes.

Table 7.10 Summary of particle size analysis across the array area (GEOxyz, 2022a)

Sediment Type	Minimum Fraction (%)	Mean Fraction (%)	Maximum Fraction (%)	Standard Deviation
Fines	0.00	1.32	14.53	2.34
Sands	18.58	70.34	99.99	25.96
Gravel	0.01	28.35	81.08	25.23

Offshore Export Cable Corridor

63. Bathymetry along the Offshore ECC has been characterised using EMODnet data, to be supplemented with Project-specific geophysical information when it becomes available. Moving southwest from the array area, water depths range generally between 10m to 30m (LAT). This is dependent on bathymetric features, with the lowest depths corresponding to the Outer Dowsing Shoal (see Figure 7.1). The ECC then crosses through an area of relatively flat seabed with depth of 20m to 25m (LAT), before crossing the Triton Knoll and Dudgeon Shoal sandbanks, which at their highest point have water depths of around 10m (LAT). South of the Inner Silver Pit, water depths generally range between 10m and 30m (LAT) within the glacial outwash feature, described further in paragraph 102. From around 12km offshore, water depths typically shallow uniformly from around 14m towards the coast (EMODnet, 2022).

64. Surficial sediments in the Offshore ECC area are characterised mainly by sandy gravel, with some mud component to the south of Inner Silver Pit (Figure 7.11; BGS, 2022). The offshore area of the Triton Knoll ECC is comprised of silty gravelly sand and gravelly sand dominating, with poorly sorted gravelly sand identified from the Triton Knoll bank. In addition, a large number of boulders were identified along the ECC, the largest of which are over 1m in diameter (TKOWFL, 2014). The results of PSA along the Project ECC are shown in Table 7.11 (GEOxyz, 2022b). The results indicate a variable sediment type with a general dominance of sand, with higher fines content than the array area, consistent with the BGS data presented in Figure 7.11. Closer to the coast, the proportion of sand generally decreases, with a corresponding increase in gravel and fines content. The overall mean sediment size within the offshore ECC was 0.7mm, with the sand fraction generally classified as coarse sand under the Wentworth Classification

Table 7.11 Summary of particle size analysis across the offshore ECC (GEOxyz, 2022b)

Sediment Type	Minimum Fraction (%)	Mean Fraction (%)	Maximum Fraction (%)	Standard Deviation
Fines	0.00	6.38	26.03	7.43
Sands	6.74	71.57	99.94	19.65
Gravel	0.02	23.37	98.11	17.92

Coast

65. Water depths typically shallow uniformly towards the coast, from around 14m (LAT) at 12km offshore (EMODnet, 2020). The present form of the Lincolnshire beaches has been directly influenced by an annual beach nourishment scheme which has involved the placement of almost 17 million square metres of sand since 1994 (Environment Agency, 2019a; 2019b). Prior to the nourishment scheme, the beach consisted of a thin veneer of sand overlying clay, which matches historical borehole data described previously in paragraph 56. Analysis of the nourishment material has shown that it can be best described as poorly sorted gravelly sand, with a mean grain size considerably coarser than the natural beach sediment, although considerable variation was identified within each dredger load and at different locations along the coast (Blott and Pye, 2004).

Compensation Areas

66. Water depths in the northern ANS area are generally between, approximately, 20m to 30m (LAT) (Figure 7.1), with surficial sediments comprising of mainly gravel and sandy gravel (Figure 7.11; BGS, 2022). The southern ANS area has similar water depths across the majority of it, although it overlies the Coal Pit channel, within which depths may reach up to, approximately, 70m LAT (Figure 7.1)) and is characterised by gravelly sand. The bathymetry and surficial sediment cover within the biogenic reef creation area may be generally characterised using the information provided in paragraph 63 and 64.

7.4.2.3 Sediment Transport

67. Sediment transport is a crucial link in the interaction between hydrodynamic regime and coastal morphological evolution. There are two main mechanisms of sediment transport:
- Bedload transport, which refers to the movement of grains along the seabed by currents, which primarily relates to coarse material including sands and gravels; and
 - Suspended load transport, which refers to particles of sediment carried in suspension in the water column.
68. The sediment transport regime across the study area has been characterised using regional scale assessments including the Southern North Sea Sediment Transport Study Phase 2 (SNSSTS II) (HR Wallingford *et al.*, 2002), the work of Kenyon and Cooper (2005), and Tappin *et al.* (2011), in addition to modelling studies for other OWFs in the area. This supports estimations of potential sediment mobility calculated from Project numerical model outputs, in addition to the results of Project-specific sediment transport model.
69. Modelling studies and analysis of bedform indicators, such as sandwaves and tidal banks, have demonstrated that tidal currents are the dominant mechanisms responsible for bedload transport in the Humber region (van der Molen, 2002; Kenyon and Cooper, 2005). Offshore, some areas show evidence of surge current dominance, which also have the ability to temporarily reverse or reinforce tidally-driven sediment transport pathways (TKOWFL, 2011). Waves tend to only influence offshore sediment transport during extreme events but exert the dominant forcing to littoral transport within the nearshore zone (HADA, 2012a).
70. The main pattern is of a northerly/north-westerly directed offshore stream and a southerly inshore stream, separated by a bedload parting between just south of Sand Hole, across the Silver Pit and through the Race Bank – North Ridge – Dudgeon Shoal (Kenyon and Cooper, 2005; Tappin *et al.*, 2011; Figure 7.12). Superimposed on this are numerous smaller scale pathways and circulatory systems, particularly in areas of complex bathymetry such as around sandbank features (HADA, 2012b).
71. Modelled current time-series data from the Project numerical model outputs (the details of which are provided within Volume 3, Appendix 7.2: Marine Physical Processes Modelling Report (document reference 6.3.7.2)) have been used to estimate the potential mobility of sediments across the study area during a spring and neap tidal phase in 2015. Current time-series were extracted from the hydrodynamic model at 27 points, the locations of which are shown in Figure 7.14. The bed shear stresses and corresponding critical depth-averaged current speed values required for the transportation of different sediment grain sizes have been calculated using standard methods described by Soulsby (1997), with the results are presented in Table 7.17, with a summary provided in Table 7.12.

Table 7.12 Summary of estimated potential sediment mobility across the study area

Size Class	Sediment Mobility ¹⁴ (Spring)			Sediment Mobility (Neap)		
	Minimum	Mean	Maximum	Minimum	Mean	Maximum
Granule gravel	0%	2%	12%	0%	0%	0%
Very coarse sand	2%	29%	55%	0%	2%	15%
Coarse sand	30%	62%	86%	1%	21%	49%
Medium sand	49%	73%	97%	9%	38%	62%
Fine sand	53%	76%	98%	12%	43%	65%
Very fine sand	53%	76%	99%	12%	43%	66%
Coarse silt	56%	77%	99%	14%	45%	66%

72. This analysis indicates that over the 27 locations identified, sediments with grain sizes of less than 0.5mm (medium sand and smaller) are mobilised more than 70% of the time during spring tides, and between 38% and 45% during neap tides. Gravel-sized sediment is rarely mobilised, and only during spring tides. The estimated potential sediment mobility varies with location, with higher values generally identified at extraction points located on sandbanks (Table 7.17; Figure 7.14).
73. Further evidence of sediment transport patterns is provided by a combination of geomorphological analysis of Project bathymetric data and a set of coupled tidal flow, wave and sediment transport models, as analysed by East Point Geo Ltd. (2023). Despite simplifying assumptions, comparable bedform migration directions and rates of bed elevation change were observed between the sediment transport model and those calculated by geomorphological analysis.
74. Suspended Particulate Matter (SPM) provides an indication of turbidity and is highly variable according to water depth and the marine processes in the area (i.e., tide, current and wind regimes). The offshore region of the study area is generally characterised by low surface concentrations of SPM due to distance from terrestrial sources and low seabed fines content. Fines transported southwards from the erosion of the Holderness Cliffs combine with muds transported out of the Humber Estuary, forming a plume which moves offshore to the south-east and towards the southern North Sea. The majority of the plume's suspended load is deposited outside UK Territorial Waters (Defra, 2002).

¹⁴ Percentage of time that sediment is mobile.

Offshore Array

75. Regional-scale assessments identify a net north-westerly direction of bedload transport for the Project array area, which is located seaward of the bedload parting zone, as shown in Figure 7.12 (Kenyon and Cooper, 2005). This is supported by modelled near-bed current velocities from the centre of the array, which have a residual direction towards the northwest (Plate 7.3). Areas of mobile sediment waves are present across the array area, particularly in the north and northeast as well as on the north-eastern flanks of sandbank features, as shown on Figure 7.15 (Dove et al., 2017). These sediment waves generally face towards the north and northwest, further supporting net bedload transport towards this direction (Tappin et al., 2011).
76. A geomorphological analysis of Project geophysical data has been used to create a high-level terrain map in order to provide context to the geomorphological processes operating across the Project site, with sandwave crest mapping conducted in order to provide estimates of bedform migration (East Point Geo Ltd., 2023). Generally, the array area may be subdivided into static areas, within which mobile sediment availability is low and surface sediments are sufficiently competent to resist scour, and dynamic areas, comprising areas of sandwaves and megaripples. The central southern part of the array area is generally static, whereas dynamic areas characterise the northern, western, and eastern parts.
77. Migration is generally to the north-northwest in the western half of the site, and to the southeast east of the adjacent large sandbank. The majority of those features migrating north-northwest show asymmetry with their lee side facing north, however further east, where bedforms are generally smaller, asymmetry is less pronounced. Few features have their lee side facing south regardless of their observed migration direction. Rates of migration vary between 0m/year and 40m/year, with an average of 12m/year, and are slightly higher in the centre and north of the array (East Point Geo Ltd., 2023).
78. Overall, the central northern part of the array area shows the largest rates of migration, with bedforms observed to have migrated primarily to the northwest. To the east of the array area, there is a change in bedform behaviour to oscillating migration and then migration to the southeast, albeit at small rates. In the southern, central, and western parts of the array area, features either oscillate (between northwest and southeast migration) or have low migration rates to the north (East Point Geo Ltd., 2023). These results generally corroborate the net north-westerly direction of bedload transport identified in regional-scale assessments, although indicate that this may be reversed in the east of the array.
79. A set of coupled tidal flow, wave and sediment transport models were developed by East Point Geo Ltd. (2023) to supplement these results. The model suggests that residual sediment transport directions are influenced by wave height. Under frequent conditions with fairly low waves, sediment transport occurs mainly during low tides, when currents are directed to the north. However, under more energetic wave conditions, transport occurs during the entire tidal cycle and the residual transport is therefore generally to the south, which correlates with geomorphological mapping showing transport to the south in some sandwave areas.

80. A tidal current time-series from the SWLB has been used to estimate the potential sediment mobility of sediments within the array area during a spring and neap tidal phase in May 2022. The bed shear stresses and corresponding critical depth-averaged current speed values required for the transportation of different sediment grain sizes have been calculated using standard methods described by Soulsby (1997), and are provided in Table 7.13 for depth-averaged tidal currents. Based on this analysis, sediments with grain sizes smaller than 0.5mm (medium sand and smaller) will be mobilised over 50% of the time during springs, and between 5% and 9% of the time during neaps.
81. These results are somewhat similar to the sediment mobility results calculated from current time-series data extracted from the Project numerical model outputs, as described in paragraph 71 and presented in Table 7.17. Point 25 is located approximately within the centre of the Project array area (as shown on Figure 7.14), similar to the SWLB, with the analysis suggesting the mobilisation of medium sand and finer over 60% of the time during springs, and between 28% and 36% of the time during neaps. The difference in these results may be due to variations in current speeds between the locations, or between the identified spring and neap tides.

Table 7.13 Estimated potential sediment mobility within the array area calculated from depth-averaged tidal currents

Size Class	Grain Size (upper boundary) (mm)	Threshold of Bed Shear Stress (N/m ²)	Corresponding Critical Depth-averaged Current Speeds (m/s)	Sediment Mobility ¹⁵ (Spring)	Sediment Mobility (Neap)
Granule gravel	4.0	3.007	1.32	0%	0%
Very coarse sand	2.0	1.166	0.908	4%	0%
Coarse sand	1.0	0.481	0.643	41%	1%
Medium sand	0.5	0.262	0.524	56%	5%
Fine sand	0.25	0.189	0.492	59%	7%
Very fine sand	0.125	0.153	0.489	60%	7%
Coarse silt	0.0625	0.120	0.477	61%	9%

¹⁵ Percentage of time that sediment is mobile.

82. Suspended sediment in the region is mainly sourced from the eroding Holderness cliffs, which consist of 67% mud (Tappin *et al.*, 2011). As a result of distance from these terrestrial sources, combined with a generally low fine seabed sediment signature, low surface concentrations of up to 5mg/l were recorded between the period 1998 to 2015 (Cefas, 2016) within the Project array area (see Figure 7.13). Higher values will occur during spring tides and storm conditions, with the greatest concentrations encountered close to the bed. Turbidity values recorded at the SWLB are presented in Table 7.14 to corroborate these low surface concentrations. Data was collected from April 2022 to May 2023, with part of the data excluded due to data processing concerns, although the presented data is considered to adequately cover both summer and winter conditions. The data indicates mean near-surface and near-bed concentrations of 2.4mg/l and 9.2mg/l, respectively, during the summer, and 2.3mg/l and 8.9mg/l, respectively, during the winter. The maximum suspended sediment concentration found on analysing the site water samples collected on 8 August 2022 and 28 February 2023 (both during a neap tide according to the National Tidal and Sea Level Facility (NTSLF)) was 13.2 mg/l (Fugro, 2023).

Table 7.14 Near-surface and near-bed turbidity values recorded at the SWLB (located in water depths of 22.9m (LAT))

Measurement Period	Near-bed		Near-surface	
	Minimum (mg/l)	Mean (mg/l)	Minimum (mg/l)	Mean (mg/l)
Summer (deployed from 17/04/2022 to 04/08/2022)	Minimum (mg/l)	3.4	Minimum (mg/l)	1.4
	Mean (mg/l)	9.2	Mean (mg/l)	2.4
	Maximum (mg/l)	17.4	Maximum (mg/l)	3.9
	Standard Deviation (mg/l)	3.6	Standard Deviation (mg/l)	0.5
Winter (deployed from 26/11/2022 to 12/05/2023)	Minimum (mg/l)	3.0	Minimum (mg/l)	1.3
	Mean (mg/l)	8.9	Mean (mg/l)	2.3
	Maximum (mg/l)	17.7	Maximum (mg/l)	3.6
	Standard Deviation (mg/l)	3.7	Standard Deviation (mg/l)	0.3

83. Time-series data of near-bed turbidity alongside current velocity and significant wave height are shown in Plate 7.5 and Plate 7.6 for the summer and winter phases (as defined in Table 7.14), respectively. During summer, a statistically significant¹⁶ correlation can be identified between near-bed turbidity and deterministic significant wave height (Pearson coefficient¹⁷ = 0.2113). During winter, statistically significant correlations are also identified between near-bed turbidity and current velocity (Pearson coefficient = 0.3606), and deterministic significant wave height (Pearson coefficient = 0.3836). In addition, turbidity values throughout the water column in winter show statistically significant positive correlation with significant and maximum wave height, which generally increases towards the seabed. During both seasons, wave direction also has a statistically significant impact on the level of turbidity, with the highest turbidity associated with waves approaching from the west (during summer) and west-southwest (during winter).

¹⁶ With a p-value of below 0.05.

¹⁷ The Pearson correlation measures the strength of the linear relationship between two variables, with the coefficient value ranging from -1 (perfect negative correlation) to +1 (perfect positive correlation), with the value of zero representing no linear relationship.

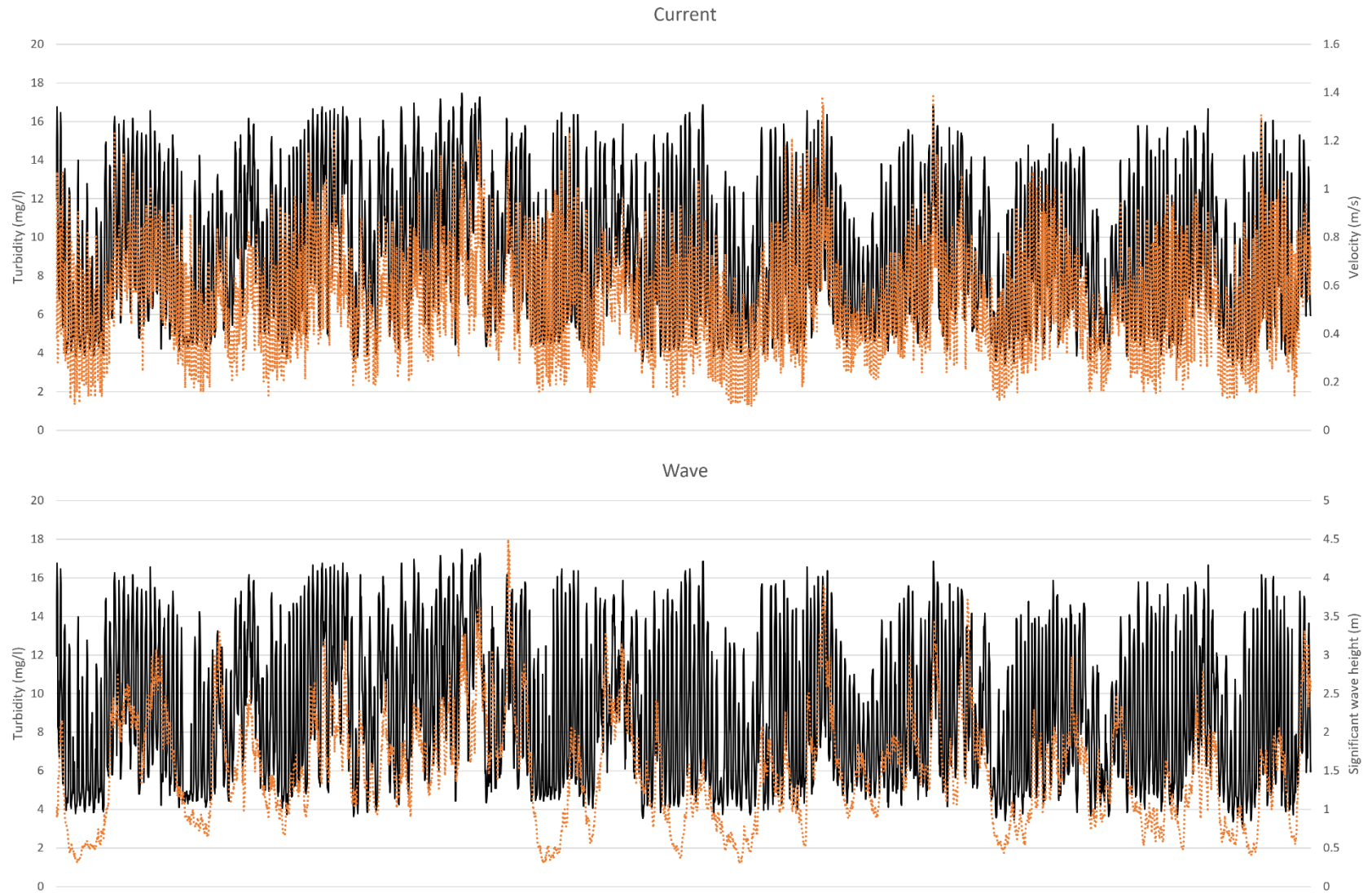


Plate 7.5 Time-series of near-bed turbidity (orange) against current velocity and significant wave height taken from the SWLB from April to August 2022

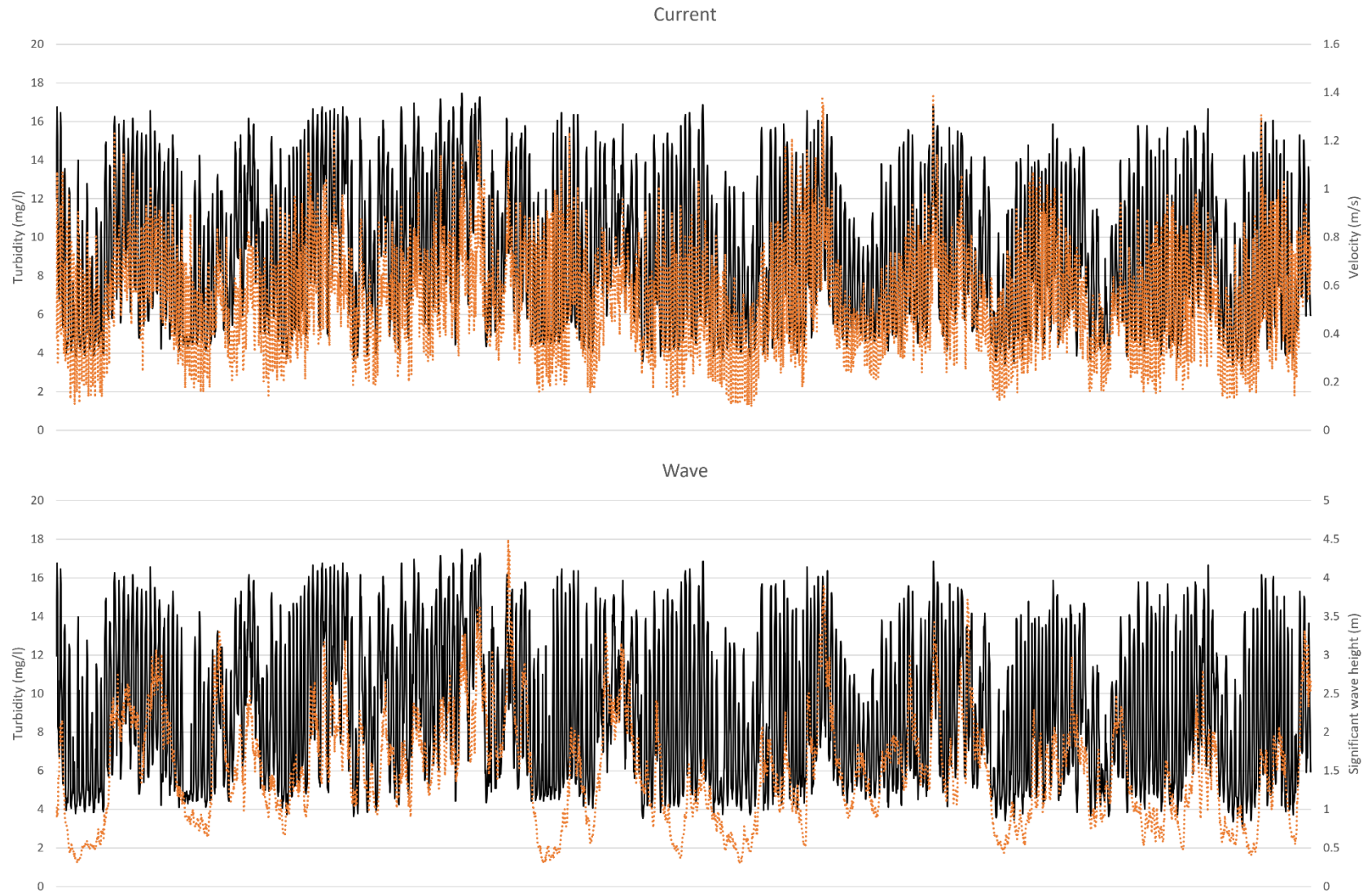


Plate 7.6 Time-series of near-bed turbidity (orange) against current velocity and significant wave height taken from the SWLB from November 2022 to May 2023

Offshore Export Cable Corridor

84. Bedload sediment transport in the most offshore part of the ECC is directed towards the northwest, as in the Project array area. Where the flow is diverted, such as around the margins of the Triton Knoll and Inner Dowsing sandbanks, localised changes to the broad scale sediment transport paths occur (TKOWFL, 2014). The ECC crosses a bedload parting, approximately, 35km offshore, with bedload transport directed to the south (Figure 7.12). Further inshore, there is a dominant southwards bedload sediment transport direction pathway, with an inshore direction into the Wash. Littoral transport diverges along the Lincolnshire coastline such that sediment is transported towards the mouth of the Wash and the Humber Estuary, with a southward transport direction at the Landfall site (Figure 7.12).
85. Geomorphological analysis indicates that the bedload parting zone is located approximately along the axis of the North Ridge sandbank (as shown on Figure 7.14). To the east of the sandbank, bedform migration is generally towards the northwest, at low rates, with southward migration to the west. This pattern is identified along the flanks of the sandbank itself, suggesting anticlockwise sediment movement (East Point Geo Ltd., 2023).
86. Estimates of potential sediment mobility for the Triton Knoll ECC found that silt and sand is expected to be mobile during both spring and neap tides, except for very coarse sand (~1,500µm), which is only expected to be mobile during spring tides. Gravel sized material is predicted to be immobile or only mobilised during the highest spring tides (TKOWFL, 2014). This supports the sediment mobility results calculated from current time-series data extracted from the Project numerical model outputs, as described in paragraph 71 and presented in Table 7.17, with locations shown on Figure 7.14.
87. Surface SPM levels within the nearshore zone of the Offshore ECC are directly under the influence of terrestrial sources from the Humber Estuary and Holderness Cliffs, such that concentrations reach around 60mg/l, between the period 1998 to 2015 (Cefas, 2016). Maximum values coincide with the winter months when a greater frequency of storm events and fluvial inputs (including storm runoff) can be expected to occur. During the summer months, for example July, maximum values are of the order of 12mg/l (Figure 7.13). There is an east to west gradient in SPM throughout the year, although this is most pronounced during the winter.

Coast

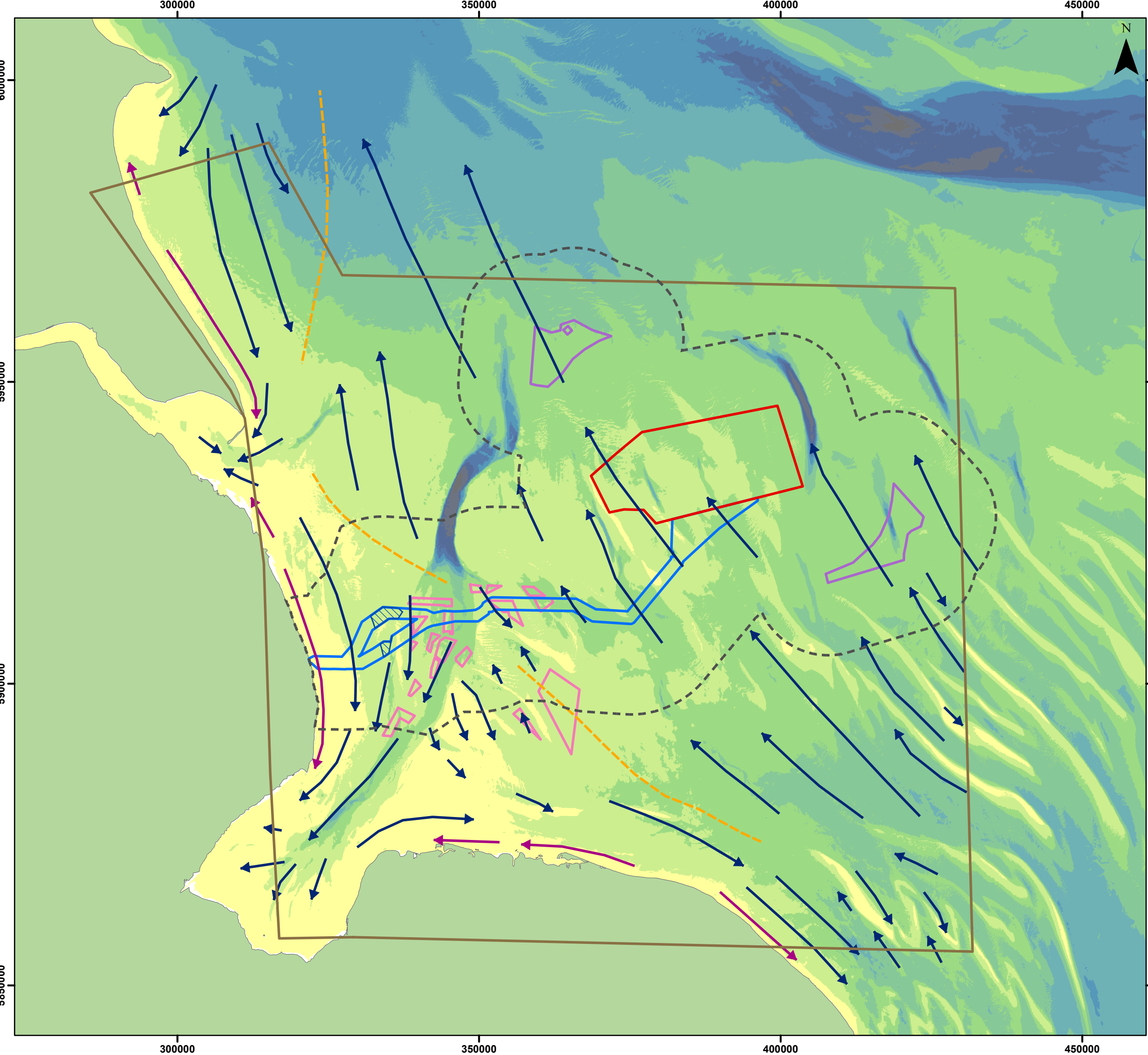
88. As outlined previously, the dominant wave direction along the Lincolnshire coast is from the northeast, which produces a net southerly drift of beach material along the Lincolnshire coast and into the Wash (HR Wallingford *et al.*, 2002; Environment Agency, 2011). The wave regime is the dominant driver of littoral transport in the nearshore zone and is an important determinant of beach morphology in the area, outlined further in paragraph 107.

89. Between 0.1 and 0.3 million cubic metres of sediment derived from the Holderness cliffs is deposited on the Lincolnshire coast each year, in addition to the combined riverine input from the Humber Estuary, which provides approximately 0.1 million m³/year to the system, and the beach nourishment scheme carried out on the Lincolnshire coast, which represents an important artificial source of sediment to beaches in this area (Environment Agency, 2019a). The majority of the sediments crossing the Humber Estuary are retained at Donna Nook, a sediment sink, with the potential mean longshore transport rate of only 12,000m³/annum to the south (HR Wallingford *et al.*, 2002; HADA, 2012b).
90. Estimates of longshore sediment transport rates were made using HR Wallingford’s 2D Nearshore Profile Model (NEARSHORE) in 1991 for Anderby Creek, at the northern end of the Landfall area (shown in Figure 7.17). Sediment transport calculations were made at 50m intervals along shore-normal profiles extending seaward from the seawall¹⁸ for spring and neap tides, with data provided in Table 7.15 (HR Wallingford *et al.*, 2002). Interpreted longshore drift were provided in HR Wallingford *et al.* (2002) as between 100,000m³/year and 300,000m³/year towards the south for the wider coast at the Landfall location.

Table 7.15 Estimated longshore sediment transport rates at Anderby Creek (HR Wallingford *et al.*, 2002)

Distance from seawall (m)	Spring tide cumulative longshore transport rate (10 ⁶ m ³ /year) (-ve southwards)	Neap tide cumulative longshore transport rate (10 ⁶ m ³ /year) (-ve southwards)
0	0.00	0.00
50	-0.07	0.00
100	-0.10	-0.23
150	-0.22	-0.41
200	-0.28	-0.56
250	-0.35	-0.76
300	-0.46	-0.98
350	-0.55	-1.13
400	-0.62	-1.24
450	-0.98	-1.48

¹⁸ According to both the Environment Agency (2011) and contemporary satellite images, there are currently no visible hard defences at Anderby Creek, and instead the beach is backed by a vegetated dune bank.



Legend

- Array Area
- Offshore Export Cable Corridor
- ORCP Area
- Artificial Nesting Structure Area
- Biogenic Reef Restoration Area
- Physical Processes Zone of Influence
- Longshore Transport
- Bed Load Transport
- - - Bed Load Parting
- SEA Boundary

Depth (m)

- 0 - 10
- 10 - 20
- 20 - 30
- 30 - 40
- 40 - 50
- 50 - 60
- 60 - 70
- 70 - 80
- 80 - 90
- 90 - 100

Longshore Transport, Bed Load Transport and Bed Load Parting from Kenyon and Cooper, 2005



Coordinate System: WGS 1984 UTM Zone 31N
 0 10 20 km
 Scale: 1:600,000
 A3 Page Size

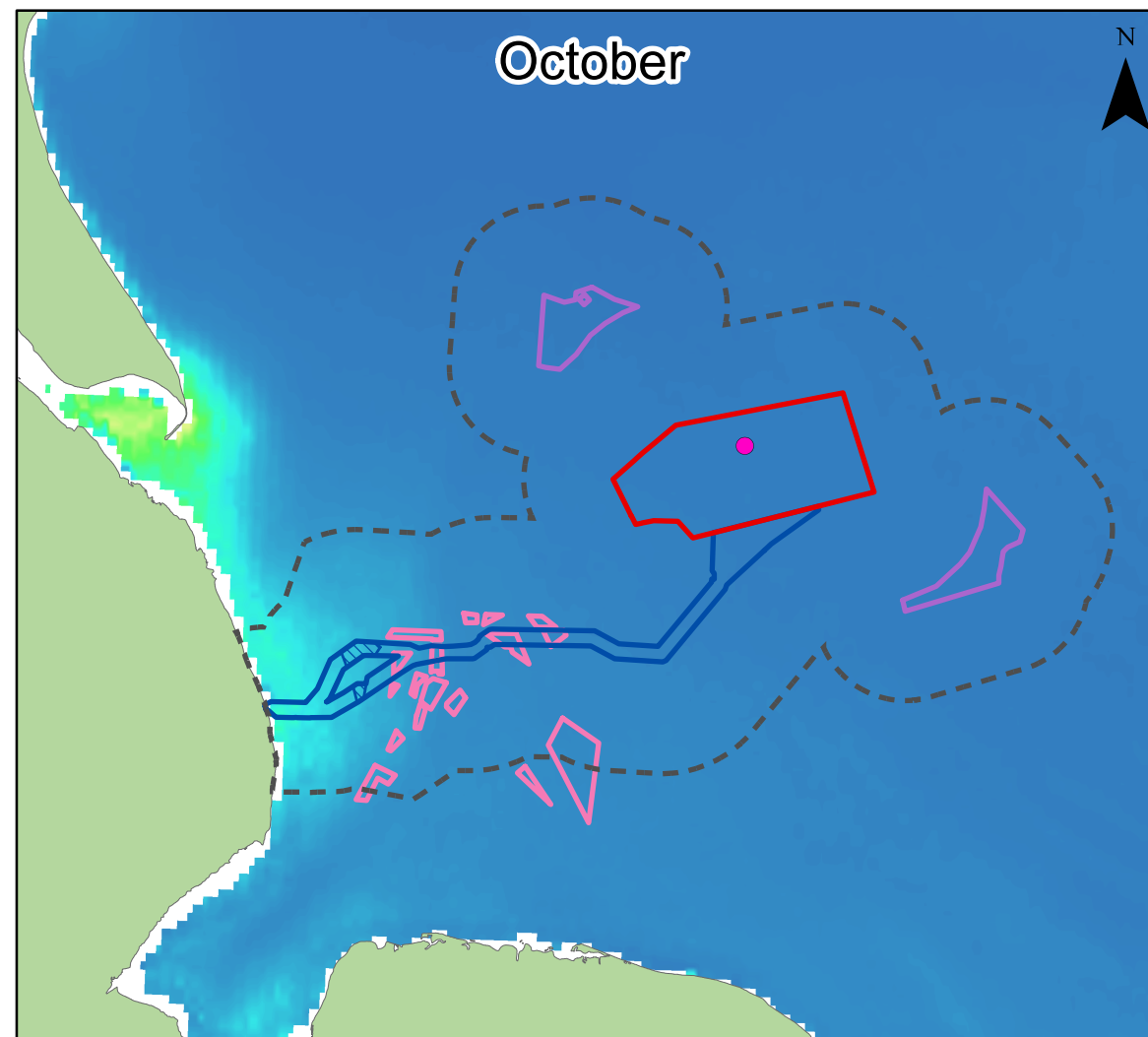
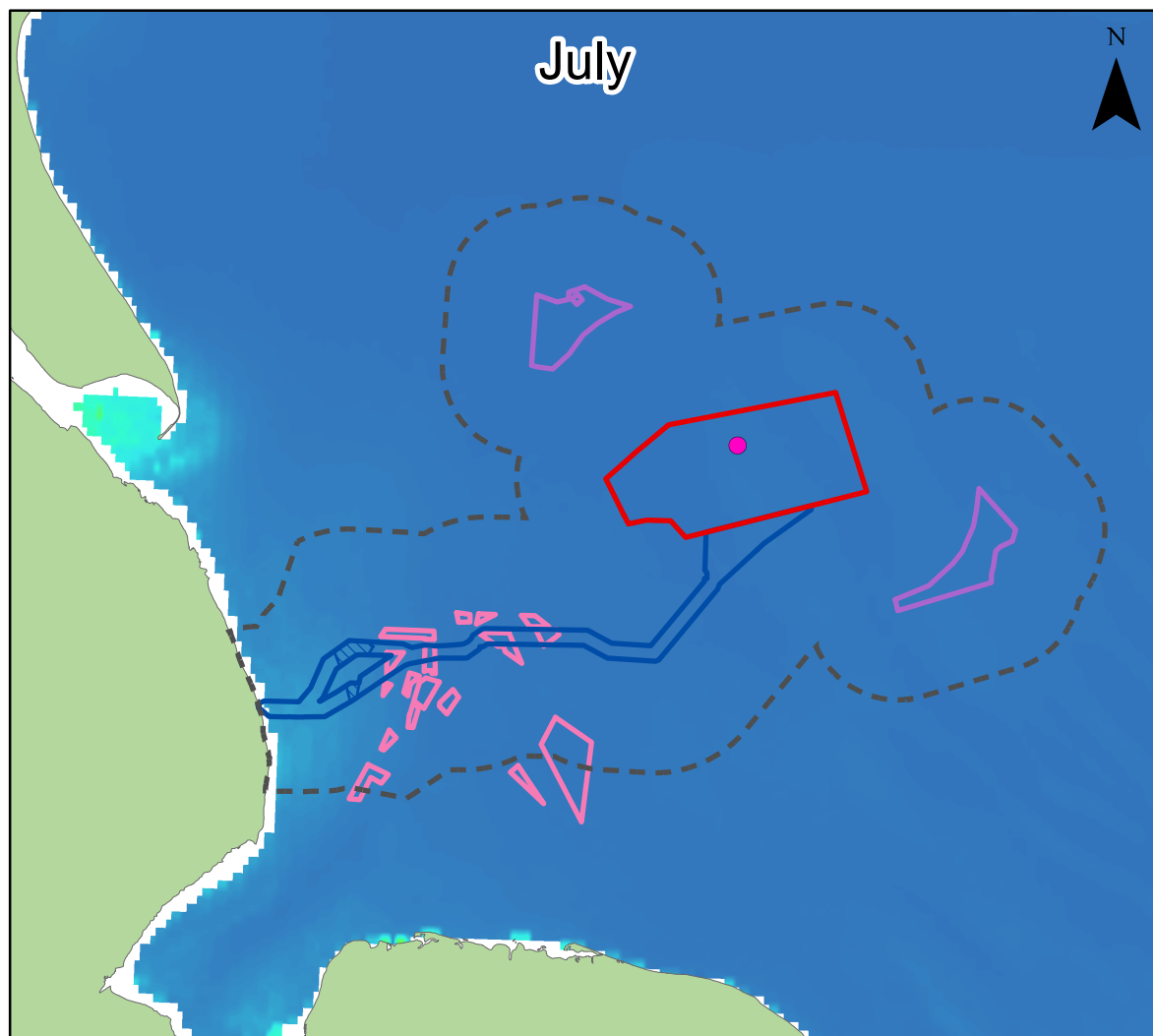
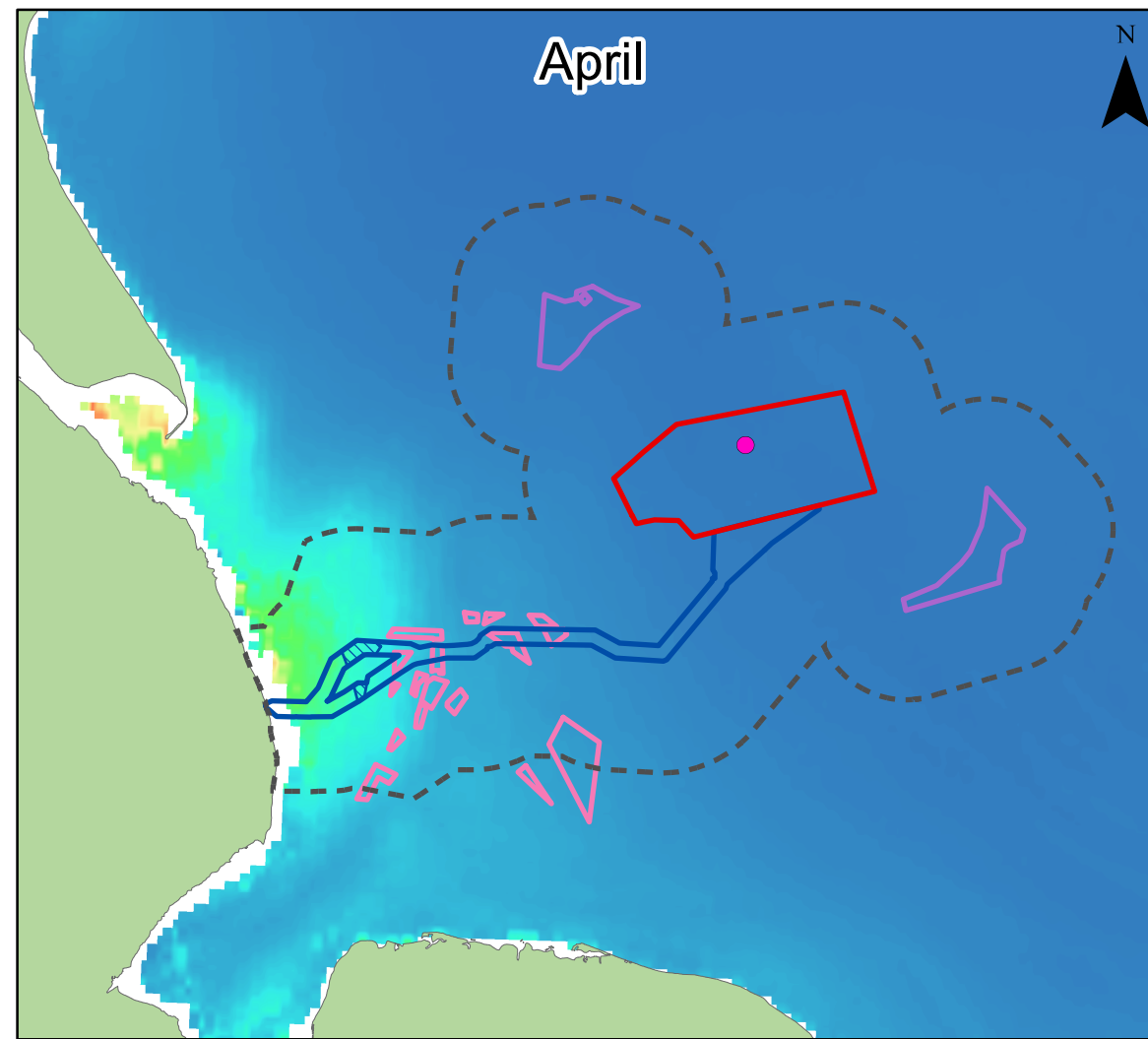
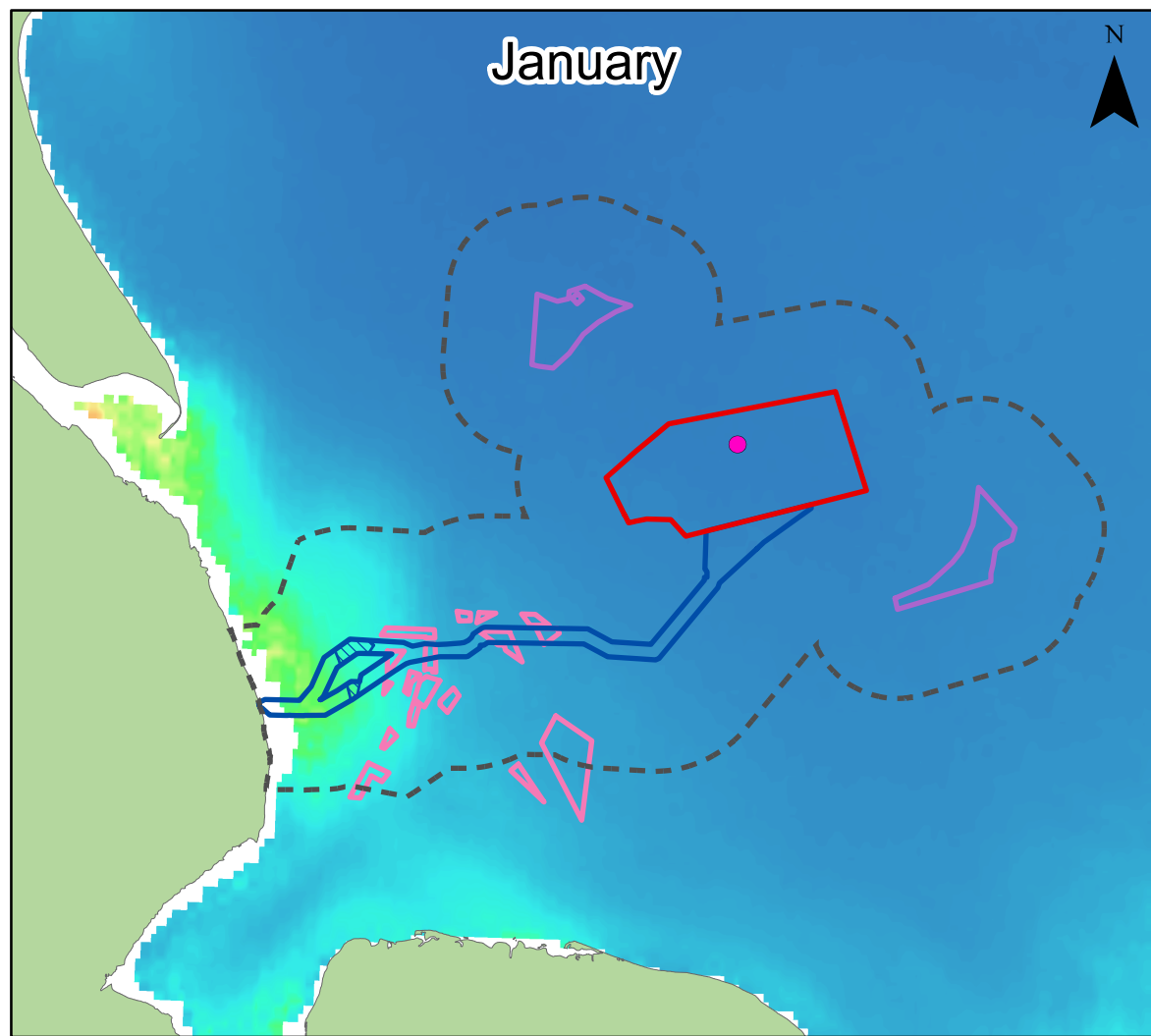
Environmental Statement
 Bedload Sediment Pathways
 (adapted from Kenyon and Cooper, 2005)
 Figure 7.12



Date: 16/02/2024
 Produced By: BPHB
 Revision: 0.1

Contains ESRI Basemapping; EMDOnet Geology 2016

Document Path: Z:\GIS\GIS - Projects\0152 Outer Dowsing ELA\GIS\Figures\ES\Physical Processes Technical Report\DOOW_0152_PPTR_Fig7_12_Bedload_Sediment_Pathways.mxd



Legend

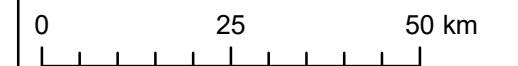
- Array Area
- Offshore Export Cable Corridor
- ORCP Area
- Artificial Nesting Structure Area
- Biogenic Reef Restoration Area
- Physical Processes Zone of Influence
- Lidar Buoy SWLB059

SPM Concentrations (mg/l) (CEFAS, 1998-2015)

High : 100
 Low : 0



Coordinate System: WGS 1984 UTM Zone 31N



Scale: 1:1,000,000

A3 Page Size

Environmental Statement

Average Suspended Particulate Matter
 (Cefas, 2016)

Figure 7.13



Date: 16/02/2024
 Produced By: BPHB
 Revision: 0.1



Contains ESRI Basemapping:

Compensation Areas

91. Regional-scale assessments indicate a net north-westerly direction of bedload sediment transport for the ANS areas, as shown in Figure 7.12, with generally low suspended sediment concentrations. The biogenic reef creation area crosses a bedload parting, as characterised in paragraph 84 and shown in Figure 7.12, with increasing suspended sediment concentrations closer to the coast.

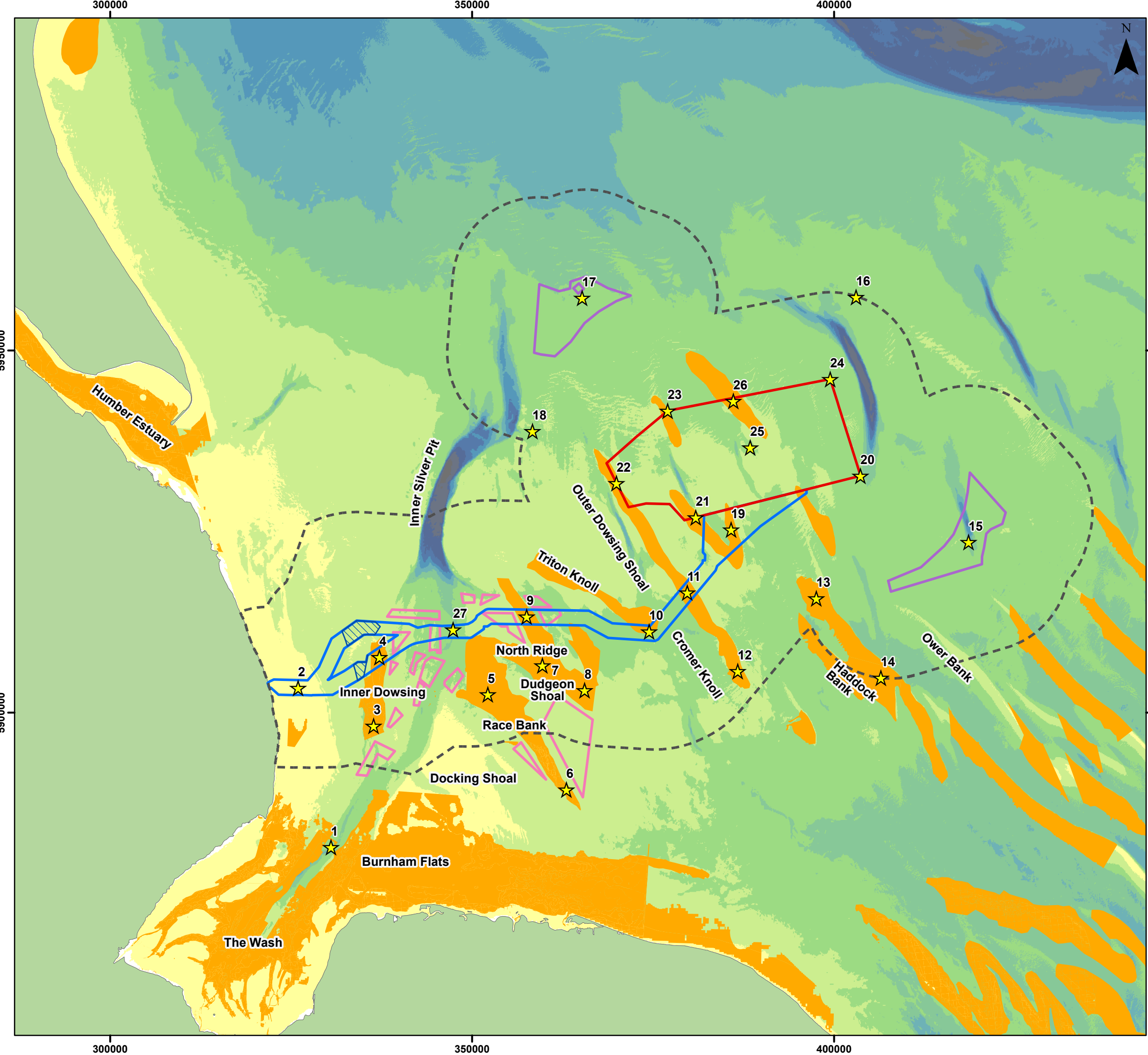
7.4.3 Morphology

92. The large-scale seabed morphology in the ZOI is characterised by a broad, arcuate, low-relief bathymetric high extending eastwards from the Holderness and Lincolnshire coasts, with a series of large valleys incised approximately perpendicularly into this high (Dove *et al.*, 2017). The ZOI is bordered to the northwest by the Outer Silver Pit, and to the southwest by the major embayment of the Wash. To the south are the Norfolk Banks, a series of northwest to southeast trending sandbanks (Tappin *et al.*, 2011; Figure 7.10). Water depths generally increase eastward from the coast with a gently undulating character, apart from areas of prominent, localised relief formed by a number of large-scale features (Tappin *et al.*, 2011). This conspicuous variation in the region's seabed morphology is largely due to the presence of glacial landforms, with the exception of superficial Holocene sediment banks and waves (Cathie, 2021).

93. The most prominent of these landforms are the major deeps of Inner Silver Pit and Sole Pit, which form elongate, curvilinear submarine valleys up to 90m deep (Tappin *et al.*, 2011). These 'tunnel valleys', as well as smaller deeps across the study area, are generally aligned with the tidal currents and form geomorphological divides, with sediment being transported parallel to them rather than across them (see Figure 7.12). The floors of these deeps typically remain unfilled with contemporary sediments, and instead have exposures of bedrock and Pleistocene deposits as shown in Figure 7.7 (HADA, 2012a). A series of large-scale sediment banks is also present across the region, generally oriented northwest to southeast, which form sinuous features in the southwest (HADA, 2012a; Figure 7.14). The present-day seabed morphology has been interpreted as the result of a combination of glacial processes and the post-glacial reworking of outwash deposits (Tappin *et al.*, 2011).

Offshore Array

94. The array area is bound to the eastern (seaward) edge by Sole Pit, and on the western (landward) boundary by the Outer Dowsing Channel, as shown in Figure 7.1. Several sandbanks are located within the array area, as identified on the geophysical survey and shown in Figure 7.15, with heights from seabed of between 10m and 12m, as well as areas of northwest-facing sand waves with wave heights of 2m to 3m. The sandwaves within the array area are complex, characterised both by symmetrical and asymmetrical (lee sides with angles of 5°) sandwaves, some with superimposed megaripples indicating a current direction of north-northwest to south-southeast. In addition, two deeps known as the Dowsing Deepes are located in the centre of the array area, reaching a maximum depth of 45m (LAT). They are aligned in a north-northwest to south-southeast direction and extend up to 10km in length (Figure 7.15; Cathie, 2021). These features are likely to have been formed by similar processes to larger-scale submarine valleys in the region such as the Sole and Inner Silver Pits (Tappin *et al.*, 2011).
95. Sole Pit is an offshore depression considered to have formed during Quaternary glaciations, specifically by erosion underneath grounded ice sheets and later by tidal scour (Balson, 1999; Briggs *et al.*, 2007). Approximately 34km long, 2.5km wide and 80m deep, with marginal slope gradients of up to 12°, it is curvilinear in shape, with marginal channels entering at inflexions on its flanks. Jurassic bedrock and earlier Pleistocene deposits are exposed within the Sole Pit either at seabed or beneath a thin sediment cover (Figure 7.7), likely due to erosion increased tidal current speeds (Tappin *et al.*, 2011).
96. The Outer Dowsing Channel, as well as the other smaller deeps in the region, is mainly linear. It is oriented mainly north-northwest to south-southeast and has steep flanks of between 7° and 10° (Tappin *et al.*, 2011). To the east, partially located within the western extent of the array area, the Outer Dowsing Shoal is a shallow water bank aligned north-northwest to south-southeast, which shallows to a depth of 4m with associated gravel and sand deposits (Museum of London Archaeology, 2010). Combining with Cromer Knoll to the southeast, it forms a single morphologic feature approximately 50km long, rising 5m to 6m above the surrounding seabed, with the steepest flanks towards the southwest (Tappin *et al.*, 2011).
97. In the southeast of the Zol and extending into the southern part of the array area, Haddock Bank has an irregular plan shape and exhibits complex fining patterns across an uneven seabed topography (Holmes and Wild, 2003). The surficial medium to very coarse sands exhibit a generally steady decrease in mean grain size from the south-west to the north-east across the bank (Holmes and Wild, 2003).



Legend

- Array Area
- Offshore Export Cable Corridor
- ORCP Area
- Artificial Nesting Structure Area
- Biogenic Reef Restoration Area
- Physical Processes Zone of Influence
- ★ HD Model Timeseries Extraction Points
- Annex I Sandbanks (JNCC)

Depth (m)

- 0 - 10
- 10 - 20
- 20 - 30
- 30 - 40
- 40 - 50
- 50 - 60
- 60 - 70
- 70 - 80
- 80 - 90
- 90 - 100



Coordinate System: WGS 1984 UTM Zone 31N

0 10 20 km

Scale: 1:500,000

A3 Page Size

Environmental Statement

Major Sandbanks within the Study Area

Figure 7.14

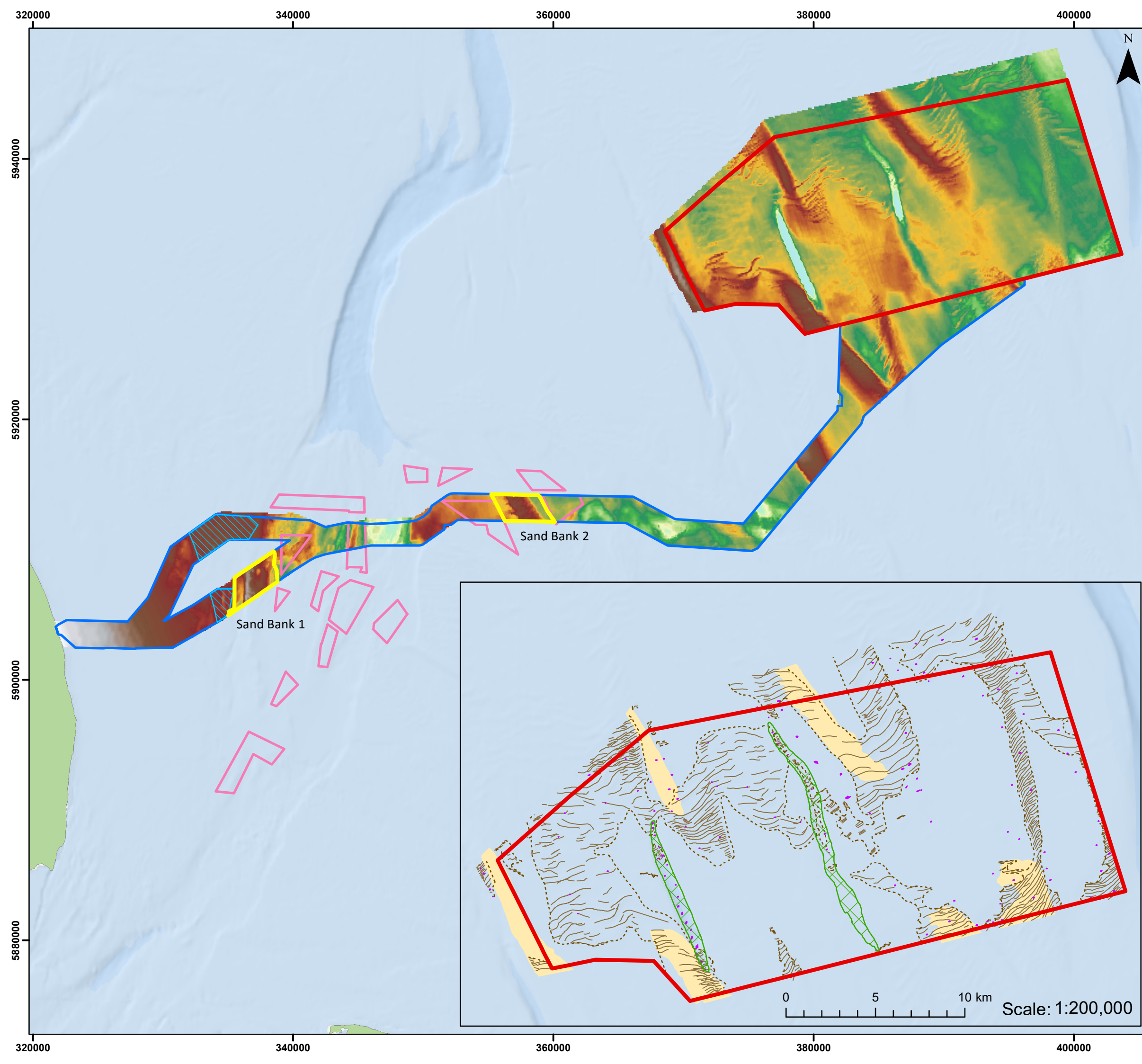


Date: 16/02/2024
 Produced By: BPHB
 Revision: 0.1

GoBe

Contains ESRI Basemapping;
 EMDOnet 2020 bathymetry

Document Path: Z:\GIS\GIS - Projects\0152 Outer Dowsing EIA\GIS\Figures\ES\Physical Processes Technical Report\DOOW_0152_PPT-R_Fig7_14_Major_Sandbanks1.mxd



Legend

- Array Area
- Offshore Export Cable Corridor
- ORCP Area
- Biogenic Reef Restoration Area
- Sand Bank Zones
- Sandwaves Area
- Sandwaves Crest
- Sandbank
- Megaripples Crest
- Canyon

Depth (m) (EMODnet, 2020)

0
32

Seafloor Morphology data provided by Enviros and is detailed in report 'Outer Dowsing Round 4 Draft Final Report - ENV21-21042-GTR4-04' May 2022



Coordinate System: WGS 1984 UTM Zone 31N

0 5 10 km

Scale: 1:275,000 A3 Page Size

Environmental Statement

Morphology of Array Area, Offshore ECC and at Landfall

Figure 7.15



Date: 16/02/2024
Produced By: BPHB
Revision: 0.1

GoBe Contains ESRI Basemapping; Esri, Garmin, GEBCO, NOAA NGDC, and other contributors

Document Path: Z:\GIS\GIS - Projects\0152 Outer Dowsing EIA\GIS\Figures\ES\Physical Processes Technical Report\ODOW_0152_PPTR_Fig7.15_Morphology.mxd

Offshore Export Cable Corridor

98. The Race Bank – North Ridge – Dudgeon Shoal and Inner Dowsing Annex I sandbank systems are located across the western half of the offshore ECC (Figure 7.1 and Figure 7.14). The Inner Dowsing sandbank is considered to be a relict feature, although it has experienced some changes in crest level, and is maintained by tidal currents (Centrica, 2007; JNCC, 2010). It is approximately 14km long with an undulating crest 5m to 10m above the general level of the seabed, with megaripples and sandwaves associated (HADA, 2012a).
99. The Race Bank – North Ridge – Dudgeon Shoal system is an example of an active sinusoidal sandbank feature located at a sediment transport bedload parting (TKOWFL, 2010). The banks are approximately 15km to 20km long, 1.5km to 3km wide and around 10m high, with sandwaves trending southeast to northwest (HADA, 2012a). Sediment transport modelling undertaken as part of the Race Bank OWF ES illustrated predominantly north-westerly sediment transport pathways across the majority of the site in question (Centrica, 2008). In addition, a general trend of westward migration of the North Ridge sandbank has been observed, with approximate lateral migration rates of 3.5m/year (East Point Geo Ltd., 2023).
100. There is evidence identified within the literature of clockwise sediment transport around Race Bank and North Ridge (HR Wallingford *et al.*, 2002; TKOWFL, 2010), primarily driven by tidal forcing (Centrica, 2009). However, geomorphological analysis as carried out by East Point Geo Ltd. (2023) identified bedform migration to the northwest on the eastern flank of the North Ridge sandbank, with southward migration on the western flank, suggesting anticlockwise sediment movement, which would be consistent with published current data indicating anticlockwise circulation at this location. Sandbank geometry can indicate regional-scale tidal flow and net sediment transport pathways, while sediment waves associated with sandbanks are a result of localised sediment transport regimes (Creane *et al.*, 2022). Open-shelf sinuous sandbanks are identified in Kenyon and Cooper (2005) as indicating no preferred direction of bedload transport, as evidenced by the position of the banks on a bedload parting. The bedform migration identified on the North Ridge sandbank may therefore be due to more localised sediment transport processes occurring within the wider sandbank system.
101. The offshore ECC route crosses through the Inner Dowsing sandbank and the North Ridge sandbank, the locations of which are shown in (Figure 7.15). The bathymetric profile at these locations is presented in Plate 7.7, indicating the presence of sandwaves and megaripples. The migration of these features is estimated to result in a change in seabed elevation of approximately between 5m and 6m at Inner Dowsing (referred to as Sand Bank 1), and approximately between 2m and 3m at North Ridge (referred to as Sand Bank 2).

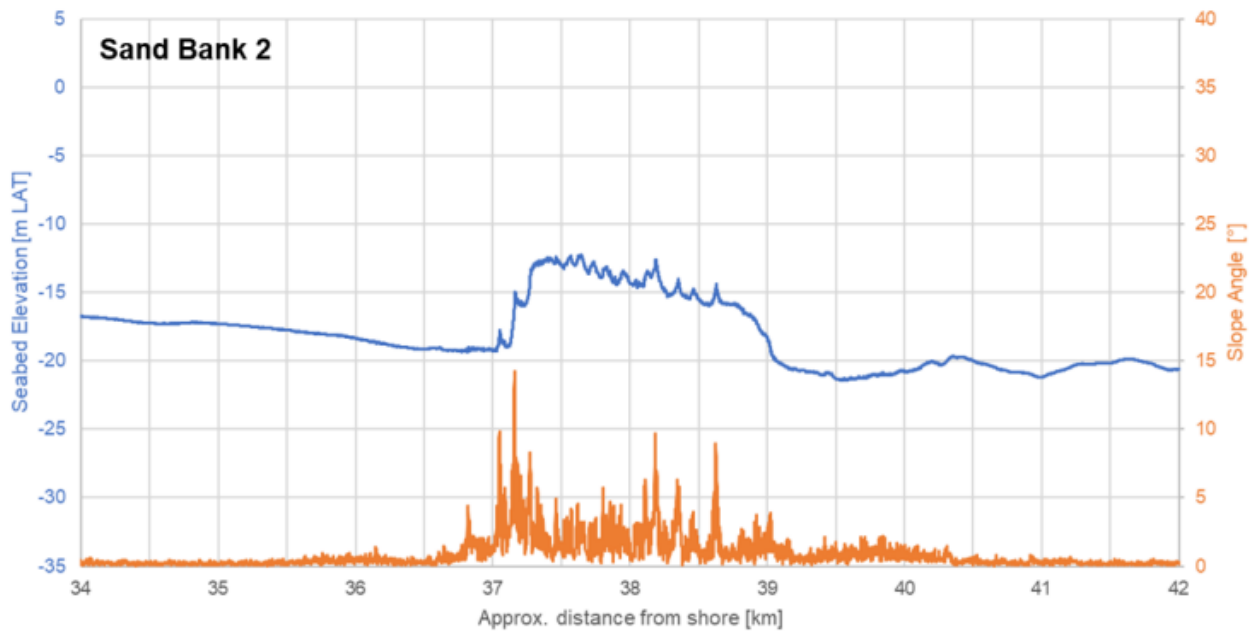
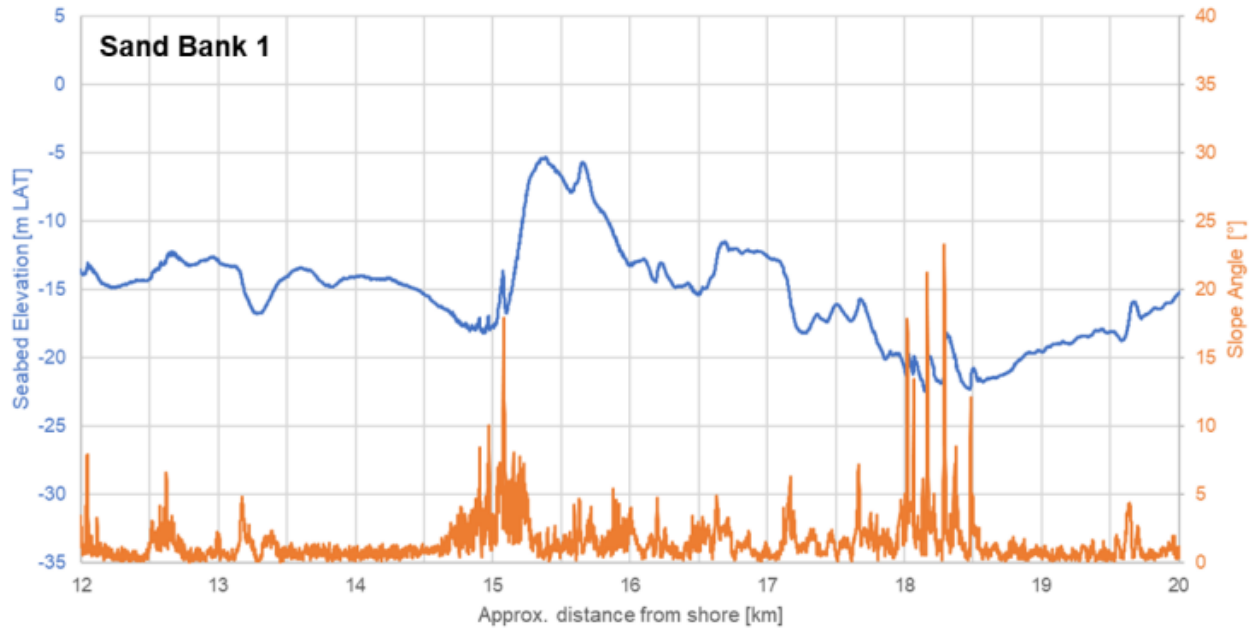


Plate 7.7 Bathymetric and gradient profile along the offshore ECC at the Inner Dowsing (Sand Bank 1) and North Ridge (Sand Bank 2) sandbanks, as labelled in Figure 7.15. Data from Project Cable Burial Risk Assessment (CBRA).

102. Inner Silver Pit, located landward of the array area and on the northern boundary of the offshore ECC, is an elongated, over-deepened and enclosed paleo-valley partly filled with unconsolidated sediments (Figure 7.1). Geological evidence suggests that this bathymetric deep may have been formed by similar processes as Sole Pit, specifically by erosion underneath a grounded ice sheets and later by tidal scour, although Tappin *et al.* (2011) highlights the complex, polygenetic origin of these bathymetric features. It is approximately 38km long, 2.5km wide and 100m deep, with changes in water depth in excess of 60m over 0.5km (Tappin *et al.*, 2011). Proctor *et al.* (2001) suggest that the depth enables tidal currents of sufficient strength to erode most materials, including gravels, that are deposited there, meaning there is little to no sediment accumulation. These sediments are moved along the Inner Silver Pit both to the north and south where they are transported out of the depression by tidal currents. This mechanism is enhanced by wave activity, particularly storm events, which can mobilise sediments throughout most of the deepest parts of the valley (TKOWFL, 2011).
103. An extensive channel system is located at the southern end of Inner Silver Pit and extends southwards towards the Lynne Deeps and the Wash, interpreted as a glacio-fluvial outwash fan (Tappin *et al.*, 2011). As with other deeps in the area, such as Sole Pit, erosion exposes bedrock at the seabed within the Inner Silver Pit, with chalk strata with a strike of east-northeast to west-southwest well defined on geophysical survey data as shown in Figure 7.9 (Tappin *et al.*, 2011).

Coast

104. The Lincolnshire coast has a roughly convex outline, bound by the River Humber to the north and the Wash in the south (Environment Agency, 2011). The coast is characterised generally by wide sandy beaches, overlying Bolder Clay, which reduce in width towards the south. Gibraltar Point is located at a distinct orientation change of the coastline into the Wash, and represents a spit maintained by sediment transport from the Lincolnshire and North Norfolk coasts, in addition to that from offshore sandbanks just offshore of Skegness (Environment Agency, 2010). Between Mablethorpe and Skegness, a stretch of coast approximately 24km, the coast has a convex outline and is east-facing, increasing its exposure to the prevailing north-easterly waves. The wave regime is the main driver of sediment transport in the nearshore zone, with the inner depth of closure¹⁹, corresponding to the seaward limit of the upper shoreface, calculated as approximately 7.1m²⁰.

¹⁹ The inner depth of closure marks the transition from upper to lower shoreface and corresponds to the depth where only 12 hours per year wave action is strong enough to produce substantial suspended sediment transport.

²⁰ Using Houston's (1995) expression of Hallermeier's (1981) formula for inner closure depth, using annual mean significant wave height from the Chapel Point Waverider Buoy (Environment Agency, 2021).

105. This section of coast has historically been highly sensitive to wave action and has suffered from long-term erosion, with an estimated erosion rate of approximately 1.3m/year (HADA, 2012a; TKOWFL, 2015). Much of the surficial beach layer has been removed by contemporary hydrodynamic processes, and an annual beach nourishment scheme has been in operation since 1994 (as outlined previously in paragraph 65), increasing the stability of the coast (Environment Agency, 2019a; 2019b). Much of the frontage from Mablethorpe to Skegness has been engineered and there is a legacy of timber groynes, although many of these are historic and those that have not been removed have deteriorated or have been buried by renourished sediment (Environment Agency, 2011).
106. The coast between Anderby Creek and Chapel St Leonards (indicated on Figure 7.1) shows less variability than further north along the coast, although the general trend is erosional and beach levels have been regularly renourished since the late 1990s. The coastal frontage at the proposed Landfall site is characterised by the presence of a sandy beach backed by vegetated sand dunes, indicating that the upper beach has remained stable over time (HADA, 2012a). These vegetated sand dunes can be identified on the aerial imagery in Plate 7.8 and Plate 7.9, providing further evidence of stability approximately within the last decade.
107. Similarly to many beaches along the Lincolnshire coast, there is a distinctive ridge and runnel pattern on the beach as seen on Plate 7.8, with ridges becoming more prominent in calm, low energy conditions following a storm event, and are understood to return sediment removed offshore during storms (Environment Agency, 2011). However, these features vary over spatial and temporal scales, partly driven by variation in the wave regime, with steeper waves during winter transporting sands offshore and less steep waves during summer returning sands to the beach (TKOWFL, 2015). An outfall located in the northern half of the offshore ECC shown on Plate 7.8 and Plate 7.9, acts as a groyne, with sediment build-up on the northern side, reflecting the southerly direction of sediment transport.
108. Annual topographic surveys, collected by the Environment Agency, have been used to give an indication of morphology and trends along this area of the coast. An analysis of topographic surveys taken between 1991 and 2006 found that the beach nourishment programme (as outlined previously in paragraph 65) successfully led to accreting beach profiles, however between annual nourishment events the beach continued to erode, demonstrating a continuing natural erosional trend (Environment Agency, 2011). The erosion is concentrated around the low water mark, with an accretionary trend displayed by the upper beach (HADA, 2012a).
109. This pattern is ongoing, with the beach at Wolla Bank displaying a distinctive seasonal shift in the foreshore width, the timing of which is affected by nourishment activities. The difference in the foreshore, as shown from surveys, at 25m intervals between 2010 and 2011, before and after nourishment activities is presented in Figure 7.16. Elevation changes between 2011 and 2013, with an erosional trend in the mid-beach region, with accretion on the upper beach are shown in Figure 7.17 and Plate 7.10 (Environment Agency, 2013a). This is thought to be partly due to the pooling of standing water on the beach, which is slow to percolate through the sand and drain into the sea, as indicated on Plate 7.8.



Plate 7.8 Aerial photograph of the beach at transect L048 (see Figure 7.16), showing outfall and wet sand with channels running out to sea on the lower beach. Photo from 26 May 2012 (Environment Agency, 2013a). Transect is located in the northern half of the offshore ECC.

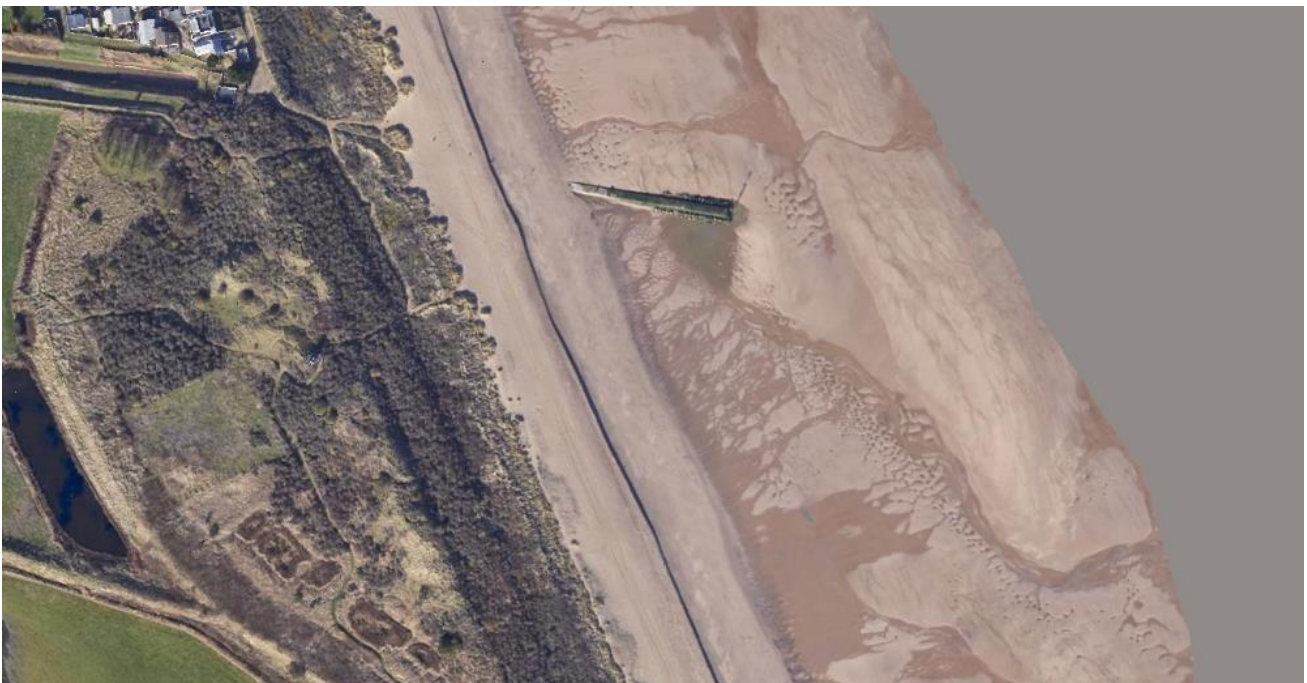


Plate 7.9 Aerial photograph of the beach approximately at transect L048 (see Figure 7.16), showing outfall and wet sand with channels running out to sea on the lower beach (APEM, 2023). Transect is located in the northern half of the offshore ECC.



Legend

- Offshore Export Cable Corridor
- Survey Transects

Difference (m)

- >=4.5
- 3 - 4.5
- 2.5 - 3
- 2 - 2.5
- 1.5 - 2
- 1 - 1.5
- 0.5 - 1
- 0.25 - 0.5
- 0.25 - 0.25
- 0.5 - -0.25
- 1 - -0.5
- 1.5 - -1
- 2 - -1.5
- 2.5 - -2
- 3 - -2.5
- 3.5 - -3
- <= -3.5

Coordinate System: British National Grid

0 100 200 m

Scale: 1:5,000 A3 Page Size

Environmental Statement

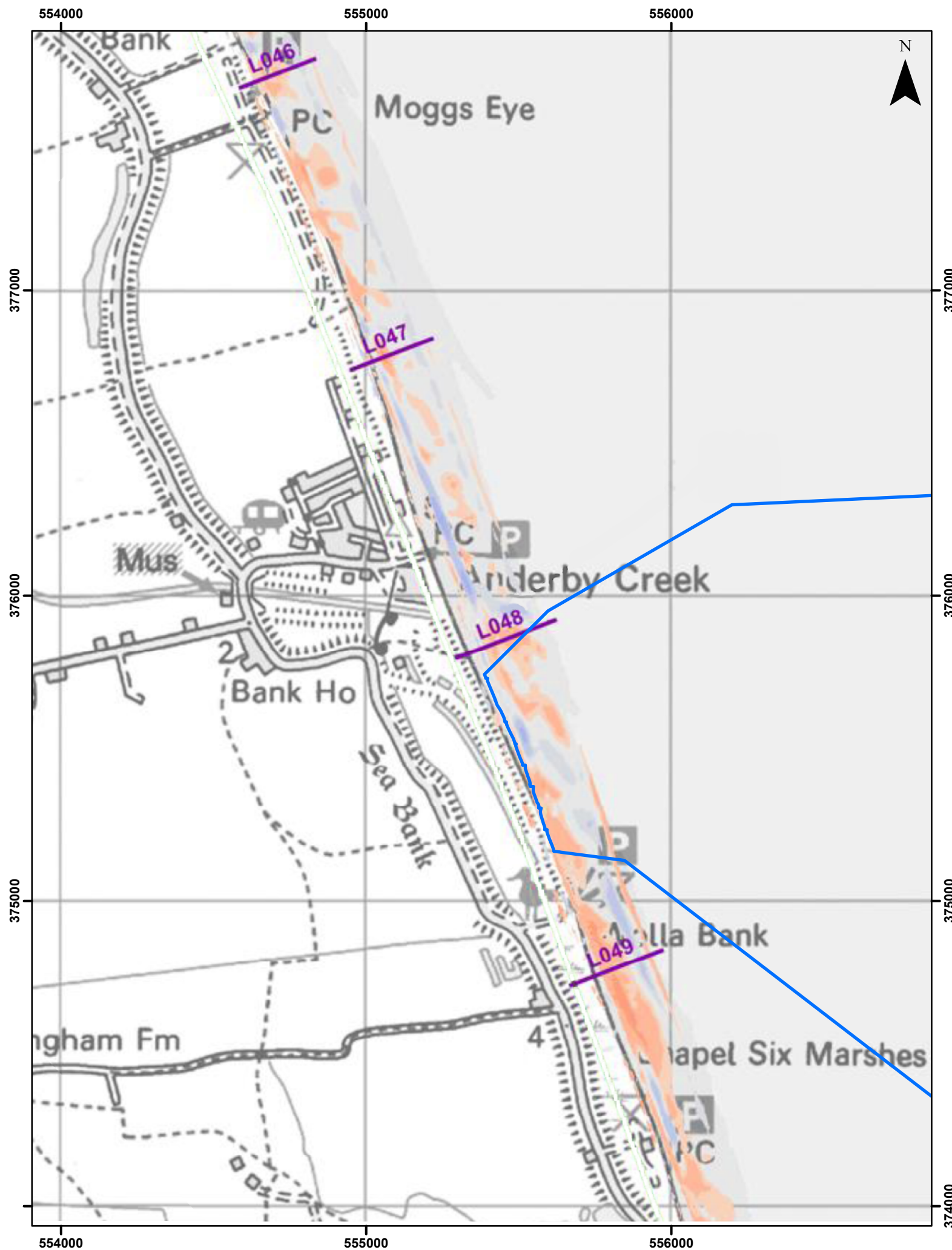
Beach Elevation Change from Surveys at 25m Intervals between 2011 and 2010 (Pre and Post Nourishment Activities) at Wolla Bank

Figure 7.16

Date: 15/02/2024
 Produced By: BPHB
 Revision: 0.1

Contains ESRI Basemapping; EMDOnet 2020 bathymetry

Document Path: Z:\GIS\GIS - Projects\0152 Outer Dowsing ELA\GIS\Figures\ES\Physical Processes Technical Report\ODOW_0152_PPTR_Fig7_16 Beach Elevation Change 2010_2011.mxd



Legend

- Offshore Export Cable Corridor
- Survey Transects

Difference (m)

- >=4.5
- 3 - 4.5
- 2.5 - 3
- 2 - 2.5
- 1.5 - 2
- 1 - 1.5
- 0.5 - 1
- 0.25 - 0.5
- 0.25 - 0.25
- 0.5 - -0.25
- 1 - -0.5
- 1.5 - -1
- 2 - -1.5
- 2.5 - -2
- 3 - -2.5
- 3.5 - -3
- <= -3.5

Coordinate System: British National Grid

0 500 1,000 m

Scale: 1:15,000 A3 Page Size

Environmental Statement

Beach Elevation Change between 2013 and 2011 between Moggs Eye and Wolla Bank

Figure 7.17

Date: 15/02/2024
 Produced By: BPHB
 Revision: 0.1

Contains ESRI Basemapping;
 EMDOnet 2020 bathymetry

Document Path: Z:\GIS\GIS - Projects\0152 Outer Dowsing EIA\GIS\Figures\ES\Physical Processes Technical Report\DOCW_0152_P1R_Fig7_17 Beach Elevation Change 2011_2013.mxd

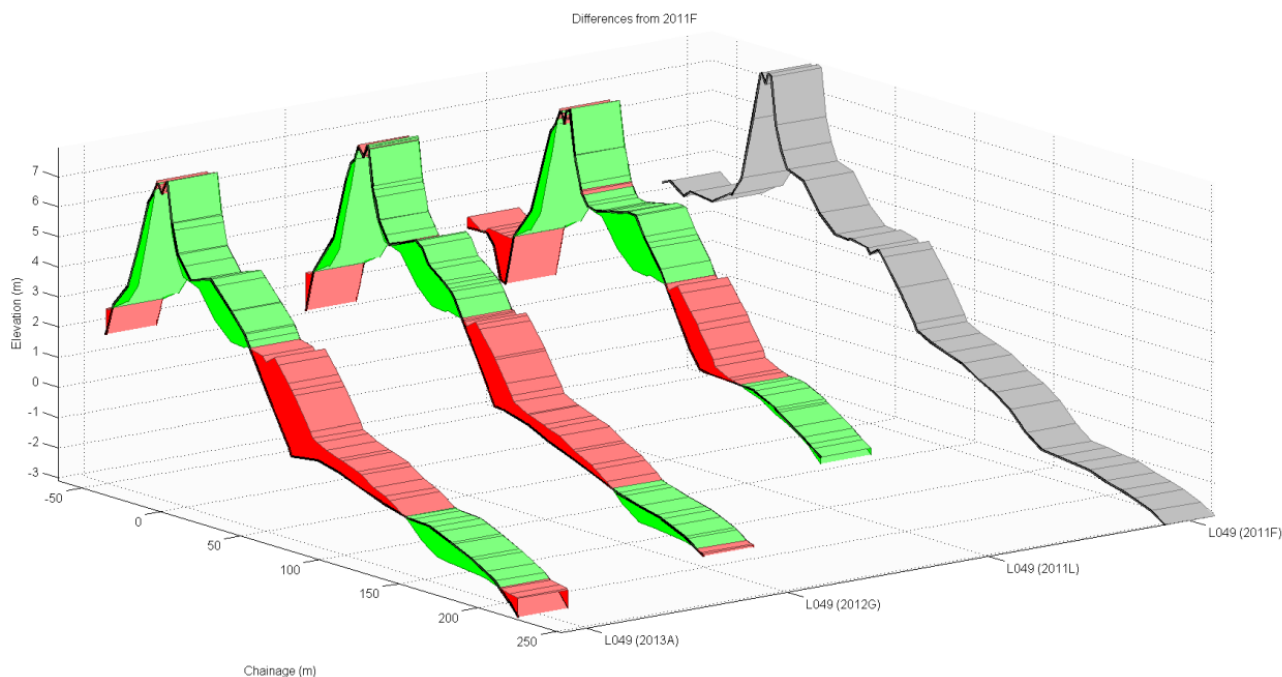


Plate 7.10 Difference in the beach profile at transect L049 (see Figure 7.17) over the last three surveys compared to the beach in June 2011. Lowering is shown in red (Environment Agency, 2013a)

110. Light Detection and Ranging (LiDAR) data from the National Network of Regional Coastal Monitoring Programmes (NNRCMP) has been used to assess change in the beach topography between 2016 and 2020 (as shown in Figure 7.18 to Figure 7.20 and Plate 7.11). This indicates that the mid-beach has generally experienced erosion since 2016, with accretion in the upper and lower beach, although patterns are highly variable as a result of ridge and runnel patterns and the identification of minor shelf features, as demonstrated in Plate 7.9. This pattern is the same as that identified within the topographic survey data collected by the Environment Agency, which similarly identified an erosional pattern in the mid-beach and potentially attributed it to the influence of standing water which is slow to percolate through the sand (Figure 7.17; Plate 7.11; Environment Agency, 2013a). Due to the continued artificial beach nourishment and natural erosional processes taking place during this time period, it is difficult to distinguish individual processes. The data does however demonstrate the highly dynamic nature of the beach and intertidal area, with elevation differences over the four year period in some cases reaching over 2m.

111. Sand dune systems are an important natural coastal flood defence, providing protection to the low-lying hinterland of East Lincolnshire. The degree of mobility of both individual dunes and dunefields as a whole is dependent on two main factors. These are, firstly, erosion/accretion at the dune beach-dune interface, which reflects the sediment budget of the upper beach and the foredunes, and secondly, the balance between vegetation cover and wind stresses across the wider dune system. The morphology and mobility of frontal dunes is therefore closely related to that of the adjoining beach and nearshore zone (Pye *et al.*, 2007).

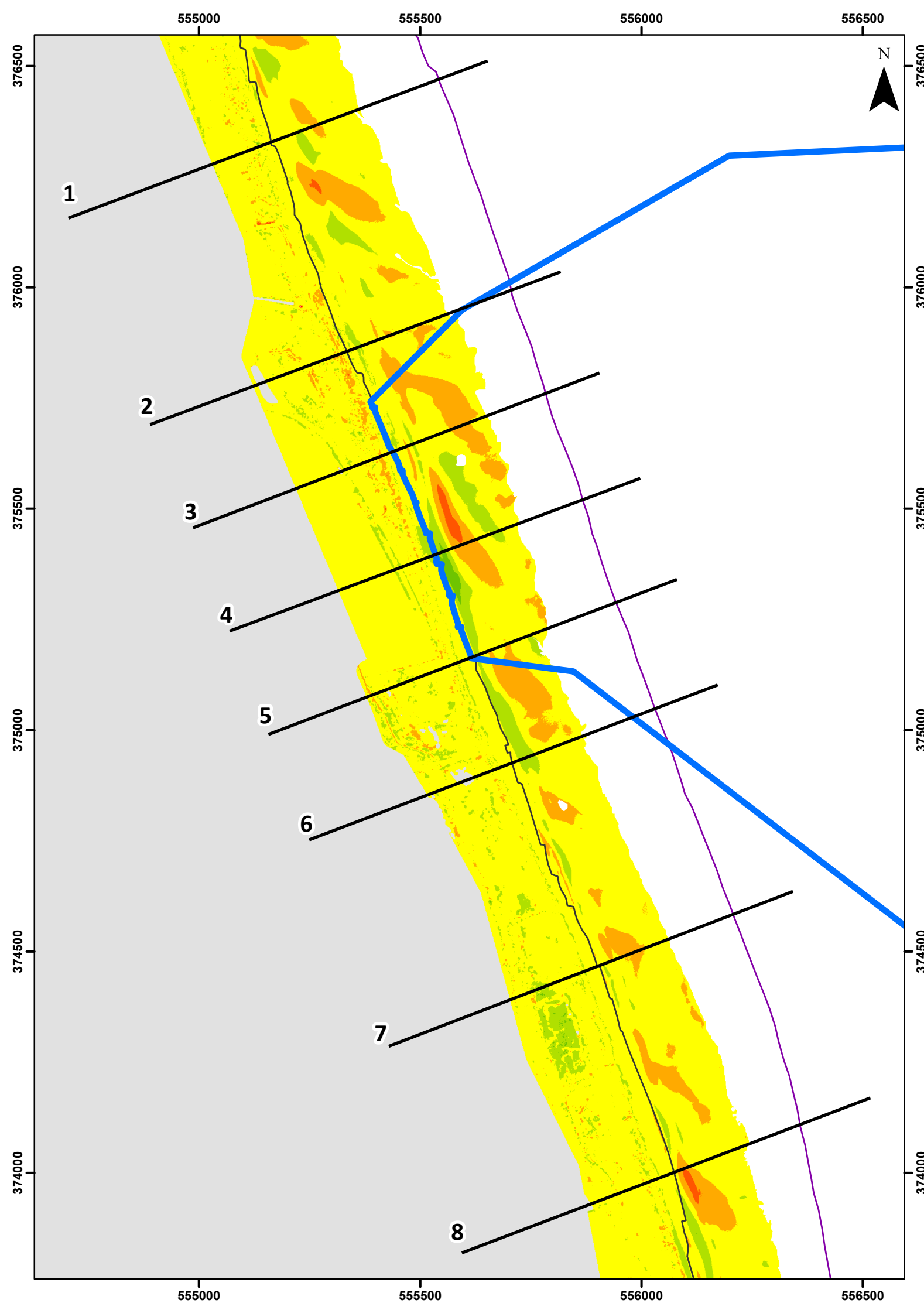
112. Characterisation work carried out by Pye *et al.* (2007) compiled available information on the geomorphological and sedimentological character and management status of coastal dune systems across England. For the stretch of coast between Sutton on Sea and Chapel St Leonards, the dune morphology was classified as ‘foredunes’, using the scheme proposed by Pye (1983). Dunes were identified as being typically between 4m and 8m Ordnance Datum (OD), with renewed dune growth since 2000 as a result of beach nourishment (Pye *et al.*, 2007). Sediment samples were collected along transects perpendicular to the coastline as part of the development of a coastal dune sediment database, with five sample sites at the Landfall area, as shown on Figure 7.17 (Saye and Pye, 2004). The results of particle size analysis for these samples are shown in Table 7.16, indicating that the dunes are primarily composed of medium sand. LiDAR data between 2016 and 2020 (Plate 7.11) indicates little to no change across the dunes, suggesting that these are stable features.

Table 7.16 Particle size characteristics of dune sediments collected from dune sites at the Landfall area (Saye and Pye, 2004)

Sample ID	Mean (µm)	Median (µm)	Mode (µm)	Clay (%)	Silt (%)	Sand (%)
CLEO 5A	374.0	370.5	356.1	0.000	0.37	99.63
CLEO 5B	328.8	342.4	356.1	0.130	1.99	97.88
CLEO 5C	335.4	359.3	356.1	0.140	2.77	97.09
CLEO 4A	366.0	371.3	356.1	0.089	0.75	99.16
CLEO 4B	421.6	424.8	429.2	0.000	0.59	99.41

Compensation Areas

113. The northern ANS area is located close to the northern reaches of the Inner Silver Pit, characterised previously in paragraph 102, and in an area of sandwaves with amplitudes ranging generally from 2m to 8m and crests oriented roughly east-northeast to west-southwest (Tappin *et al.*, 2011; EMODnet, 2020). The southern ANS area overlies the Coal Pit, a linear submarine valley likely to have formed in a similar manner to other tunnel-valleys across the region, as outlined in paragraph 93. The morphology within the biogenic reef creation area may be generally characterised using the information provided in paragraph 92 *et seq.*



Legend

- Offshore Export Cable Corridor
- MHWS
- MLWS
- Coastal Lidar Transects

Height Difference (m)

- 2 - -3
- 1 - -2
- 0 - -1
- 0
- 0 - 1
- 1 - 2

Coordinate System: British National Grid
 0 200 400 m
 Scale: 1:10,000 A3 Page Size

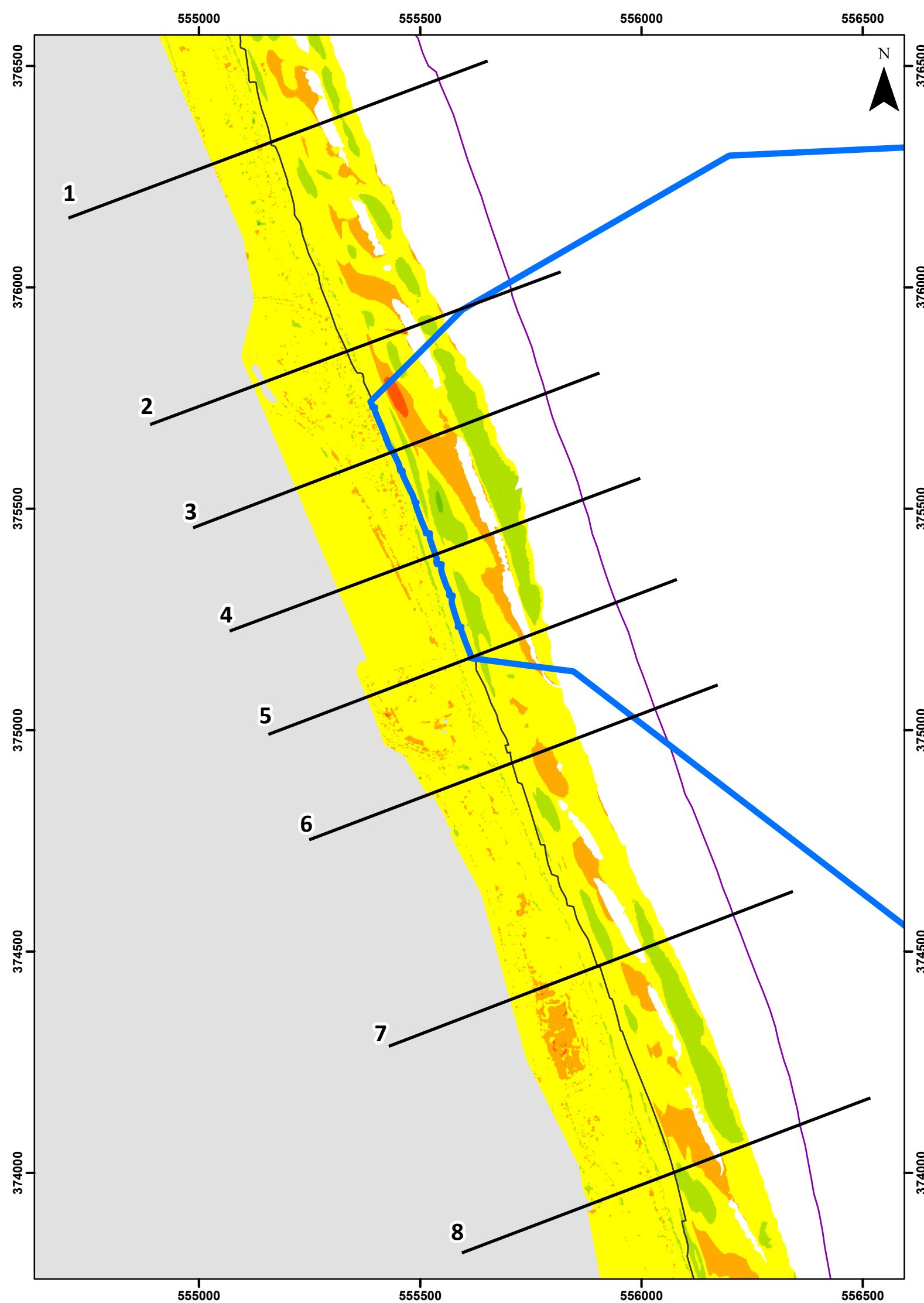
Environmental Statement
 Elevation Change from Coastal LiDAR Data
 between 2018 and 2016 at the landfall location

Figure 7.18

Date: 15/02/2024
 Produced By: BPHB
 Revision: 0.1

Contains ESRI Basemapping;
 EMDOnet 2020 bathymetry

Document Path: Z:\GIS\GIS - Projects\0152 Outer Dowsing EIA\GIS\Figures\ES\Physical Processes Technical Report\ODOW_0152_PPTR_Fig7_18 Beach Elevation Change 2018_2016.mxd



Legend

- Offshore Export Cable Corridor
- MHWS
- MLWS
- Coastal Lidar Transects

Height Difference (m)

- 2 - -3
- 1 - -2
- 0 - -1
- 0 - 1
- 1 - 2
- 2 - 3



Coordinate System: British National Grid
 0 200 400 m
 Scale: 1:10,000 A3 Page Size

Environmental Statement
 Elevation Change from Coastal LiDAR Data
 between 2020 and 2018 at the landfall location

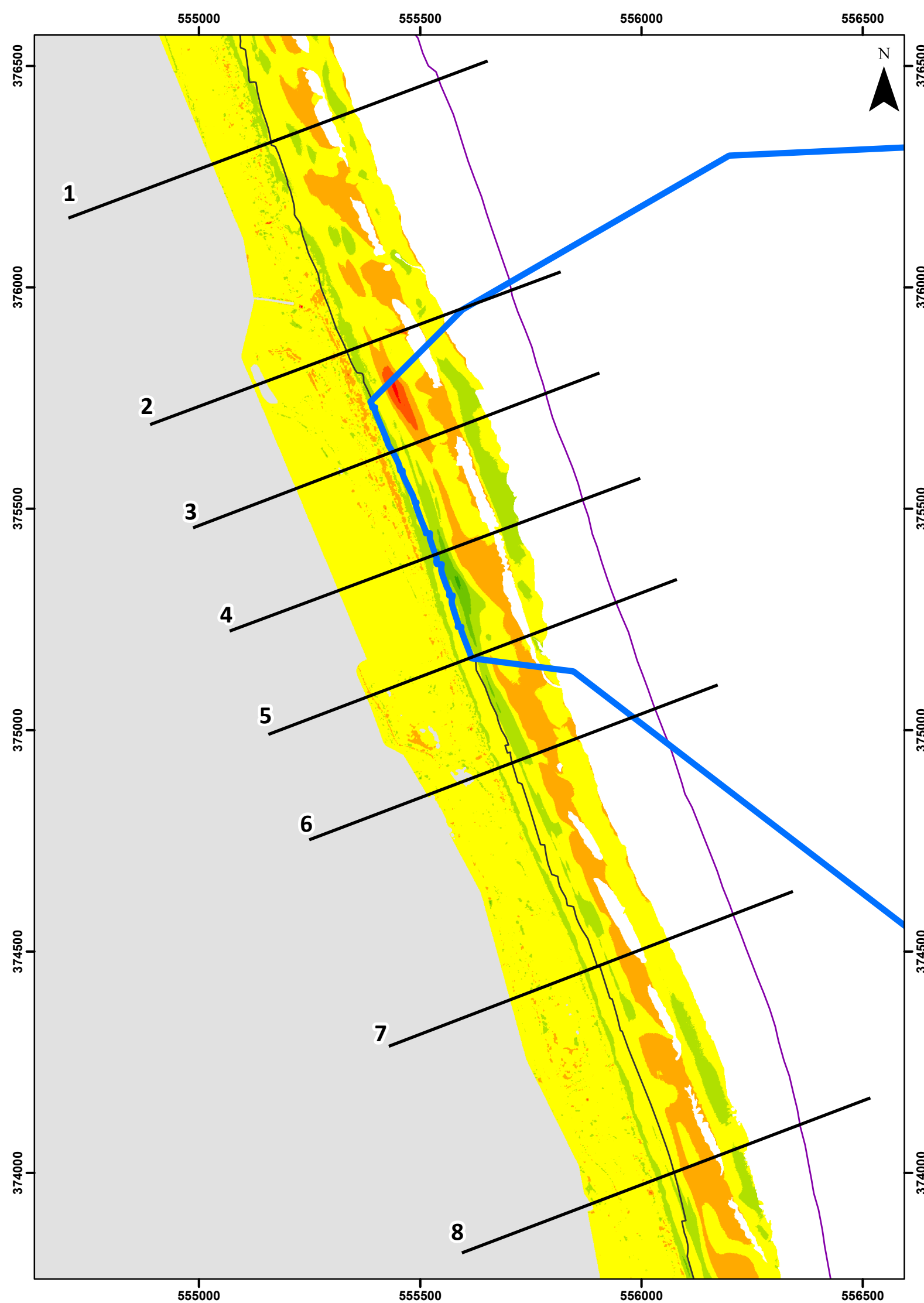
Figure 7.19



Date: 15/02/2024
 Produced By: BPHB
 Revision: 0.1



Contains ESRI Basemapping;
 EMDOnet 2020 bathymetry



Legend

- Offshore Export Cable Corridor
- MHWs
- MLWS
- Coastal Lidar Transects

Height Difference (m)

- 2 - -3
- 1 - -2
- 0 - -1
- 0 - 1
- 1 - 2
- 2 - 3

Coordinate System: British National Grid

0 200 400 m

Scale: 1:10,000 A3 Page Size

Environmental Statement

Elevation Change from Coastal LiDAR Data between 2020 and 2016 at the landfall location

Figure 7.20

OUTER DOWSING OFFSHORE WIND

Date: 15/02/2024
 Produced By: BPHB
 Revision: 0.1

GoBe

Contains ESRI Basemapping; EMDOnet 2020 bathymetry

Document Path: Z:\GIS\GIS - Projects\0152 Outer Dowsing EIA\GIS\Figures\ES\Physical Processes Technical Report\ODOW_0152_PPT-R_FIG7.20 Beach Elevation Change 2020_2016.mxd



Plate 7.11 Difference plots between LiDAR data across the dune and beach frontage between 2016 and 2020, with transect locations shown in Figure 7.20. MHWS and MLWS are indicated by the blue and red dots, respectively.

7.5 Future Baseline Environment

114. A consideration of the future baseline, including the associated variation, is provided in the context of the operating lifetime of the Project. For the current purposes of this scoping document, the Representative Concentration Pathway (RCP) 8.5 (high emissions) scenario (Palmer *et al.*, 2018) has been presented.
115. The UK Climate Projections 2018 (UKCP18) suggests an increase in mean sea level (MSL) of over 0.7m by 2100 along the Lincolnshire coast (Palmer *et al.*, 2018). This effect would also redefine both tidal levels and extreme water levels presented in Table 7.7 and Table 7.8, respectively, translating the position of high water further landward and increasing the potential of coastal erosion and flooding events. However, the tidal response along this part of the coastline is predicted to be small (less than 5% change in standard deviation of tide) even under a large time-mean sea level increase (Palmer *et al.*, 2018). Future changes in storm surges are predicted to be undistinguishable from background variation (Lowe *et al.*, 2009).
116. Wave energy is predicted to decrease, such that by 2100 a decrease larger than 10% has been modelled in the North Sea (RCP8.5 scenario; Bonaduce *et al.*, 2019; Meucci *et al.*, 2020). Inter-decadal variability may be largely due to the influence of local weather in the North Sea (EDF ENERGY, 2021).
117. The preferred management strategy in place along this part of the coast (between Mablethorpe and Skegness) from 2025 to 2055 is to maintain flood defences in their current position and to raise and improve them to counter sea level rise as required (Environment Agency, 2019a). Beach nourishment is currently ongoing, and it is predicted that the levels and frequency of sand required will increase due to climate change impacts. The proposed strategy over the next 100 years is therefore to implement a combination of rock structures and beach nourishment. This will be a phased process with beach nourishment continuing in its current form until 2024, with structures to be implemented between 2025 and 2030 (Environment Agency, 2019). Data from the National Coastal Erosional Risk Mapping 2018 – 2021 (NCERM2) dataset predicts no future erosion over the frontages located at landfall over the next 100 years (Environment Agency, 2024)

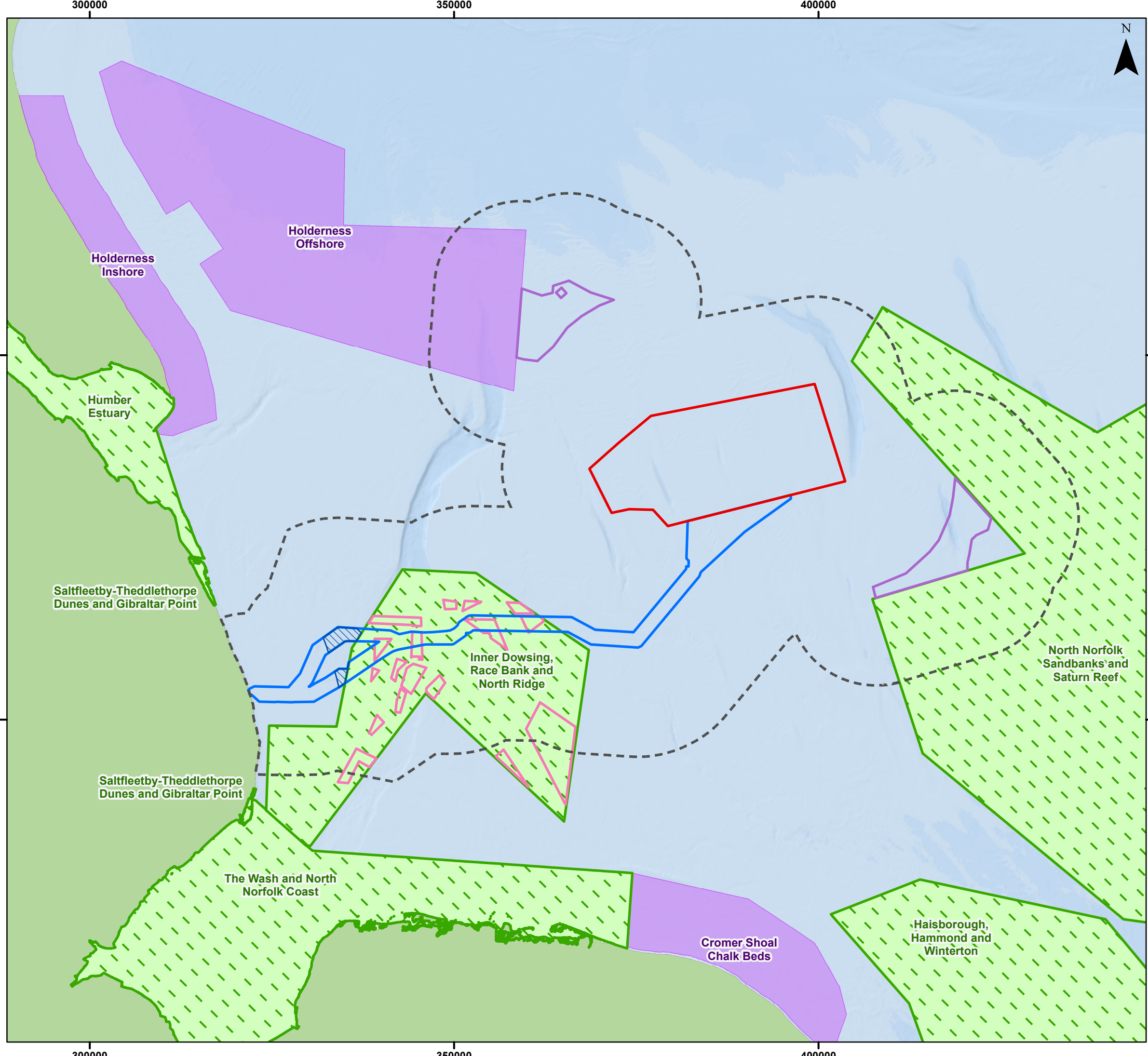
7.6 Designated Sites and Protected Species

118. Designated sites in the vicinity of the study area, which are designated for the protection and conservation of marine habitats up to MHWS are shown in Figure 7.21. A list of designated sites within the Marine Processes ZoI, with detail of the relevant protected features, is provided below:
- North Norfolk Sandbanks and Saturn Reef Special Area of Conservation (SAC):
 - Reefs; and
 - Sandbanks which are slightly covered by sea water all of the time.
 - Inner Dowsing, Race Bank and North Ridge SAC:
 - Reefs; and

- Sandbanks which are slightly covered by sea water all of the time.

119. One coastal (Sites of Special Scientific Interest (SSSI)) site is also present:

- Chapel Point – Wolla Bank SSSI: national importance in the Geological Conservation Review.



Legend

- Array Area
- Offshore ECC Boundary
- ORCP Area
- Artificial Nesting Structure Area
- Biogenic Reef Restoration Area
- Physical Processes Zone of Influence
- Marine Conservation Zones
- Special Areas of Conservation



Coordinate System: WGS 1984 UTM Zone 31N
 0 10 20 km
 Scale: 1:500,000 A3 Page Size

Environmental Statement
 Designated Sites of relevance to
 Marine Physical Processes

Figure 7.21



Date: 16/02/2024
 Produced By: BPHB
 Revision: 0.1

Contains ESRI Basemapping;
 Esri, Garmin, GEBCO, NOAA
 NGDC, and other contributors

Document Path: Z:\GIS\GIS - Projects\0152 Outer Dowsing EIA\GIS\Figures\ES\Physical Processes Technical Report\DOOW_0152_PPT_R_Fig7_21_Designated Sites.mxd

7.7 References

ABPmer (2018). SEASTATES Metocean Data and Statistics Interactive Map. Available online at: www.seastates.net [Accessed September 2022].

ABPmer, Met Office and POL (2008). 'Atlas of UK Marine Renewable Energy Resources: Atlas Pages. A Strategic Environmental Assessment Report, March 2008'. BP Marine Environmental Research Ltd. Produced for BERR. Report and associated GIS layers available at: <http://www.renewables-atlas.info/> [Accessed: May 2022].

Balson, P. S. (1999), 'The Holocene Coastal Evolution of Eastern England: Evidence from the southern North Sea'. *Proceedings of Coastal Sediments*, 99,1284-1293.

Belderson, R.H., Johnson, M.A., Kenyon, N.H. (1982), 'Bedforms', in Stride, A.H. (ed.), *Offshore tidal sands: Processes and deposits*'. Chapman and Hall, London, 27-57.

Blott, S.J. and Pye, K. (2004), 'Morphological and sedimentological changes on an artificially nourished beach, Lincolnshire, UK'. *Journal of Coastal Research*, 20(1), 214-233.

Bonaduce, A., Staneva, J., Behrens, A., Bidlot, J-R., and Wilcke, R.A.I, (2019), 'Wave Climate Change in the North Sea and Baltic Sea'. *Journal of Marine Science and Engineering*, 2019(7), DOI:10.3390/jmse7060166.

Briggs, K., Thomson, K., and Gaffney, V. (2007), 'A geomorphological investigation of submerged depositional features within the Outer Silver Pit, Southern North Sea', in Gaffney, V.L., Thomson, K. and Fitch, S. (eds.), *Mapping Doggerland: the Mesolithic landscapes of the southern North Sea*. Archaeopress (Oxford).

Cameron, T.D.J., Crosby, A., Balson, P.S., Jeffery, D.H., Lott, G.K., Bulat, J., and Harrison, D.J. (1992), 'The Geology of the Southern North Sea'. (London: HMSO).

Cathie (2021), 'Desktop Study and Preliminary Ground Model'. UK Round 4 Offshore Windfarm – Outer Dowsing. Report for Total E&P.

Cefas (2016), 'Sediment Climatologies around the UK'. Report for the UK Department for Business, Energy & Industrial Strategy (BEIS) Offshore Energy Strategic Environmental Assessment (OESEA) programme.

Centrica (2007), 'Lincs Offshore Windfarm Environmental Statement. Chapter 5: Description of the Existing Environment'.

Centrica (RBW) Ltd (2008), 'Race Bank Environmental Statement. Chapter 5: Physical Environment'.

Creane, S., Coughlan, M., O'Shea, M. and Murphy, J. (2022), 'Development and dynamics of sediment waves in a complex morphological and tidal dominant system: southern Irish Sea'. *Geosciences*, 12(12), p.431.

Defra (2002). 'Futurecoast'.

Defra (2022), 'Inner Silver Pit South: Consultation factsheet for candidate Highly Protected Marine Area (HPMA)'. https://consult.defra.gov.uk/hpma/consultation-on-highly-protected-marine-areas/supporting_documents/Annex%20E%20Inner%20Silver%20Pit%20South%20candidate%20HPMA%20factsheet.pdf [Accessed September 2022].

Department of Energy and Climate Change (DECC) (2016), 'Offshore Energy Strategic Environmental Assessment 3 (OESEA3) Environmental Report'.

Dove, D., Evans, D.J., Lee, J.R., Roberts, D.H., Tappin, D.R., Mellett, C.L., Long, D. and Callard, S.L. (2017), 'Phased occupation and retreat of the last British–Irish Ice Sheet in the southern North Sea; geomorphic and seismostratigraphic evidence of a dynamic ice lobe', *Quaternary Science Reviews*, 163: 114-134.

East Point Geo Ltd. (2023), 'Outer Dowsing Offshore Wind – Seabed Mobility Study'. CONFIDENTIAL.

EDF ENERGY, SZC and CGN (2020), 'The Sizewell C Project. Volume 2 Main Development Site, Chapter 20 Coastal Geomorphology and Hydrodynamics'. Revision 1.0. The Inspectorate Reference Number: EN010012.

EMODnet. (2020), 'European Marine Observation and Data Network (EMODnet) Bathymetry data'. <https://portal.emodnet-bathymetry.eu> [Accessed: September 2022].

EMU Ltd and Osiris (2008), 'Geophysical investigations at the proposed Race Bank and Docking Shoal Wind Farm sites with associated cable route corridors Section 2 – Race Bank'. Projects Report JVEO.1.02.0886 – 02.

Environment Agency (2011), 'Coastal Morphology Report: Lincolnshire (Mablethorpe to Skegness)'.

Environment Agency (2013a), 'Coastal Morphology Technical Note, Lincshire'.

Environment Agency (2013b), 'Sea State Report: Chapel Point wave buoy, 2012-2013'.

Environment Agency (2018), 'Coastal flood boundary conditions for UK mainland and islands'. Project: SC060064/TR2: Design Sea Levels.

Environment Agency (2019a), 'Saltfleet to Gibraltar Point Strategy'.

Environment Agency (2019b), 'Saltfleet to Gibraltar Point Strategy. Strategic Environmental Assessment: Environmental Report'.

Environment Agency (2021), 'Chapel Point Annual Wave Report 2021'.

Enviros (2022), 'Outer Dowsing Offshore Wind Farm Geophysical UHRS and Light Geotechnical Survey, East Anglia, Offshore UK'.

Equinor (2022), 'Sheringham Shoal and Dudgeon Offshore Wind Farm Extension Projects Environmental Statement. Volume 1 Chapter 6 – Marine Geology, Oceanography and Physical Processes.'

Environment Agency (2024), 'National Coastal Erosion Risk Mapping (NCERM) – National (2018 – 2021)'. <https://www.data.gov.uk/dataset/7564fcf7-2dd2-4878-bfb9-11c5cf971cf9/national-coastal-erosion-risk-mapping-ncerm-national-2018-2021> [Accessed: February 2024].

Flather, R.A. and Williams, J.A. (2000), 'Climate change effects on storm surges: methodologies and results', in Beersma, J., Agnew, M., Viner, D., Hulme, M. (eds.), 'Climate scenarios for water-related and coastal impact' (Norwich: CRU, ECLAT-2 Workshop Report, No.3).

Fugro (2023), 'Final Metocean Data Report'.

GEOxyz. (2022a), 'Benthic Ecology OWF Area Results Report (Vol. 1) UK4855H-824-RR-01'.

GEOxyz. (2022b), 'Benthic Ecology ECC Area Results Report (Vol. 2) UK4855H-824-RR-02'.

GEOxyz. (2022c), 'Environmental, Geophysical and Geotechnical Site Investigations 2022 – Outer Dowsing OWF, Funnel and ECC. Field Report – Geo Ocean III – Offshore Phase 2. Geophysical and UHRS (OWF, Funnel & ECC)'.

Hallermeier, R.J. (1980). 'A profile zonation for seasonal sand beaches from wave climate'. Coastal engineering, 4, 253-277.

Houston, J.R. (1995), 'Beach-fill volume required to produce specified dry beach width'. Coastal Engineering Technical Note, 11-32.

Holmes, R., and Wild, J.B.I (2003), 'DTI Strategic Environmental Assessment Area 2 (SEA2) geological processes (interpretation of multibeam, sidescan sonar, chirp and grain size data acquired in 2001 from the seafloor of the Norfolk Banks and Dogger Bank, southern North Sea)'. BGS Internal Report CR/03/188.

HR Wallingford, Posford Haskoning, CEFAS and Dr Brian D'Olier (2002), 'Southern North Sea Sediment Transport Study (SNSSTS) Phase 2: Sediment Transport Report'. Report No. EX4526, August 2002.

Humber Aggregate Dredging Association (HADA) (2012a), 'Marine Aggregate Regional Environmental Assessment of the Humber and Outer Wash Region'. <http://marine-aggregate-rea.info/sites/www.marine-aggregate-rea.info/files/private/volume-i-marea-final-hada-report-10-may-2012.pdf> [Accessed: May 2022].

Humber Aggregate Dredging Association (HADA) (2012b), 'Marine Aggregate Regional Environmental Assessment of the Humber and Outer Wash Region Appendix E - Physical Processes Study: Baseline Characterisation'. <http://marine-aggregate-rea.info/sites/www.marine-aggregate-rea.info/files/private/appendix-e-abpmer-phys.pdf> [Accessed: September 2022].

JNCC (2010). 'Special Area of Conservation (SAC): Inner Dowsing, Race Bank and North Ridge. SAC Selection Assessment Version 5.0'. <http://publications.naturalengland.org.uk/publication/3288484?category=3229185> [Accessed: November 2022].

Kenyon, N. and Cooper, B. (2005), 'Sand banks, sand transport and offshore windfarms: Technical Report', DTI SEA 6 Technical Report.

Lowe, J., Howard, T., Paradaens, A., Tinker, J., Holt, J., Wakelin, S., Milne, G., Leake, J., Wolf, J., Horsburgh, K., Reeder, T., Jenkins, G., Ridley, J., Dye, S., Bradley, S. (2009), 'UK Climate Projections Science Report: Marine and coastal projections'. Met Office Hadley Centre: Exeter.

MetOceanWorks (2021a), 'Metocean Data Overview: Outer Dowsing Offshore Wind Farm'. Commercial in Confidence.

MetOceanWorks (2021b), 'Outer Dowsing Offshore Wind Farm: Metocean Design Criteria. Location: CENTRAL'. Commercial in Confidence.

MetOceanWorks (2021c), 'Outer Dowsing Offshore Wind Farm: Metocean Design Criteria. Location: EAST'. Commercial in Confidence.

MetOceanWorks (2021d), 'Outer Dowsing Offshore Wind Farm: Metocean Design Criteria. Location: WEST'. Commercial in Confidence.

Orsted (2021), 'Hornsea Project Four: Environmental Statement – Volume A5, Annex 1.1: Marine Processes Technical Report'.

Palmer., M, Howard., T, Tinker., J, Lowe., J, Bricheno., L, Calvert., D, Edwards., T, Gregory., J, Harris., G, Krijnen., J, Pickering., M, Roberts., C and Wolf., J. (2018), 'UKCP18 Marine report'. November 2018.

Pingree, R.D. and Griffiths, D.K. (1979), 'Sand transport paths around the British Isles resulting from M2 and M4 tidal interactions'. *Journal of the Marine Biological Association of the United Kingdom*, 59(2), 497-513.

Proctor, R., Holt, J.T. and Balson, P.S. (2001), 'Sediment deposition in offshore deeps of the Western North Sea: questions for models'. *Estuarine, Coastal and Shelf Science*, 53(4), 553-567.

Pye, K.. (1983), 'Coastal dunes', *Progress in Physical Geography*, 7(4), pp.531-557.

Pye, K., Saye, S.E., and Blott, S.J. (2007), 'Sand Dune Processes and Management for Flood and Coastal Defence (Parts 1-5)', Joint Defra/Environment Agency Flood & Coastal Erosion Risk Management R&D Programme TR, London: DEFRA.

Saye, S.E. and Pye, K. (2004), 'Development of a coastal dune sediment database for England and Wales: forensic applications', *Geological Society, London, Special Publications*, 232(1), pp.75-96.

Soulsby R.L. (1997), 'Dynamics of marine sands: A manual for practical applications'. Thomas Telford, London.

Spencer, T., Brooks, S.M., Evans, B.R., Tempest, J.A. and Möller, I. (2015), 'Southern North Sea storm surge event of 5 December 2013: Water levels, waves and coastal impacts', *Earth-Science Reviews*, 146: 120-145.

Sündermann, J. and Pohlmann, T. (2011), 'A brief analysis of North Sea physics'. *Oceanologia*, 53(3), 663-689.

Tappin, D. R., Pearce, B., Fitch, S., Dove, D., Gearey, B., Hill, J. M., Chambers, C., Bates, R., Pinnion, J., Diaz Doce, D., Green, M., Gallyot, J., Georgiou, L., Brutto, D., Marzialetti, S., Hopla, E., Ramsay, E., and

Fielding, H. (2011), 'The Humber Regional Environmental Characterisation', British Geological Survey Open Report OR/10/54.

TKOWFL (2011), 'Triton Knoll Offshore Wind Farm Physical Processes Technical Documentation'.

TKOWFL (2012), 'Triton Knoll Offshore Wind Farm Environmental Statement: Physical Processes'.

TKOWFL (2014), 'Triton Knoll Electrical System Preliminary Environmental Information: Marine Physical Environment Baseline'.

TKOWFL (2015), 'Triton Knoll Electrical System Environmental Statement: Marine Physical Environment'.

7.8 Annex A

120. Modelled current time-series data from the Project numerical outputs (the details of which are provided in document reference 6.3.7.2) have been used to estimate the potential sediment mobility of sediments across the study area, the results of which are shown in Table 7.17. Potential sediment mobility across a spring and neap tidal cycle are presented at 27 points, the locations of which are shown in Figure 7.14.

Table 7.17 Estimated potential sediment mobility across the study area from modelled tidal currents

Point	Size Class	Grain Size (upper boundary) (mm)	Approximate Water Depth (m)	Threshold of Bed Shear Stress (N/m ²)	Corresponding Critical Depth- averaged Current Speeds (m/s)	Sediment Mobility ²¹ (Spring)	Sediment Mobility (Neap)
1	Granule Gravel	4	25	3.007	1.32	6%	0%
	Very Coarse Sand	2	25	1.166	0.908	32%	2%
	Coarse Sand	1	25	0.481	0.643	56%	13%
	Medium Sand	0.5	25	0.262	0.524	65%	30%
	Fine Sand	0.25	25	0.189	0.492	66%	35%
	Very Fine Sand	0.125	25	0.153	0.489	66%	36%
	Coarse Silt	0.0625	25	0.120	0.477	67%	38%
2	Granule Gravel	4	5	3.007	1.049	9%	0%
	Very Coarse Sand	2	5	1.166	0.721	42%	6%
	Coarse Sand	1	5	0.481	0.511	66%	33%
	Medium Sand	0.5	5	0.262	0.416	74%	50%
	Fine Sand	0.25	5	0.189	0.391	76%	54%
	Very Fine Sand	0.125	5	0.153	0.388	76%	54%

²¹ Percentage of time that sediment is mobile.

Point	Size Class	Grain Size (upper boundary) (mm)	Approximate Water Depth (m)	Threshold of Bed Shear Stress (N/m ²)	Corresponding Critical Depth- averaged Current Speeds (m/s)	Sediment Mobility ²¹ (Spring)	Sediment Mobility (Neap)
3	Coarse Silt	0.0625	5	0.120	0.379	77%	56%
	Granule Gravel	4	15	3.007	1.227	12%	0%
	Very Coarse Sand	2	15	1.166	0.844	51%	7%
	Coarse Sand	1	15	0.481	0.598	69%	33%
	Medium Sand	0.5	15	0.262	0.487	76%	49%
	Fine Sand	0.25	15	0.189	0.458	78%	53%
	Very Fine Sand	0.125	15	0.153	0.454	78%	54%
4	Coarse Silt	0.0625	15	0.120	0.444	79%	55%
	Granule Gravel	4	5	3.007	1.049	4%	0%
	Very Coarse Sand	2	5	1.166	0.721	36%	3%
	Coarse Sand	1	5	0.481	0.511	64%	18%
	Medium Sand	0.5	5	0.262	0.416	74%	38%
	Fine Sand	0.25	5	0.189	0.391	78%	44%
	Very Fine Sand	0.125	5	0.153	0.388	78%	44%
5	Coarse Silt	0.0625	5	0.120	0.379	78%	47%
	Granule Gravel	4	15	3.007	1.227	0%	0%
	Very Coarse Sand	2	15	1.166	0.844	32%	1%
	Coarse Sand	1	15	0.481	0.598	82%	25%
	Medium Sand	0.5	15	0.262	0.487	95%	50%
	Fine Sand	0.25	15	0.189	0.458	97%	57%
	Very Fine Sand	0.125	15	0.153	0.454	97%	58%
6	Coarse Silt	0.0625	15	0.120	0.444	98%	60%
	Granule Gravel	4	15	3.007	1.227	0%	0%
6	Very Coarse Sand	2	15	1.166	0.844	37%	4%

Point	Size Class	Grain Size (upper boundary) (mm)	Approximate Water Depth (m)	Threshold of Bed Shear Stress (N/m ²)	Corresponding Critical Depth- averaged Current Speeds (m/s)	Sediment Mobility ²¹ (Spring)	Sediment Mobility (Neap)
	Coarse Sand	1	15	0.481	0.598	68%	36%
	Medium Sand	0.5	15	0.262	0.487	82%	52%
	Fine Sand	0.25	15	0.189	0.458	85%	57%
	Very Fine Sand	0.125	15	0.153	0.454	85%	57%
	Coarse Silt	0.0625	15	0.120	0.444	86%	58%
7	Granule Gravel	4	15	3.007	1.227	0%	0%
	Very Coarse Sand	2	15	1.166	0.844	39%	1%
	Coarse Sand	1	15	0.481	0.598	84%	23%
	Medium Sand	0.5	15	0.262	0.487	97%	45%
	Fine Sand	0.25	15	0.189	0.458	98%	53%
	Very Fine Sand	0.125	15	0.153	0.454	99%	54%
	Coarse Silt	0.0625	15	0.120	0.444	99%	57%
8	Granule Gravel	4	5	3.007	1.049	0%	0%
	Very Coarse Sand	2	5	1.166	0.721	55%	7%
	Coarse Sand	1	5	0.481	0.511	86%	40%
	Medium Sand	0.5	5	0.262	0.416	96%	59%
	Fine Sand	0.25	5	0.189	0.391	97%	63%
	Very Fine Sand	0.125	5	0.153	0.388	98%	64%
	Coarse Silt	0.0625	5	0.120	0.379	98%	66%
9	Granule Gravel	4	15	3.007	1.227	0%	0%
	Very Coarse Sand	2	15	1.166	0.844	23%	0%
	Coarse Sand	1	15	0.481	0.598	81%	19%
	Medium Sand	0.5	15	0.262	0.487	96%	44%
	Fine Sand	0.25	15	0.189	0.458	98%	51%

Point	Size Class	Grain Size (upper boundary) (mm)	Approximate Water Depth (m)	Threshold of Bed Shear Stress (N/m ²)	Corresponding Critical Depth- averaged Current Speeds (m/s)	Sediment Mobility ²¹ (Spring)	Sediment Mobility (Neap)
10	Very Fine Sand	0.125	15	0.153	0.454	98%	52%
	Coarse Silt	0.0625	15	0.120	0.444	99%	54%
	Granule Gravel	4	25	3.007	1.32	0%	0%
	Very Coarse Sand	2	25	1.166	0.908	7%	0%
	Coarse Sand	1	25	0.481	0.643	56%	12%
	Medium Sand	0.5	25	0.262	0.524	69%	29%
	Fine Sand	0.25	25	0.189	0.492	73%	36%
	Very Fine Sand	0.125	25	0.153	0.489	74%	37%
11	Coarse Silt	0.0625	25	0.120	0.477	76%	39%
	Granule Gravel	4	5	3.007	1.049	0%	0%
	Very Coarse Sand	2	5	1.166	0.721	29%	1%
	Coarse Sand	1	5	0.481	0.511	74%	30%
	Medium Sand	0.5	5	0.262	0.416	85%	50%
	Fine Sand	0.25	5	0.189	0.391	87%	54%
	Very Fine Sand	0.125	5	0.153	0.388	88%	55%
12	Coarse Silt	0.0625	5	0.120	0.379	89%	57%
	Granule Gravel	4	15	3.007	1.227	0%	0%
	Very Coarse Sand	2	15	1.166	0.844	46%	10%
	Coarse Sand	1	15	0.481	0.598	68%	42%
	Medium Sand	0.5	15	0.262	0.487	75%	56%
	Fine Sand	0.25	15	0.189	0.458	77%	60%
	Very Fine Sand	0.125	15	0.153	0.454	78%	60%
13	Coarse Silt	0.0625	15	0.120	0.444	79%	62%
	Granule Gravel	4	15	3.007	1.227	0%	0%

Point	Size Class	Grain Size (upper boundary) (mm)	Approximate Water Depth (m)	Threshold of Bed Shear Stress (N/m ²)	Corresponding Critical Depth- averaged Current Speeds (m/s)	Sediment Mobility ²¹ (Spring)	Sediment Mobility (Neap)
	Very Coarse Sand	2	15	1.166	0.844	24%	0%
	Coarse Sand	1	15	0.481	0.598	58%	21%
	Medium Sand	0.5	15	0.262	0.487	69%	40%
	Fine Sand	0.25	15	0.189	0.458	71%	45%
	Very Fine Sand	0.125	15	0.153	0.454	71%	46%
	Coarse Silt	0.0625	15	0.120	0.444	72%	48%
14	Granule Gravel	4	5	3.007	1.049	8%	0%
	Very Coarse Sand	2	5	1.166	0.721	53%	15%
	Coarse Sand	1	5	0.481	0.511	71%	49%
	Medium Sand	0.5	5	0.262	0.416	77%	62%
	Fine Sand	0.25	5	0.189	0.391	79%	65%
	Very Fine Sand	0.125	5	0.153	0.388	79%	66%
15	Coarse Silt	0.0625	5	0.120	0.379	80%	66%
	Granule Gravel	4	35	3.007	1.385	0%	0%
	Very Coarse Sand	2	35	1.166	0.952	8%	0%
	Coarse Sand	1	35	0.481	0.675	45%	9%
	Medium Sand	0.5	35	0.262	0.55	58%	23%
	Fine Sand	0.25	35	0.189	0.517	62%	28%
	Very Fine Sand	0.125	35	0.153	0.513	62%	30%
16	Coarse Silt	0.0625	35	0.120	0.501	63%	32%
	Granule Gravel	4	25	3.007	1.32	0%	0%
	Very Coarse Sand	2	25	1.166	0.908	2%	0%
	Coarse Sand	1	25	0.481	0.643	30%	1%
	Medium Sand	0.5	25	0.262	0.524	49%	9%

Point	Size Class	Grain Size (upper boundary) (mm)	Approximate Water Depth (m)	Threshold of Bed Shear Stress (N/m ²)	Corresponding Critical Depth- averaged Current Speeds (m/s)	Sediment Mobility ²¹ (Spring)	Sediment Mobility (Neap)
17	Fine Sand	0.25	25	0.189	0.492	53%	12%
	Very Fine Sand	0.125	25	0.153	0.489	53%	12%
	Coarse Silt	0.0625	25	0.120	0.477	56%	14%
	Granule Gravel	4	25	3.007	1.32	0%	0%
	Very Coarse Sand	2	25	1.166	0.908	17%	0%
	Coarse Sand	1	25	0.481	0.643	50%	6%
	Medium Sand	0.5	25	0.262	0.524	64%	18%
	Fine Sand	0.25	25	0.189	0.492	67%	23%
	Very Fine Sand	0.125	25	0.153	0.489	67%	23%
18	Coarse Silt	0.0625	25	0.120	0.477	68%	26%
	Granule Gravel	4	25	3.007	1.32	0%	0%
	Very Coarse Sand	2	25	1.166	0.908	22%	0%
	Coarse Sand	1	25	0.481	0.643	56%	10%
	Medium Sand	0.5	25	0.262	0.524	68%	27%
	Fine Sand	0.25	25	0.189	0.492	71%	31%
	Very Fine Sand	0.125	25	0.153	0.489	71%	32%
19	Coarse Silt	0.0625	25	0.120	0.477	72%	34%
	Granule Gravel	4	15	3.007	1.227	0%	0%
	Very Coarse Sand	2	15	1.166	0.844	32%	1%
	Coarse Sand	1	15	0.481	0.598	62%	23%
	Medium Sand	0.5	15	0.262	0.487	71%	41%
	Fine Sand	0.25	15	0.189	0.458	73%	47%
	Very Fine Sand	0.125	15	0.153	0.454	73%	48%
Coarse Silt	0.0625	15	0.120	0.444	74%	49%	

Point	Size Class	Grain Size (upper boundary) (mm)	Approximate Water Depth (m)	Threshold of Bed Shear Stress (N/m ²)	Corresponding Critical Depth- averaged Current Speeds (m/s)	Sediment Mobility ²¹ (Spring)	Sediment Mobility (Neap)
20	Granule Gravel	4	25	3.007	1.32	0%	0%
	Very Coarse Sand	2	25	1.166	0.908	5%	0%
	Coarse Sand	1	25	0.481	0.643	40%	2%
	Medium Sand	0.5	25	0.262	0.524	56%	15%
	Fine Sand	0.25	25	0.189	0.492	60%	20%
	Very Fine Sand	0.125	25	0.153	0.489	60%	20%
	Coarse Silt	0.0625	25	0.120	0.477	61%	23%
21	Granule Gravel	4	15	3.007	1.227	1%	0%
	Very Coarse Sand	2	15	1.166	0.844	39%	3%
	Coarse Sand	1	15	0.481	0.598	67%	29%
	Medium Sand	0.5	15	0.262	0.487	76%	48%
	Fine Sand	0.25	15	0.189	0.458	78%	52%
	Very Fine Sand	0.125	15	0.153	0.454	78%	53%
	Coarse Silt	0.0625	15	0.120	0.444	79%	55%
22	Granule Gravel	4	5	3.007	1.049	0%	0%
	Very Coarse Sand	2	5	1.166	0.721	34%	1%
	Coarse Sand	1	5	0.481	0.511	67%	19%
	Medium Sand	0.5	5	0.262	0.416	79%	39%
	Fine Sand	0.25	5	0.189	0.391	82%	46%
	Very Fine Sand	0.125	5	0.153	0.388	82%	46%
	Coarse Silt	0.0625	5	0.120	0.379	83%	49%
23	Granule Gravel	4	15	3.007	1.227	0%	0%
	Very Coarse Sand	2	15	1.166	0.844	24%	0%
	Coarse Sand	1	15	0.481	0.598	55%	12%

Point	Size Class	Grain Size (upper boundary) (mm)	Approximate Water Depth (m)	Threshold of Bed Shear Stress (N/m ²)	Corresponding Critical Depth- averaged Current Speeds (m/s)	Sediment Mobility ²¹ (Spring)	Sediment Mobility (Neap)
	Medium Sand	0.5	15	0.262	0.487	67%	29%
	Fine Sand	0.25	15	0.189	0.458	70%	33%
	Very Fine Sand	0.125	15	0.153	0.454	70%	34%
	Coarse Silt	0.0625	15	0.120	0.444	71%	36%
24	Granule Gravel	4	25	3.007	1.32	0%	0%
	Very Coarse Sand	2	25	1.166	0.908	7%	0%
	Coarse Sand	1	25	0.481	0.643	45%	6%
	Medium Sand	0.5	25	0.262	0.524	58%	19%
	Fine Sand	0.25	25	0.189	0.492	62%	25%
	Very Fine Sand	0.125	25	0.153	0.489	63%	25%
	Coarse Silt	0.0625	25	0.120	0.477	64%	27%
25	Granule Gravel	4	25	3.007	1.32	0%	0%
	Very Coarse Sand	2	25	1.166	0.908	15%	0%
	Coarse Sand	1	25	0.481	0.643	53%	12%
	Medium Sand	0.5	25	0.262	0.524	65%	28%
	Fine Sand	0.25	25	0.189	0.492	68%	34%
	Very Fine Sand	0.125	25	0.153	0.489	68%	34%
	Coarse Silt	0.0625	25	0.120	0.477	69%	36%
26	Granule Gravel	4	15	3.007	1.227	0%	0%
	Very Coarse Sand	2	15	1.166	0.844	21%	0%
	Coarse Sand	1	15	0.481	0.598	54%	12%
	Medium Sand	0.5	15	0.262	0.487	67%	29%
	Fine Sand	0.25	15	0.189	0.458	70%	34%
	Very Fine Sand	0.125	15	0.153	0.454	70%	35%

Point	Size Class	Grain Size (upper boundary) (mm)	Approximate Water Depth (m)	Threshold of Bed Shear Stress (N/m ²)	Corresponding Critical Depth- averaged Current Speeds (m/s)	Sediment Mobility ²¹ (Spring)	Sediment Mobility (Neap)
27	Coarse Silt	0.0625	15	0.120	0.444	72%	37%
	Granule Gravel	4	25	3.007	1.32	2%	0%
	Very Coarse Sand	2	25	1.166	0.908	42%	2%
	Coarse Sand	1	25	0.481	0.643	65%	19%
	Medium Sand	0.5	25	0.262	0.524	74%	39%
	Fine Sand	0.25	25	0.189	0.492	77%	44%
	Very Fine Sand	0.125	25	0.153	0.489	77%	45%
	Coarse Silt	0.0625	25	0.120	0.477	77%	46%

7.9 Annex B - DETERMINATION OF MARINE PROCESSES REALISTIC WORST-CASE



**OUTER DOWSING OFFSHORE WIND. ANNEX B: EIA -
DETERMINATION OF MARINE PROCESSES REALISTIC
WORST-CASE**

GoBe

March 2024

OUTER DOWSING OFFSHORE WIND. ANNEX B: EIA - DETERMINATION OF MARINE PROCESSES REALISTIC WORST-CASE

Document-control grid

This document has been prepared by Cooper Marine Advisors Ltd.

Title	Outer Dowsing Offshore Wind. Annex B: EIA - Determination of Marine Processes Realistic Worst-Case	
Author(s)	Bill Cooper, Director, Cooper Marine Advisors Ltd [REDACTED]	
Origination Date	04 July 2023	
Date of last revision	21 March 2024	
Version	1.2	
Status	Final	
Summary of Changes	Aligned to latest version of project spreadsheet (ES Inputs 13-09-2023.xls)	
Circulation	MetOceanWorks / GoBe	
Filename	[REDACTED] [REDACTED] [REDACTED] [REDACTED]	
Approval	Bill Cooper	[REDACTED]

Disclaimer

This document has been prepared by Cooper Marine Advisors Ltd in accordance with the client's instructions and for their stated purpose. Cooper Marine Advisors Ltd does not accept any liability to any other party for any other purpose.

Contents

Abbreviations	iv
1. Introduction.....	1
1.1. Document structure	1
1.2. Supporting documents.....	1
2. Marine physical processes interactions.....	2
3. Project development cycle.....	3
3.1. Overview.....	3
3.2. Construction Phase.....	3
3.2.1. Construction programme	5
3.2.2. Seabed preparation.....	5
3.2.2.1. Sandwave clearance	6
3.2.2.2. Seabed levelling	10
3.2.3. Pile drilling for foundation installation.....	14
3.2.4. Cable installation.....	19
3.2.5. Horizontal direction drilling	22
3.3. Operation and Maintenance	22
3.3.1. Array-scale blockage.....	23
3.3.2. Cable repairs	24
3.4. Decommissioning.....	24
4. References	25

List of Figures

Figure 1. Schematic of interpreted units within the Outer Dowsing array area (west – east) (Enviros, 2022)	14
Figure 2. Indicative stratigraphic areas	16

List of Tables

Table 1. Theoretical settling velocities for representative sediment types	5
Table 2. Overspill discharge rates of fine sediments from sandwave clearance between WTG-20 to WTG-21 (indicative layout).	7
Table 3. Spoil disposal rates of fine sediments from sandwave clearance between indicative locations WTG-20 to WTG-21.	8
Table 4. Overspill discharge rates of fine sediments from sandwave clearance along a nearshore section of the ECC.	9
Table 5. Spoil disposal rates of fine sediments from sandwave clearance along a nearshore section of the ECC	10
Table 6. Comparison of total seabed levelling volumes (m ³) for different WTG types and numbers.	11
Table 7. Overspill discharge rates of fine sediments from seabed levelling per TSHD load	12
Table 8. Spoil disposal rates of fine sediments from seabed levelling per TSHD load	14
Table 9. Comparison of drill cuttings volumes (m ³) for different foundation types and areas	18
Table 10. RWC release rates of fine sediments from foundation drilling	19
Table 11. Summary of cable trenching options and production rates	19
Table 12. Mass input of fine sediments for MFE array trenching between WTG-9 to WTG-10	20
Table 13. Mass input of fine sediments for MFE array trenching around ECC_41	21
Table 14. Normalised blockage factor for individual WTG foundation types	23
Table 15. Normalised blockage factor for array	23

Abbreviations

ANS	Artificial Nesting Structure
COWRIE	Collaborative Offshore Wind Research Into The Environment
ECC	Export Cable Corridor
ECR	Export Cable Route
EIA	Environmental Impact Assessment
GW	Gigawatt
HDD	Horizontal Directional Drilling
MFE	Mass Flow Excavator
MLWS	Mean Low Water Spring
MSL	Mean Sea Level
MW	Megawatt
ORCP	Offshore Reactive Compensation Platform
OSP	Offshore Sub-station Platform
ODOW	Outer Dowsing Offshore Wind
PSA	Particle Size Analysis
RWC	Realistic Worst-Case
TSHD	Trailer Suction Hopper Dredger
WTG	Wind Turbine Generator

1. Introduction

This Technical Annex establishes the Marine Physical Processes realistic worst-case (RWC) options related to the Outer Dowsing Offshore Wind (ODOW) project description made available to support the Environmental Impact Assessment (EIA).

1.1. Document structure

Section 1 explains the scope and purpose of the Technical Annex.

Section 2 identifies the primary marine physical processes interactions anticipated from an offshore windfarm development.

Section 3 establishes the realistic worst-case options through the project development cycle from presently available information.

Section 4 lists the references of relevant literature.

1.2. Supporting documents

The marine processes RWC has been established with consideration to the following documents:

- Volume 1, Chapter 3: Project Description (document reference 6.1.3)
- COWRIE (2009). Coastal Process Modelling for Offshore Wind Farm Environmental Impact Assessment: Best Practice Guide. COWRIE Coast-07-08
- The Planning Inspectorate. (2018). Using the Rochdale Envelope. Advice Note Nine: Rochdale Envelope. Version 3
- GEOxyz (2022). Benthic Ecology OWF Area Results Report (Vol. 1). UK4855H-824-RR-01. Revision 1 (document reference 6.1.9.1)
- GEOxyz (2022). Benthic Ecology ECC Results Report (Vol. 2). UK4855H-824-RR-02. Revision 1 (document reference 6.1.9.2)
- Enviros. (2022). Outer Dowsing Offshore Wind Farm Geophysical UHRS and Light Geotechnical Survey, East Anglia, Offshore UK. ENV21-21042-GTR4-02_Rev.01

The marine processes RWC has also taken into account relevant feedback received from stakeholders through the Section 42 consultation on the Preliminary Environmental Information Report and through the Evidence Plan Process. Full details of the consultation with regard to marine processes is presented within Volume 1, Chapter 7: Marine Physical Processes (document reference 6.1.7).

2. Marine physical processes interactions

The expected interactions between marine physical processes and offshore windfarm development can be grouped into two main 'sources' of near-field effects:

- a. **Seabed disturbance** – a seabed response to a short-term mechanical activity, typically occurring during installation and decommissioning periods, which result in sediment plumes that temporarily and locally increase turbidity in the water column and with subsequent deposition creating the risk of smothering of seabed receptors. In addition, some seabed disturbance activities may also occur during the operational and maintenance period, notably if remedial work is required for cable repairs, etc. Examples of activities which may lead to seabed disturbance include; seabed levelling, disposal of spoil, pile drilling, cable trenching, punch-out of Horizontal Directional Drilling (HDD), etc.

- b. **Blockage** – interaction of installed structures (across the array and along the cable routes) with waves and flows over the duration of the operational period (the longest period in the development cycle) which results in modifications to wave energy transmission to the coast and / or development of local flow wakes which may increase turbulence, induce local scour and interfere with general sediment transport processes.

Where more than one project development option is retained for consent, the RWC represents the option which is expected to lead to the highest level of seabed disturbance for a specific activity during the development period and / or the greatest level of blockage during the operational phase.

3. Project development cycle

3.1. Overview

A consideration of offshore activities which are planned during each phase of the project development cycle provides a basis to identify the type, magnitude, location, and duration of marine physical process effects which are expected to occur. Where the spread of these effects (impact pathways) needs to be explored in greater detail, then relevant source terms are established for modelling scenarios, based on the identified RWC option.

3.2. Construction Phase

The construction programme provides adequate temporal separation between planned activities and their short-term effects on the marine environment such that they do not act in-combination (i.e., separate sources and sediment plumes do not overlap).

During the construction phase the main effects on the marine environment are expected to be related to seabed preparation for foundations and cables, drilling for foundations (where required), cable laying, and HDD in the nearshore. These activities will each develop different rates and volumes of sediment disturbance into the water column based on the methods employed. The fate of this disturbed sediment depends on several factors, notably the settling velocity of different sediment particle sizes which influences the time spent in the water column, and the tidal flows which can act on the particles during settling and can carry the sediments further afield.

Where present, the larger and heavier coarse sediments (i.e., very fine gravel to medium sand) have the fastest settling velocities which will mean they will fall rapidly back to the seabed. The smaller and lighter fine sediments (i.e., fine sand to silts and muds) have the slowest settling velocities, meaning they take the longest to settle back to the seabed. These fine sediments will therefore be more susceptible to advection by tidal flows during this period and will have the potential to form sediment plumes.

Table 1 provides indicative settling velocities (based on Soulsby, 1997) for representative sediment types present within the development area (assuming still water conditions).

Table 1. Theoretical settling velocities for representative sediment types

Sediment type		Size range (mm)	Representative size (mm)	Settling velocity (m/s)
Coarse	Gravel	> 2.000	3.000	0.216
	Very coarse sand	1.000 to 2.000	1.500	0.147
	Coarse sand	0.500 to 1.000	0.750	0.093
	Medium sand	0.250 to 0.500	0.375	0.049
Fine	Fine sand	0.125 to 0.250	0.188	0.018
	Very fine sand	0.063 to 0.125	0.094	0.005
	Coarse silt	0.031 to 0.063	0.047	0.0014
	Medium silt / muds	< 0.031	0.023	0.0003

3.2.1. Construction programme

The indicative construction programme ensures a sequential set of activities which limits the opportunity for cumulative impacts occurring between sediment plumes which might lead to a greater scale of impact.

3.2.2. Seabed preparation

An initial activity during the construction phase includes seabed preparation to remove boulders and sandwaves (where present) along the Export Cable Route (ECR) and inter-array cable routes to aid effective use of cable burial tools. Seabed levelling is also required around specific foundation types which need to be placed onto a flat seabed (e.g., suction bucket foundations) and for areas of scour protection.

Seabed preparation is expected to be conducted by up to two Trailer Suction Hopper Dredgers (TSHD). The capacity of the hopper defines the volume of sediments that can be removed per transit, the time on site when the drag-head might develop a (minor) near-bed sediment plume, and the amount of overspill when the hopper is being filled which develops a separate near-surface sediment plume. The capacity of the TSHD is likely to be around 22,000 m³ (equivalent to a jumbo dredger) with an associated loading rate of between 7,500 to 15,000 m³/hour, equating to loading times of around 3 to 1.5 hours, respectively. The faster loading time of 1.5 hours is considered to generate the highest rates of overspill discharged back to sea.

When the loading cycle is complete the dredger will transit to a suitable location for disposal of spoil (through the bottom doors of the hopper). This discharge represents the largest volume of near-instantaneous sediment release of any sediment disturbance event during the dredging cycle. All release locations will remain within the project boundary and are likely to be associated with other local areas with

a similar sediment type (e.g., sandwave dredge arisings disposed of on an adjacent area of sandwaves). In particular, any seabed preparation within the SAC areas will be retained within the same area.

The behaviour of sediment plumes due to seabed disturbance depends mainly on the density and size of sediment particles, the height of the discharge above the seabed, and the local tidal conditions. The primary dataset to define particle size distributions across the array area is provided by the benthic survey (GEOxyz, 2022). For sandwave clearance, the expectation is removal of dominantly coarse-grained and well-sorted sediments (i.e., sands), whereas seabed levelling could occur in any sediment type identified across the array area and could involve a more mixed sediment type.

3.2.2.1. Sandwave clearance

Two representative locations are investigated for sandwave clearance, one within the array area for inter-array cables, and one along the Export Cable Corridor (ECC).

a. Array Area

The largest total volume of sandwave clearance within the array area is estimated to be 11,615,616 m³. This value is established for sections along 611.17 km of cables (377.42 km of array cables, 123.75 km of interlink cables and 110.00 km of export cables falling within the array boundary) where sandwaves are present for a clearance width of 33 m and an average depth of removal of 2.5 m. This volume is related to the wind turbine generator (WTG) capacity option which utilises the largest number of wind turbines and foundations (100).

The sandwave clearance volume equates to around 520 hopper loads when assuming a bulking factor of 1.2 (mid-range of 1.15 to 1.25 for sand, medium soft to hard (Bray, Bates, & Land, 1996)), and a cumulative overspill loss of 18% representative of medium sand (Miedema, 2013). Consequently, the total overspill losses are estimated to be 2,090,911 m³ of the total clearance volume, equivalent to 4,024 m³ per load. The actual number of hopper loads will vary according to the final chosen capacity of the TSHD.

During the loading cycle a highly fluidised volume of sediment is pumped into the hopper from the draghead. Once in the hopper there will be some settlement of coarser sediment displacing water to the surface which will tend to retain finer sediments in suspension. Eventually, sediment laden water levels will rise to the height of the hopper weir and a period of overspill will start to occur as further loading displaces the excess water overboard. The overspill period is estimated to occur over the last one-hour period of the loading cycle. During this period the fine sediments in the overspill have the potential to form a sediment plume.

During the loading cycle the TSHD is expected to travel across a distance of around 1.725 km to fill the hopper, a distance equivalent to the indicative spacing between adjacent wind turbine generators (WTG).

Based on the indicative layout, the transit between WTG-20 to WTG-21 falls within an area identified with sandwaves by the geophysical survey (Enviros, 2022), and also a site with the highest relative contribution of fine sediments (42.7%), established by grab sample OWF_33 (GEOxyz, 2022). **Error! Reference source not found.** provides details of overspill rates for fine sediments discharged from the sea surface for this operation. The estimated time for different particle sizes to fall out of suspension from the sea surface to a nominal representative depth of 24 m is also provided, indicating that the smallest particles (medium silt and smaller) could take around 22 hours to fully settle out (in still water conditions). The coarser sediment would quickly fall to the seabed, with limited opportunity to be advected away by tidal currents.

Table 2. Overspill discharge rates of fine sediments from sandwave clearance between WTG-20 to WTG-21 (indicative layout).

Sediment type	Size range (mm)	Time to fall out of suspension (s)	% Contribution	Mass input (g/s)
Fine sand	0.125 to 0.250	1,333	29.6	632,008
Very fine sand	0.063 to 0.125	4,800	6.4	136,650
Coarse silt	0.031 to 0.063	17,143	0.5	10,676
Medium silt / muds	< 0.031	80,000	6.2	132,380

Once the hopper is full then the TSHD will transit to a nominated area close by for spoil disposal. The default location for spoil disposal will be the centre of four adjacent foundations and away from any other site planned for installation of infrastructure. The preference is to also dispose of dredged sediment onto a comparable seabed sediment type.

Hopper doors will discharge sediments to the seabed which will initially form a downward gravity-driven density flow (convective descent) to develop a spoil mound on the seabed. The discharge is expected to be near instantaneous, taking around 10 minutes to empty the hopper. Any finer sediment fractions present may be susceptible to forming a further sediment plume from the location of the spoil release. Thereafter, the spoil mound becomes susceptible to local wave and tidal processes which have the potential to winnow away mobile sediment fractions and integrate back into the general sediment transport regime.

The RWC scenario for modelling sandwave clearance within the array area (MetOceanWorks, 2023) is based on the following schedule:

- Dredging commences from indicative locations WTG-20 to WTG-21 to remove sandwaves along inter-array cable line
- No overspill for the initial 30 minute period as hopper starts to fill, distance covered in this period is around 0.575 km
- Overspill commences after 30 minutes at a loss rate of 18% of volume received into hopper
- Distance covered by the dredger during the overspill period around 1,150 m
- Hopper is full after 90 minutes of dredging, overspill ends

- Transit to adjacent spoil disposal location taking 25 minutes, no discharge in this period
- Arrive at disposal location to discharge hopper load, taking 10 minutes
- Fine sediments develop a sediment plume and coarse sediments a spoil mound
- Repeat clearance activity for along inter-array cable alignment to attain full clearance width of 30 m

Table 3 provides release rates for fine sediments discharged from the hopper over 10 minutes. The release would be from the base of the loaded hopper which is estimated to be around 12 m below the sea surface, hence the sediment would fall another 12 m to reach a local depth of 24 m. The conservative assumption is made that all fines are immediately available to form a sediment plume during disposal, whereas in reality the higher volume of coarse sediments will induce density-driven convective flows towards the seabed, which will trap some of the fines within the spoil mound.

Table 3. Spoil disposal rates of fine sediments from sandwave clearance between indicative locations WTG-20 to WTG-21.

Sediment type	Size range (mm)	Time to fall out of suspension (s)	% Contribution	Mass input (g/s)
Fine sand	0.125 to 0.250	667	29.6	17,274,889
Very fine sand	0.063 to 0.125	2,400	6.4	3,735,111
Coarse silt	0.031 to 0.063	8,571	0.5	291,806
Medium silt / muds	< 0.031	40,000	6.2	3,618,389

The coarser sediments, representing 57.8% of the dredged material, will quickly fall to the seabed as a gravity-driven convective flow to form a spoil mound. The convective flow draws down some of the fine sediments at the same rate (i.e., faster than settling) with some of the material potentially being stripped out to initiate a sediment plume.

The form (area and height) of this mound will depend on the local water depth and flow conditions, the transit speed of the TSHD, and the sediment sizes representing the spoil. Annex B presents the results of the spoil mound assessment related to sandwave clearance for the array area.

b. Export cables

The largest total volume of sandwave clearance along the ECR (excluding sections within the array area) is estimated to be 4,518,513m³. This value is established where sandwaves are present along 330 km of export cables (four times 82.5 km), for a clearance width of 33 m and an average depth of removal of 2.5 m.

The sandwave clearance volume along the ECR equates to around 202 hopper loads when assuming a bulking factor of 1.2 (mid-range of 1.15 to 1.25 for sand, medium soft to hard (Bray, Bates, & Land, 1996)), and a cumulative overspill loss of 18% representative of medium sand (Miedema, 2013). Consequently, the

total overspill losses are estimated to be 813,332 m³ of the total clearance volume, equivalent to around 4,024 m³ per load. The actual number of hopper loads will vary according to the capacity of the TSHD.

A nearshore area of sandwaves is identified from the ECC geophysical survey (GEOxyz, 2022), where the content of fine sediment reaches 31.9%, as determined from sediment grab sample ECC_58. These sandwaves extend for a distance of around 2.5 km along the alignment of the ECC where water depths are around 17 m (relative to mean sea level, MSL). This section of ECC is considered to be the realistic worst-case for potential development of sediment plumes being the location with the highest content of fines. Table 4 provides details of overspill rates for fine sediments discharged from the sea surface for sandwave clearance. The estimated time for different particle sizes to fall out of suspension from the sea surface to a representative depth of 17 m associated with the local area is also provided.

Table 4. Overspill discharge rates of fine sediments from sandwave clearance along a nearshore section of the ECC.

Sediment type	Size range (mm)	Time to fall out of suspension (s)	% Contribution	Mass input (g/s)
Fine sand	0.125 to 0.250	944	22.2	474,006
Very fine sand	0.063 to 0.125	3,400	0.5	10,676
Coarse silt	0.031 to 0.063	12,143	2.6	55,514
medium silt / muds	< 0.031	56,667	6.6	140,921

Once the hopper is full then the TSHD will transit to a nominated area close by for spoil disposal. This location is expected to be within the same general area of sandwaves and is nominally sited to the south of the local section of sandwave clearance.

Hopper doors will discharge sediments to the seabed which will initially form a downward gravity-driven density flow (convective descent) to develop a spoil mound on the seabed. The discharge is expected to be near instantaneous, taking around 10 minutes to empty the hopper. Any finer sediment fractions may be susceptible to forming a further sediment plume from the location of the spoil release. Thereafter, the spoil mound becomes susceptible to local wave and tidal processes which have the potential to winnow away mobile sediment fractions.

The RWC scenario for modelling sandwave clearance along the ECC (MetOceanWorks, 2023) is based on the following schedule:

- Dredging commences from the easterly side of the sandwave area within the nearshore section of the ECC
- No overspill for the initial 30 minute period as the hopper starts to fill, distance covered in this period is around 0.575 km
- Overspill commences after 30 minutes at a loss rate of 18% of volume received into the hopper

- Distance covered by the dredger during the overspill period is around 1,150 m
- Hopper is full after 90 minutes of dredging, overspill ends
- Transit to adjacent spoil disposal location taking 25 minutes, no discharge in this period
- Arrive at disposal location to discharge hopper load, taking 10 minutes
- Fine sediments develop a sediment plume and coarse sediments a spoil mound
- Repeat clearance activity for next section of sandwaves along nearshore section of ECC to attain full clearance width of 30 m

Table 5 provides release rates for fine sediments discharged from the hopper over 10 minutes. The release would be from the base of the loaded hopper which is estimated to be around 12 m below the sea surface, hence the sediment would be falling another 5 m to reach a local depth of 17 m. The conservative assumption made is that all fines are immediately available to form a sediment plume during disposal, whereas in reality the higher volume of coarse sediments will induce density-driven convective flows towards the seabed, which may trap some of the fines within the spoil mound.

Table 5. Spoil disposal rates of fine sediments from sandwave clearance along a nearshore section of the ECC

Sediment type	Size range (mm)	Time to fall out of suspension (s)	% Contribution	Mass input (g/s)
Fine sand	0.125 to 0.250	278	22.2	12,956,167
Very fine sand	0.063 to 0.125	1,000	0.5	291,806
Coarse silt	0.031 to 0.063	3,571	2.6	1,517,389
Medium silt / muds	< 0.031	16,667	6.6	3,851,833

The coarser sediments, representing 68.1% of the dredged material, will quickly fall to the seabed as a gravity-driven convective flow to form a spoil mound. The convective flow will also draw down some of the fine sediments at the same rate, with some of the material potentially being stripped out to initiate a sediment plume.

The form (area and height) of this mound will depend on the local water depth and flow conditions, the transit speed of the TSHD, and the sediment sizes representing the spoil. Annex C presents the results of the spoil mound assessment related to sandwave clearance for the ECC.

3.2.2.2. Seabed levelling

Seabed levelling is planned around all foundation types to create a suitable surface for placement of scour protection. The jacket with suction bucket foundation option also requires seabed levelling to aid successful installation on a flat seabed.

The four different types of WTG foundations being considered for consenting purposes are:

- Monopiles (up to 100% of sites)
- Jacket with Pin Piles (up to 100% of sites)
- Jacket with Suction Buckets (up to 100% of sites)
- Gravity base structures (GBS) (up to 50% of sites)

In addition, the number of WTG could also vary between a minimum of 50 to a maximum of 100, depending on the rate capacity. Table 6 summarises the total seabed levelling volumes based on the total number of turbines for each option.

Table 6. Comparison of total seabed levelling volumes (m³) for different WTG types and numbers

WTG foundation option	100	93	75	60	50
Monopiles	222,000	206,460	166,500	145,200	121,000
Jacket – Pin Piles	54,000	50,220	40,500	32,400	27,000
Jacket – Suction Buckets	445,000	413,850	333,750	306,000	255,000
GBS (up to 50% of sites)	1,815,000	1,687,950	1,361,250	1,323,300	1,102,750

According to Table 6, GBS (50% of sites) is the RWC option for the 100 WTG case, plus the remaining 50% of sites represented by the alternative WTG RWC option which is jacket with suction buckets. The total RWC seabed levelling volume is therefore 2,037,500 m³ (1,815,000 + 50% of 445,000).

Further seabed levelling in the array area is also required around five offshore platforms with a volume of 242,500 m³ (48,500 m³ per OSP GBS foundation). The overall largest total volume to be removed for seabed levelling in the array area for both WTG and OSP locations is estimated to be 2,280,000 m³.

In addition, seabed levelling is also planned at four further offshore platforms remote from the array area:

- Two Artificial Nesting Structures (ANS) at locations at least 16 km to the north-west or south-east of the array area requiring up to 36,300 m³ of sediment removal for each GBS foundation (total of 72,600 m³ for both foundations).
- Two Offshore Reactive Compensation Platforms (ORCPs) located around 12 to 17 km offshore within the ECC, requiring 48,500 m³ per GBS foundation (total of 97,000 m³ for both foundations).

The use of a jumbo TSHD (estimated capacity of 22,000 m³) is considered to be the RWC seabed levelling option compared to other methods such as MFE. When seabed sediment is dredged the material will expand in volume due to increased water content, a process referred to as bulking-up. A bulking factor of 1.25 has been assumed for present purposes, which is mid-range of 1.15 to 1.35 for sand/gravel/clay mixed sediments (Bray, Bates, & Land, 1996) which are common across the array area for sites not covered by sandwaves. The total quantity of seabed levelling across the array area requires around 111 hopper

loads when accounting for a cumulative overspill loss of 18%. The actual number of hopper loads will vary according to the final chosen capacity of the TSHD.

Given that a single GBS WTG foundation will require 36,300 m³ of sediment removal, then two TSHD loads are required per location, accounting for bulking and overspill. For the RWC assessment of seabed levelling, an area in the south-east corner of the array is selected to model sediment plumes which is a location considered to have the highest proportion of fine sediments (established by grab sample OWF_76), and is also an area devoid of any sandwaves.

Table 7 provides details of overspill rates for fine sediments discharged along with the estimated time for different particle sizes to fall out of suspension from the sea surface to a nominal representative depth of 25 m. The times to fall out of suspension indicate that the smallest particles (medium silt and smaller) could take around 23 hours to fully settle out (in still water conditions). The coarser sediment would fall directly to the seabed with limited opportunity to be advected away by tidal currents.

Table 7. Overspill discharge rates of fine sediments from seabed levelling per TSHD load

Sediment type	Size range (mm)	Time to fall out of suspension (s), depth of 25 m	% Contribution	Overspill input (g/s)
Fine sand	0.125 to 0.250	1,389	24.5	557,989
Very fine sand	0.063 to 0.125	5,000	4.3	97,933
coarse silt	0.031 to 0.063	17,857	0.7	15,943
medium silt / muds	< 0.031	83,333	6.5	148,038

At the end of the dredging cycle, the filled hopper discharges spoil from the base of the hopper (at a draught of around 12 m below sea level) with the fine sediment in the spoil developing a sediment plume, whereas coarse sediments will fall to the seabed to form a spoil mound. The conservative assumption made is that all fines will be available to form the sediment plume, whereas in reality some fines are likely to be retained in the convective flow of the discharge and retained within the spoil mound.

Table 8 provides release rates for fine sediments discharged from the base of the hopper at a depth of 12 m below the sea surface which lasts for approximately 10 minutes.

Table 8. Spoil disposal rates of fine sediments from seabed levelling per TSHD load

Sediment type	Size range (mm)	Time to fall out of suspension (s), depth of 13 m	% Contribution	Mass input (g/s)
Fine sand	0.125 to 0.250	722	24.5	14,229,580
Very fine sand	0.063 to 0.125	2,600	4.3	2,497,436
coarse silt	0.031 to 0.063	9,286	0.7	406,559
medium silt / muds	< 0.0031	43,333	6.5	3,775,195

The coarser sediments, representing 63.9% of the dredged material, will quickly fall to the seabed as a mass-driven convective flow to form a spoil mound. Annex B presents the results of the spoil mound assessment related to seabed levelling.

3.2.3. Pile drilling for foundation installation

For foundation options that require installation of piles into the seabed (i.e., monopiles and jackets with pin piles) there is a potential requirement for drilling into the seabed when pile driving is not possible.

a. Seabed geology

The geophysical survey (Enviros, 2022) has interpreted the shallow geology across the array area. Occasional shallow patches of Holocene sand (Unit A) overlay the Bolders Bank formation (Unit B - stiff clay with silt and sand, dry bulk density up to 1.95 Mg/m³, and Unit C – sand and gravels with clay and silt) which extends up to 32 m below seabed as is typically found above the Swarte formation (Unit D – clay). Mesozoic mudstone bedrock (Unit E) is expected below the Swarte formation (Figure 1).

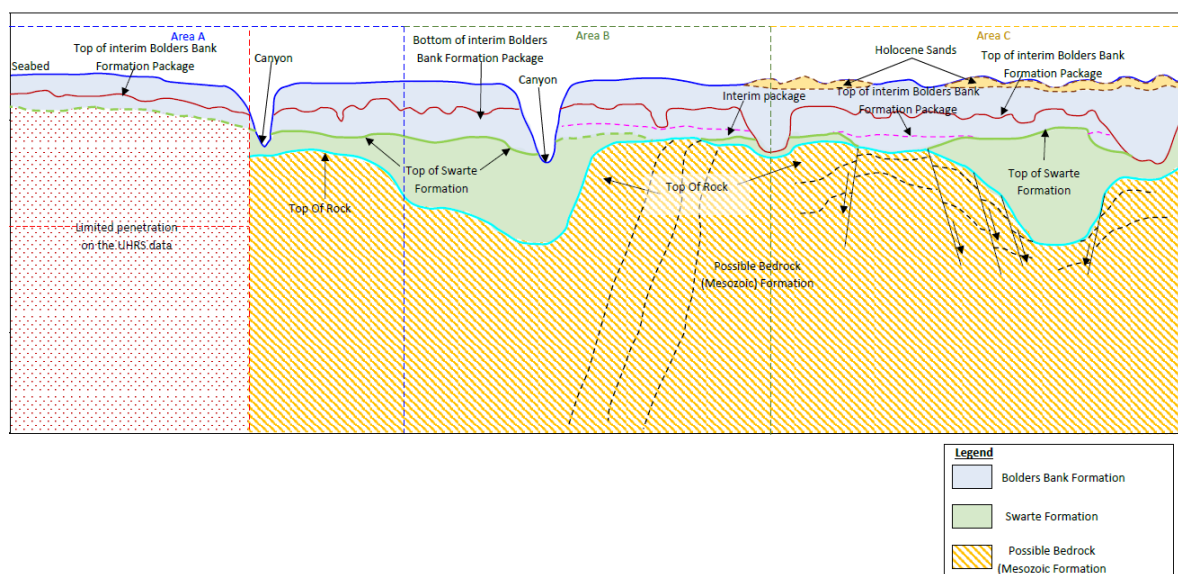


Figure 1. Schematic of interpreted units within the Outer Dowsing array area (west – east) (Enviros, 2022)

Across the western portion of the array area there are possible layers of chalk which are expected at around 20 m below seabed.

b. Drilling requirements

The drilling rate establishes the production rate of drill cuttings with faster rates having the potential to develop greater concentrations of fines in the near-field. Indicative drilling rates are expected between 0.5 to 1.5 m/hr. This rate depends on many factors, including; diameter of the pile, soil type and drill pressure, amongst others.

Drill cuttings will be discharged into the marine environment from the seabed with the finer particles having the potential to form a sediment plume and the coarser grained particles forming a cuttings mound. On completion of drilling at any one location, the time taken for a drill rig to relocate to the next foundation site is considered to be sufficiently long that any previous period of sediment plumes will have fully dispersed in the interim. Consequently, each drilling event can be considered largely independent in terms of formation and longevity of sediment plumes.

Up to two drill rigs may be operating in the array area at any time. The RWC for sediment plumes is when the two drill rigs are operating at adjacent locations along the tidal axis creating the potential for plumes to overlap during this period.

Based on an interpretation of the geophysical evidence, the likelihood for foundation drilling has been assessed as follows (areas shown in Figure 2):

- Area 1, SPA-1: 50% of foundation locations are assumed to require drilling due to flint bands or other hard layers. This area is also generally coincident with the chalk layer.
- Area 2, SPA-2: 100% of foundation locations are considered to require drilling due to shallow rockhead, 100% design embedment length.
- Area 3, SPA-3: 100% of foundation locations are considered to require drilling based on an assessment of the required penetrations and the actual variation in rockhead depth.

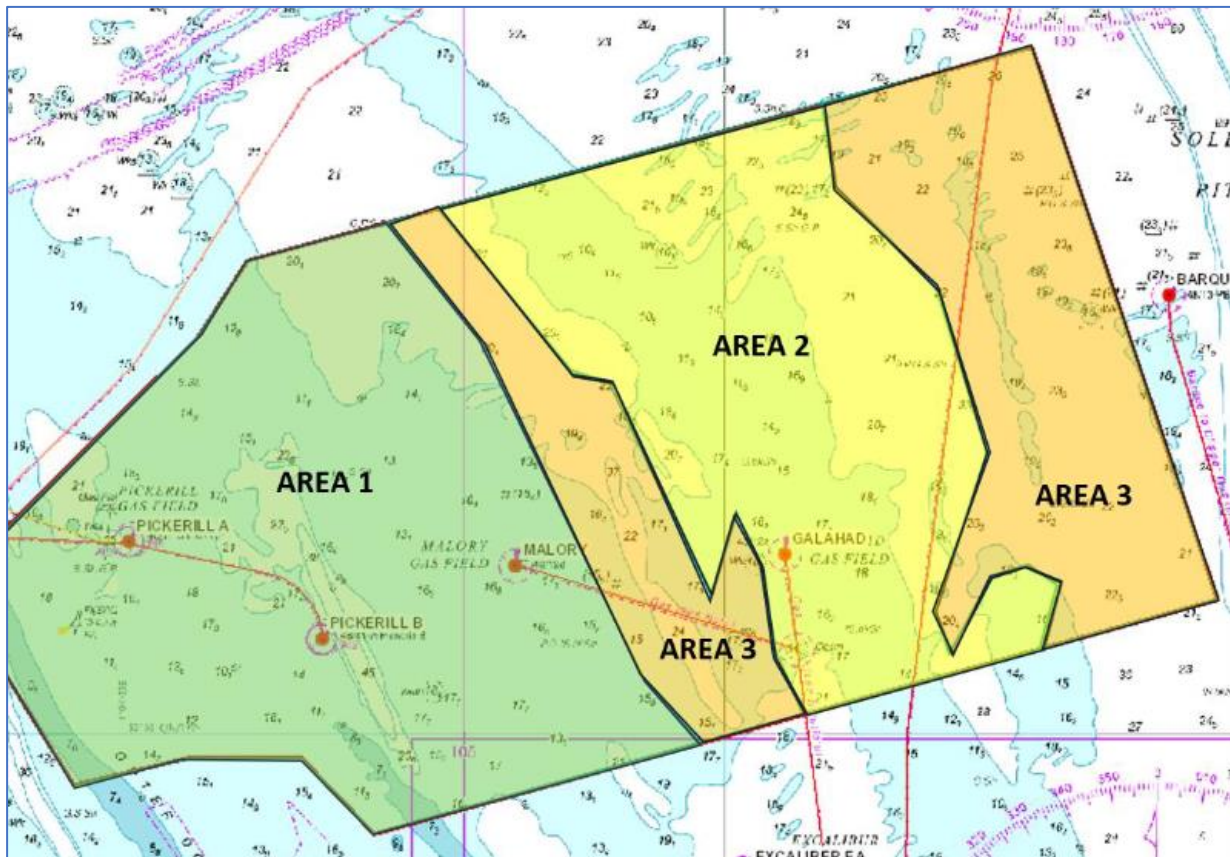


Figure 2. Indicative stratigraphic areas for the AfL array area

c. Comparison of foundation options

Foundation embedment depths vary between Area 1, 2 and 3. For example, the maximum embedment depth is 125 m for jacket pin piles located in Area 1, whereas the minimum embedment depth is estimated as 35 m in Area 2, again for jacket pin piles.

Table 9 provides details of the estimated volume of drill cuttings for an individual foundation type for each area within the array, as well as the total for all foundations which accounts for the likelihood of drilling. The OSP jacket foundation has 24 pin piles, whereas the WTG jacket foundation option has four piles.

Table 9. Comparison of drill cuttings volumes (m³) for different foundation types and areas

Foundation option	100 WTG	93 WTG	75 WTG	60 WTG	50 WTG	5 OSP
Monopile (Area 1)	7,820	7,820	7,820	8,640	8,640	10,250
Monopile (Area 2)	6,460	6,460	6,460	7,200	7,200	7,175
Monopile (Area 3)	8,160	8,160	8,160	9,000	9,000	10,250
Monopiles (Total)	609,450	565,930	457,300	406,440	340,560	34,850
Jacket pin piles (Area 1)	10,744	10,744	10,744	14,137	14,137	74,644
Jacket pin piles (Area 2)	3,958	3,958	3,958	3,958	3,958	23,750
Jacket pin piles (Area 3)	5,655	5,655	5,655	7,917	7,917	47,501
Jacket pin piles (Total)	505,828	471,899	380,573	389,055	325,155	169,646

In addition, drilling may be required at four further offshore platforms remote from the array area:

- Two ANSs at locations at least 16 km to the north-west or south-east of the array area requiring up to 11,027 m³ of drill arisings for both jacket with pin piles.
- Two ORCPs located around 12 to 17 km offshore, within the ECC requiring up to 74,644 m³ per jacket with pin piles based on an embedment depth of 110 m (total of 149,288 m³ for both foundations).

d. Realistic worst-case option

The individual foundation option which is expected to generate the largest volume of drill arising is the jacket with pin pile for an OSP located in Area 1 (74,644 m³, including overburden) with an associated embedment depth of 110 m, whereas the array total with the largest volume of drill arisings for all WTG foundations is the 100 monopile option (609,450 m³).

For development of sediment plumes, the production rate of drill cuttings becomes the determining influence which leads to the monopile OSP foundation in Area 1 being the realistic worst-case with the highest release rates (10,250 m³ in around 30 hours for a single OSP monopile compared to an estimated period of 1,760 hours for the alternative OSP jacket foundation to complete 24 piles).

The RWC scenario for sediment plumes is when there are two drilling rigs operating at adjacent foundation locations along the tidal axis in Area 1, such that plumes could potentially overlap to develop a higher overall suspended sediment concentration of fine sediments spread across a wider area. This configuration is met with drilling at OSP#104 coinciding with adjacent drilling at WTG#40. The near-bed release profiles of drill arisings for the RWC scenario are summarised in Table 10.

Table 10. RWC release rates of fine sediments from foundation drilling

Seabed layer	Time to complete (s)	Fine sand (g/s)	Very fine sand (g/s)	Coarse silt (g/s)	Medium silt (g/s)
OSP#104 overburden	16,000	18,196	13,647	45,490	318,432
OSP#104 rock layer	72,000	42,893	21,447	10,723	10,723
WTG#40 overburden	16,000	17,230	12,922	43,074	301,519
WTG#40 rock layer	67,200	37,699	18,850	9,425	9,425

According to Table 12, the total period of drilling for the OSP monopile to an embedment depth of 50 m below seabed is estimated as 24.4 hours, whereas the adjacent WTG monopile to an embedment depth of 48 m is around 23.1 hours.

3.2.4. Cable installation

a. Trenching options

Various options are available to develop the cable trench, including; jetting, ploughing, cutter, and Mass Flow Excavator (MFE), with the final selection(s) also dependent on the sediment conditions to be trenched. Each tool is likely to create a different trench cross-section at a different trenching rate and displace different volumes of sediment according to the way the tools perform. Notably, both jetting and MFE fluidise the seabed which has the greatest potential to elevate fine sediments out of the trench, whereas cutting or ploughing are likely to retain the majority of disturbed sediment within the trench. Table 11 provides a summary of key characteristics of each trenching option being considered for the Project.

Table 11. Summary of cable trenching options and production rates

Trenching tool	Jetting	Cutting	V-Plough	MFE
Trench width (m)	1.3	1.0	7.1	15.0
Trench depth (m)	3.5	3.5	2.5	2.5
Trench shape	Box	Box	V	Circle segment
Cross-section (m ²)	4.6	3.5	8.9	25.5
Trenching rate (m/hr)	300	200	180	215
Production rate (m ³ /hr)	1,365	700	1,607	5,493
Fluidising seabed	Yes	No	No	Yes

b. Realistic worst-case trenching option

The realistic worst-case trenching option is considered to be MFE as this develops the largest trench cross-section with the greatest potential to displace fine sediments into the water column to the same height above the seabed as the depth of the trench.

The worst-case trenching locations are identified where the disturbed sediment contains the largest contribution of fine sediments.

The present assumption is a single cable installation vessel will be operating on site at any time.

c. Array area

Based on the indicative array layout of WTG and OSP foundations, trenching for the inter-array cable between WTG-9 to WTG-10 along the northern boundary will encounter the highest proportion of fine sediments which have the potential to form a sediment plume, as quantified by grab sample OWF_29. The particle size analysis (PSA) data developed from benthic grab samples helps deduce the sediment as bimodal, “very poorly sorted”, “gravelly muddy Sand” (gmS) (GEOxyz, 2022) with around 59.8% coarse sediment and 40.2% fine sediment. The equivalent dry sediment density is established from vibracore R4B-VC-15 with a value of 1,900 kg/m³ (Enviros, 2022).

Table 12 provides a breakdown of the equivalent mass input for the various categories of fine sediment based on the realistic worst-case trenching option. These quantities are applied to the far-field modelling of sediment plumes for this location (MetOceanWorks, 2023). The estimated time for different particle sizes to fall out of suspension from a height of 2.5 m above the seabed is also provided indicating that the smallest particles (medium silt and smaller) may take around two hours to fully settle out (in still water conditions).

Table 12. Mass input of fine sediments for MFE array trenching between WTG-9 to WTG-10

Sediment type	Size range (mm)	Time to fall out of suspension (s)	% Contribution	Mass input (g/s)
Fine sand	0.125 to 0.250	139	27.0	782,698
Very fine sand	0.063 to 0.125	500	5.2	150,742
coarse silt	0.031 to 0.063	1,786	0.7	20,292
medium silt / muds	< 0.031	8,333	7.3	211,618

The spacing between WTG-9 to WTG-10 is around 2 km. For a trenching rate of up to 215 m/hr then this distance would be completed within a period of around nine hours with a continuous release of fine sediments. Given this section intersects with the highest contribution of fine sediments then trenching in other sections across the array (with a lower concentration of fines) is considered to develop a lower

release rate which will consequently lead to lower concentrations of suspended sediment, and less subsequent settlement.

d. ECC

The PSA data along the ECC identifies sample ECC_41 with the highest contribution of fine sediments (GEOxyz, 2022) which have the potential to form a sediment plume. The sediment at this location is described as “very poorly sorted” “gravelly muddy sand” (gmS) with around 69.5% of fine sediment. The equivalent dry sediment density is estimated to be 2,120 kg/m³, equivalent to glacial till, very mixed grained (Terzaghi, Peck, & Mesri, 1996).

Table 13 provides a breakdown of the equivalent mass input for the various categories of fine sediment based on the realistic worst-case trenching option. These quantities are applied to the far-field modelling of sediment plumes for this location (MetOceanWorks, 2023). The estimated time for different particle sizes to fall out of suspension from a height of 2.5 m above the seabed is also provided indicating that the smallest particles (medium silt and smaller) may take around two hours to fully settle out (in still water conditions).

Table 13. Mass input of fine sediments for MFE array trenching around ECC_41

Sediment type	Size range (mm)	Time to fall out of suspension (s)	% Contribution	Mass input (g/s)
Fine sand	0.125 to 0.250	139	25.3	818,339
Very fine sand	0.063 to 0.125	500	18.1	585,452
coarse silt	0.031 to 0.063	1,786	9.7	313,750
medium silt / muds	< 0.0031	8,333	16.4	530,465

For equivalence with the trenching scenario in the array area, a 2 km section of the ECC is simulated with trenching rate of up to 215 m/hr. This distance is expected to be completed within a period of around nine hours with a continuous release of fine sediments. A 2 km section is considered an appropriate distance for this scenario with variability of sediment composition (i.e., less fines) expected over greater distances.

e. Cable protection

Cable protection (e.g., use of rock berms) may be required for all laid cables, with a provision for up to 22.75% of inter-array cables, 18.75% of interlink cables, and 20.67% of offshore export cables, to help maintain the target burial depth. Rock berms would have a trapezoid shape with a width at seabed of 12 m, a height of 1.5 m and a top width of 2 m. In addition, up to 84 cable crossings may be required; 30 for inter-array, 16 for interlink, and 38 for export cables. Each crossing may be up to 500 m long. The maximum size of rock (to accommodate any anchor strikes) would be a median particle diameter (D50) of 0.125 m.

3.2.5. Horizontal direction drilling

Whilst HDD is generally considered a more benign option in comparison to open cut trenching, there are still expected to be localised and short-term effects due to:

- Excavation and backfilling of nearshore exit pits
- Potential release of bentonite during punch-out in the nearshore exit pit

a. Exit pits

Six HDD exit pits will be excavated in the nearshore at a location of no more than 700 m offshore from mean low water spring (MLWS). Each exit pit will be excavated to a depth up to 5 m over an area of 240 m², accounting for slide slopes this is conservatively estimated to be a maximum volume of 5,000 m³ per pit and a total of 30,000 m³ for all six exit pits.

The method of excavation is expected to be using a plough.

Each exit pit is expected to remain open for up to six months and then backfilled on completion.

b. Bentonite release

On completion of each HDD process the drill will emerge in the nearshore exit pit with the potential to release around 773 m³ of drilling muds (e.g., bentonite slurry) and drill cuttings as a near-bed discharge per punch-out event. Based on a typical slurry density for bentonite fluid and specific density of bentonite particles, the equivalent mass of bentonite would be 138 tonnes per exit pit.

The period of release for bentonite is estimated to be 12 hours to accommodate both initial punch-out and the subsequent reaming process. Accordingly, the estimated release rate would be 3,195 g/s over this period.

When the bentonite slurry mixes with seawater there is expected to be some flocculation. Based on laboratory measurements, the settling velocity for bentonite in seawater is expected to be around 0.000108 m/s; a conservative slower value for small flocs (Krahl, Vowinckel, Ye, Hsu, & Manning, 2022).

3.3. Operation and Maintenance

During the operation and maintenance phase (35-year design life) the main effects on the marine environment are expected to be array-scale blockage related effects on waves and tides due to the presence of multiple WTG and OSP foundations, as well as associated scour protection.

Cables may also require repairs involving recovery and relaying of cables with associated sediment disturbance which are likely to be comparable to construction related effects for the areas involved. In

addition, a provision for up to 25% of cable protection material may be required for replenishment of any rock berms.

3.3.1. Array-scale blockage

An individual foundation will locally interfere with passing waves and currents (depending on its relative size, shape, and solidity ratio) with a group of foundation structures having the potential to develop an array-scale blockage effect where the number, arrangement, and spacing is also considered.

Table 14 compares the normalised blockage factors for each WTG foundation type and size relative to the RWC case which is assessed to be the GBS flat base for the 50 WTG option. Since the number of GBS foundations are limited to up to 50% of sites then the next highest blockage case for an individual WTG foundation is also identified as jacket with suction buckets.

Table 14. Normalised blockage factor for individual WTG foundation types

WTG foundation option	100 WTG	93 WTG	75 WTG	60 WTG	50 WTG
Monopiles	0.30	0.30	0.30	0.31	0.31
Jacket - Pin Piles	0.34	0.34	0.34	0.34	0.34
Jacket - Suction Buckets	0.47	0.47	0.47	0.49	0.49
GBS – conical	0.68	0.68	0.76	0.76	0.76
GBS – flat	0.90	0.90	0.90	1.00	1.00

Table 15 considers the variation in normalised blockage effect for each array option (based on 50% of GBS (flat) sites and 50% of jacket with suction bucket WTG foundations), and indicates that the RWC array-scale blockage is the 100 WTG case.

Table 15. Normalised blockage factor for array

Array option	100 WTG	93 WTG	75 WTG	60 WTG	50 WTG
GBS + Jacket Suction B	1.00	0.93	0.75	0.65	0.54

A key assumption in this screening assessment is the scale of the array area remains constant for all foundation options. In addition, jacket structures are assumed to have a highly conservative solidity ratio of 0.3 and orientated at 45° to incident waves and flows which increases their frontal effective area. The key difference between jacket-type foundation options is that the 18 m diameter suction bucket option protrudes by 3 m above the seabed with a solidity value of 1.0.

Additional blockage in the array area is also contributed by a spread of five OSP foundations. There are also two ORCP structures closer to the coast within the ECC and two ANSs which may be placed in sites

north and south of the array area. In all cases, their respective GBS foundation options represent the RWC and for the two ORCP foundations when these foundations are at the minimum separation of 90 m apart.

3.3.2. Cable repairs

During the operational period of the windfarm there may be occasions when cable repairs need to be undertaken which may involve trenching as well as the potential introduction of cable protection measures.

Any trenching could develop short-term sediment plumes which would be comparable to the effects which are considered to occur during installation. Provisions are made for cable repairs with each repair up to 1,500 m and reburial up to 5,600 m.

Cable protection has the potential to introduce rock berms along sections of the cable needing to be reburied. The rock berm may have a height up to 1.5 m over a 12 m width. Provisions are also included for up to 25% replenishment over the operational period.

The maximum size of rock (to accommodate any anchor strikes) would be a median particle diameter (D50) of 0.125 m.

3.4. Decommissioning

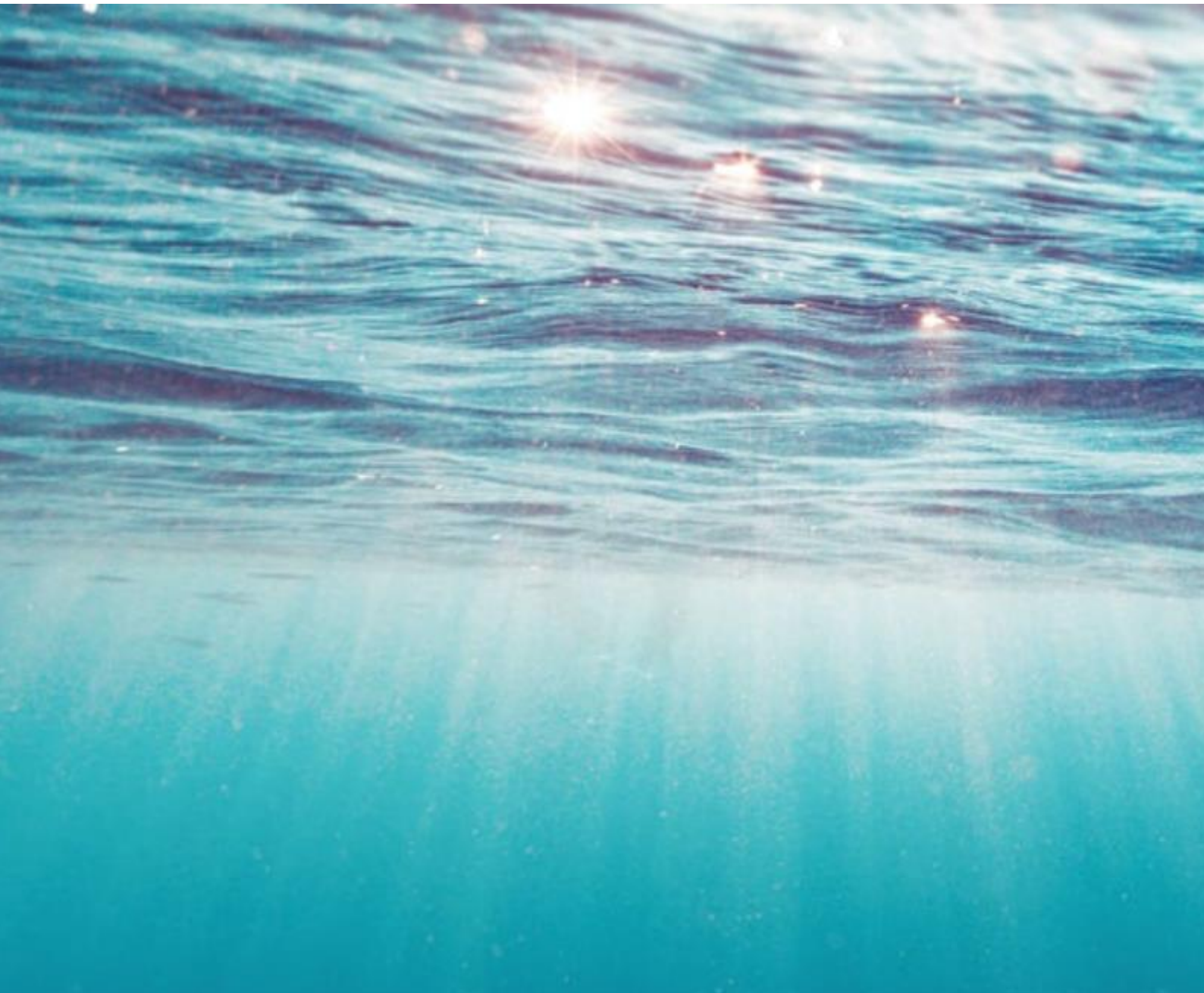
The general assumption is that sediment disturbance effects on the seabed will occur during the decommissioning phase which are comparable in type, but no greater in magnitude and extent than those which are identified to occur during the construction phase.

If all subsea cables are removed, then there is anticipated to be a short period of sediment disturbance of comparable scale to the original cable trenching activity.

If topsides of installed WTG and OSP structures are removed, then the long-term risk remains for the buried structures to be exposed at some period in the future if areas are subject to high rates of seabed mobility which lowers the level of the seabed, however, the consequence of these exposed structures may be minimised if scour protection remains in place.

4. References

- Bray, R. N., Bates, A. D., & Land, J. M. (1996). *Dredging: A Handbook for Engineers 2nd Edition*.
- COWRIE. (2009). *Coastal Process Modelling for Offshore Wind Farm Environmental Impact Assessment: Best Practice Guide*. COWRIE Coast-07-08.
- Enviros. (2022). *Outer Dowsing Offshore Wind Farm Geophysical UHRS and Light Geotechnical Survey, East Anglia, Offshore UK*. ENV21-21042-GTR4-02_Rev.01.
- GEOxyz. (2022). *Benthic Ecology ECC Area Results Report (Vol. 2)*. UK4855H-824-RR-02. Revision 1.
- GEOxyz. (2022). *Benthic Ecology OWF Area Results Report (Vol. 1)*. UK4855H-824-RR-01.
- Krahl, E., Vowinckel, B., Ye, L., Hsu, T.-J., & Manning, A. J. (2022, July 15). Impact of the Salt Concentration and Biophysical Cohesion on the Settling Behavior of Bentonites. *Frontiers in Earth Science. Marine Geoscience*, 10. doi:10.3389/feart.2022.886006
- MetOceanWorks. (2023). *Marine Physical Processes Numerical Modelling*. GoBe_C00003_R01_Marine_Physical_Processes_Modelling.
- Miedema, D. S. (2013). *Dredging Processes. The loading process of a Trailing Suction Hopper Dredge*. TUDelft.
- ODOW. (2021). *Scoping Report Project Description Outline*. Revision: v1.0. Client: GTR4 Ltd.
- Soulsby, R. (1997). *Dynamics of marine sands. A manual for practical applications*. Thomas Telford.
- Terzaghi, K., Peck, R. B., & Mesri, G. (1996). *Soil Mechanics in Engineering Practice. Third Edition*. Wiley & Sons, Inc.
- Tetra Tech. (2022). *Empire Offshore Wind LLC. Empire Wind 2 Project. Appendix C. Sediment Transport Analyses*.
- The Planning Inspectorate. (2018). *Using the Rochdale Envelope. Advice Note Nine: Rochdale Envelope. Version 3*.



www.CooperMarineAdvisors.co.uk

7.10 Annex C - Assessment of Spoil Mounds



**OUTER DOWSING OFFSHORE WIND. ANNEX C:
EIA - ASSESSMENT OF SPOIL MOUNDS**

MetOceanWorks / GoBe

March 2024

OUTER DOWSING OFFSHORE WIND. ANNEX C: EIA - ASSESSMENT OF SPOIL MOUNDS

Document-control grid

This document has been prepared by Cooper Marine Advisors Ltd.

Title	Outer Dowsing Offshore Wind. Annex C: EIA - Assessment of spoil mounds
Author(s)	Bill Cooper, Director, Cooper Marine Advisors Ltd [REDACTED]
Origination Date	21 Juy 2023
Date of last revision	21 March 2024
Version	2.0
Status	Draft
Summary of Changes	Updated from PEIR, addressed review comments (internal and MetOceanWorks)
Circulation	MetOceanWorks / GoBe
Filename	[REDACTED] [REDACTED] [REDACTED] [REDACTED]
Approval	Bill Cooper [REDACTED]

Disclaimer

This document has been prepared by Cooper Marine Advisors Ltd in accordance with the client’s instructions and for their stated purpose. Cooper Marine Advisors Ltd does not accept any liability to any other party for any other purpose.

Contents

Abbreviations	iv
1. Introduction	1
1.1. Document structure	1
1.2. Supporting documents	1
2. Assessment of spoil mounds	2
2.1. Overview	2
2.2. Approach	2
2.3. Sediment parameters	3
3. Disposal scenarios	4
3.1. Overview	4
3.1.1. TSHD dimensions	4
3.2. Sandwave clearance – Array area	5
3.2.1. Sediment volumes	5
3.2.2. Environmental conditions	5
3.2.3. Representative spoil mound	6
3.3. Sandwave clearance – ECC	8
3.3.1. Sediment volumes	8
3.3.2. Environmental conditions	9
3.3.3. Representative spoil mound	9
3.4. Seabed levelling – array area	11
3.4.1. Sediment volumes	11
3.4.2. Environmental conditions	12
3.4.3. Representative spoil mound	12
4. Summary	15
5. References	16

List of Figures

Figure 1.	Phases of the spoil disposal process following release from dredger (PNNL, 2006)	2
Figure 2.	Predicted spoil mound height and extent from array area sandwave clearance	7
Figure 3.	Predicted spoil mound height and extent for nearshore ECC sandwave clearance	10
Figure 4.	Predicted spoil mound height and extent from seabed levelling around WTG-65 to 94	13

List of Tables

Table 1.	STFATE representative sediment types, settling velocities and deposition voids ratio	3
Table 2.	Summary dimensions of representative TSHD (source: Boskalis)	4
Table 3.	Contribution of sediment types from sandwave clearance between WTG-20 to WTG-21, per hopper load	5
Table 4.	Estimated area and height of spoil mound from array area sandwave clearance.....	8
Table 5.	Contribution of sediment types from sandwave clearance along a nearshore section of the ECC	9
Table 6.	Estimated area and height of spoil mound from nearshore ECC sandwave clearance	11
Table 7.	Contribution of sediment types from seabed levelling around WTG_65 to 94.....	12
Table 8.	Area of coverage of spoil mound from seabed levelling around WTG-65 to 94	14

Abbreviations

ECC	Export Cable Corridor
EIA	Environmental Impact Assessment
MSL	Mean Sea Level
MW	Megawatt
OSP	Offshore Sub-station Platform
ODOW	Outer Dowsing Offshore Wind
OWF	Offshore Wind Farm
STFATE	Short-term Fate
TSHD	Trailer Suction Hopper Dredger
USACE	United States Army Corps of Engineers
WTG	Wind Turbine Generator
UK	United Kingdom

1. Introduction

Annex B provides an assessment of spoil mounds which are expected to develop when a trailer suction-hopper dredger (TSHD) discharges sediment at various locations across the Outer Dowsing Offshore Wind (ODOW; the Project) array area and along the export cable corridor (ECC). The sediment represents the material which has been removed from the seabed for seabed levelling and sandwave clearance, except for

- The material lost during loading the hopper as overspill, and
- fine sediments dispersing away as a sediment plume during the disposal period.

1.1. Document structure

Section 1 explains the scope and purpose of the Technical Annex.

Section 2 describes the method of assessment for spoil mounds.

Section 3 offers details of each spoil disposal scenario and presents the results.

Section 4 provides a summary of the assessment.

Section 5 lists the references related to this technical note.

1.2. Supporting documents

The assessment of spoil mounds has been established with consideration to the following project documents:

- Annex A. Outer Dowsing Offshore Wind: EIA - Determination of marine processes realistic worst-case
- Volume 1, Chapter 3: Project Description
- GEOxyz (2022). Benthic Ecology OWF Area Results Report (Vol. 1). UK4855H-824-RR-01
- GEOxyz. (2022). Benthic Ecology ECC Area Results Report (Vol. 2). UK4855H-824-RR-02.
- Enviros. (2022). Outer Dowsing Offshore Wind Farm Geophysical UHRS and Light Geotechnical Survey, East Anglia, Offshore UK. ENV21-21042-GTR4-02_Rev.01

2. Assessment of spoil mounds

2.1. Overview

Spoil mounds can form on the seabed when a TSHD discharges a hopper load of sediments which fall to the seabed due to a negatively buoyant density flow. The coarser sediment in the spoil mound is less likely to be transported away by the ambient flows so the mound remains as a semi-permanent feature (subject to a slow rate of winnowing). In some situations, multiple phases of spoil disposal across a defined area may develop overlapping mounds, and gradually modify the profile of the local seabed unless onward sediment transport can move the material away.

2.2. Approach

The near-field STFATE (Short-Term FATE) model for split barge and hopper dredge disposal operations of dredged material disposal in open water (USACE, 1995) is applied to assess individual discharges of spoil disposal from a Jumbo-sized TSHD with a capacity of 22,000 m³.

STFATE considers the spoil disposal from an instantaneous discharge with the following processes:

- Convective descent of spoil released from hopper where gravity and momentum dominate
- Dynamic collapse where the discharge encounters the seabed and spreading dominates
- Diffusive phase with passive advective transport and dispersion by currents in the short-term (of fine sediments)

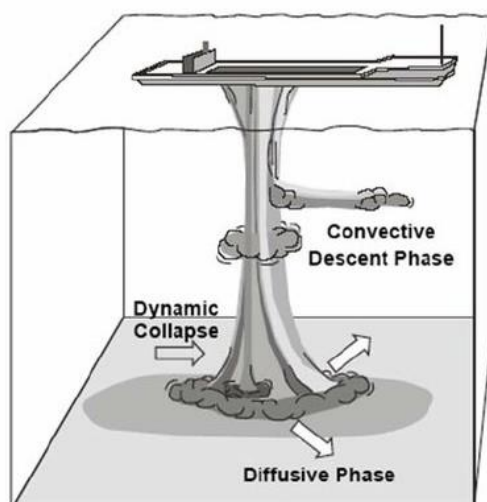


Figure 1. Phases of the spoil disposal process following release from dredger (PNNL, 2006)

Model inputs include the water depth and flow conditions at the spoil sites (provided by the hydrodynamic model; Volume 5, Appendix 1.2: Physical Processes Modelling Report, MetOceanWorks, 2023), along with the volume of spoil which is described with four different particle sizes with associated values for specific

gravity, fall velocity and deposition voids ratio. A specific gravity of 2.65 is applied to all particle sizes. The model also accounts for the basic dimensions and capacity of the TSHD. In the present case, the model is implemented with a 15 m grid in the horizontal.

STFATE complements the far-field particle tracking model (described in Volume 5, Appendix 1.2: Physical Processes Modelling Report, MetOceanWorks, 2023), which is applied to assess the wider advection, dispersion, and subsequent deposition of fine sediment as sediment plumes.

2.3. Sediment parameters

STFATE allows the hopper volume of dredged material to be characterised into up to four sediment classes. Based on sediment gradings data obtained from the benthic survey grab samples (GEOxyz, 2022) the following representative sediment types are adopted:

- Gravel
- Medium sand
- Fine sand
- Silt

Table 1 summarises the properties of the various sediment types defined in STFATE.

Table 1. STFATE representative sediment types, settling velocities and deposition voids ratio

	Sediment type	Representative size (mm)	Settling velocity (m/s)	Deposition void ratio
Coarse	Gravel	4.500	0.265	0.50
	Medium / coarse sand	0.500	0.066	0.60
Fine	Very fine / fine sand	0.125	0.009	0.70
	Silt / clay	0.030	0.0001	5.00

The coarser sediment fractions (gravel and medium sand) will fall relatively quickly to the seabed, developing a downward convective density flow with limited opportunity for wider dispersion over the release period. Most fine sediments (fine sand and silts) will be carried to the seabed within the convective flow (falling faster than associated particle settling velocities), but some will have the potential to be stripped out during this phase to become prone to tidal advection and dispersion further away from the point of release as the dynamic collapse.

3. Disposal scenarios

3.1. Overview

STFATE has been applied to investigate spoil disposal scenarios from anticipated TSHD activities during the construction period and related to:

- Sandwave clearance of inter-array cable routes within the array area
- Sandwave clearance along the ECC
- Seabed levelling around foundation locations

The disposal from a single hopper load is considered for each activity to determine a representative scale of the resulting spoil mound. The total level of activity in each case is expected to involve multiple disposals which are expected to form independently of each other across an area considered suitable for disposal.

3.1.1. TSHD dimensions

When the TSHD reaches the nominated area for spoil disposal the bottom hopper doors will open to discharge the cargo. The hopper is expected to be emptied within a period of 10 minutes.

Table 2 provides representative dimensions for the dredger (based on the Boskalis TSHD Prins der Nederlanden).

Table 2. Summary dimensions of representative TSHD (source: Boskalis)

Vessel Dimension	Value	Unit
Length	201	m
Breadth	28	m
Number of hopper doors	5	-
Hopper Capacity	20,997	m ³
Carry capacity	39,335	tonnes
Draught (empty)	7.0	m
Draught (full)	12.1	m
Max sailing speed (loaded)	15.4	knots

The number of spoil mounds and dimensions of each mound are closely related to the capacity of the dredger.

3.2. Sandwave clearance – Array area

3.2.1. Sediment volumes

The total volume of sandwave clearance within the array area is estimated to be up to 11,821,178 m³ with a clearance width of 30 m and an average removal depth of 2.5 m. This volume is related to the 15 MW wind turbine capacity option which utilise the largest number of turbines.

The number of hopper loads required to clear the anticipated volume of sandwaves will vary in proportion to the size of the TSHD. For a hopper capacity of 22,000 m³ (jumbo dredger) there is expected to be around 529 hopper loads when assuming a bulking factor of 1.2 (mid-range of 1.15 to 1.25 for sand, medium soft to hard (Bray, Bates, & Land, 1996)) and accounting for overspill losses of 18% for medium sand (Miedema, 2013).

A 1.725 km section of the cable route between wind turbine generator, WTG-20 to WTG-21 is selected for sandwave clearance, being an area where sandwaves are identified in the geophysical survey (Enviros, 2022) and where the sediment composition, as determined from grab sample OWF-33 (GEOxyz, 2022), contains the highest relative amount of fine sediments (to produce a realistic worst-case for sediment plumes from overspill and disposal).

Table 3 summarises the anticipated proportion of sediment types within a single hopper load after dredging this section of cable.

Table 3. Contribution of sediment types from sandwave clearance between WTG-20 to WTG-21, per hopper load

Sediment type		Relative proportion (%)	Sediment volume (m ³)	Mass (kg)
Coarse	Gravel	27.00	4,950	9,454,500
	Medium / coarse sand	30.30	5,555	10,610,050
Fine	Very fine / fine sand	36.00	6,600	12,606,000
	Silt / clay	6.70	1,228	2,346,117

This dredging cycle is expected to be repeated six times along this route to achieve the full planned 30 m width of sandwave clearance.

3.2.2. Environmental conditions

The environmental conditions at the representative spoil disposal site are established from the central location between adjacent wind turbines and where the sediment type and morphology are comparable (i.e., retaining sandwave clearance material within an area of adjacent sandwaves).

For sandwave clearance between WTG-20 to WTG-21 this location is determined to be slightly to the south of the dredged area where the local water depth is around 24 m. Tidal effects can increase or decrease this depth by up to 2 m at times of spring tide high and low water, respectively. Given the draught of the loaded TSHD is around 12 m (Table 2) then the distance for spoil to fall from the open hopper doors to reach the local seabed depth of 24 m is expected to be around a further 12 m.

Tidal flows have the potential to deflect the falling spoil which may slightly reduce the height and increase the spread and deposition area of the spoil mound compared to deposition during a period of slack water. The maximum depth-average flow speed is estimated to be around 1 m/s on spring tides with a typical flow speed of around 0.5 m/s.

When the dredger reaches the target disposal site then the vessel is expected to slow to discharge the loaded hopper whilst turning to return to the dredging site. This operation will also serve to distribute the spoil over a slightly wider area compared to a stationary period of disposal.

3.2.3. Representative spoil mound

STFATE predicts the area of deposition and height of the spoil mound once all the material reaches the seabed and based on the prescribed inputs. Subsequent tidal winnowing of the spoil mound is not accounted for, noting coarse sediments are unlikely to be subjected to high transport rates whereas fine sediments are likely to be rapidly moved on.

Error! Reference source not found. presents the deposition footprint of the spoil mound for sandwave clearance in the array area between WTG-20 to WTG-21. In this scenario, the dredger is moving from west to east with a nominal cross flow from north to south. The southerly cross-flow leads to wider deposition of the fine sediments, notably the silts extend up to 564 m from the centre of the spoil mound which is estimated to have a maximum height of 1.55 m and comprises the majority of coarse sediment.

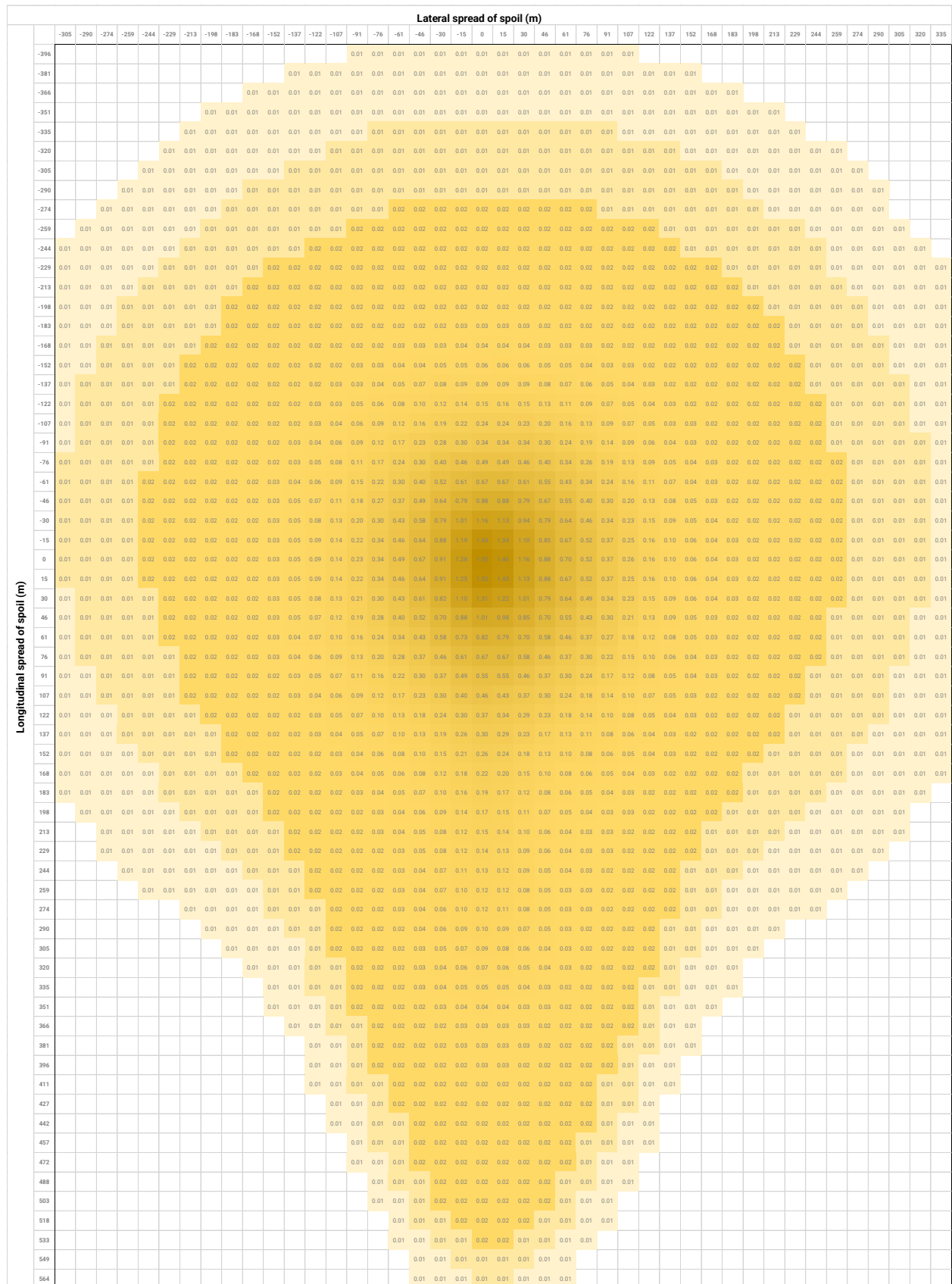


Figure 2. Predicted spoil mound height and extent from array area sandwave clearance

Table 4 provides a summary of the area of coverage for the spoil mound for different heights above the seabed, including thresholds of 0.05 and 0.30 m which are regarded as a condition which would risk the smothering of benthic receptors at “light” and “heavy” levels (Tyler-Walter, Tillin, d’Avack, Perry, & Stamp, 2018). The wider areas with heights up to 0.01 m are considered to be formed mainly of fine sediments with the overall footprint of the (single) spoil mound occupying around 0.397 km².

Table 4. Estimated area and height of spoil mound from array area sandwave clearance

Height of mound above seabed (m)	Area covered (km ²)
< 0.01	0.071
0.01 to 0.05	0.231
0.05 to 0.10	0.028
0.10 to 0.30	0.035
0.30 to 1.00	0.027
> 1.00	0.005
Total	0.397

If a subsequent disposal event from this operation fully overlapped with a prior spoil mound then the depth of deposition (net height of small mound) can be estimated as additive to the prior mound heights. Alternatively, if the footprint of a subsequent disposal was separate then the area involved would be additive. A partial overlap would result in a proportional contribution of additional depth and area involved.

3.3. Sandwave clearance – ECC

3.3.1. Sediment volumes

The largest volume of sandwave clearance for export cables within the ECC is estimated to be up to 4,312,688 m³ (excluding sections of export cables within the array area).

The number of hopper loads required to clear the anticipated volume of sandwaves will vary in proportion to the size of the TSHD. For a hopper capacity of 22,000 m³ (jumbo dredger) there is expected to be around 193 hopper loads when assuming a bulking factor of 1.2 (mid-range of 1.15 to 1.25 for sand, medium soft to hard (Bray, Bates, & Land, 1996) and accounting for overspill losses of 18% for medium sand (Miedema, 2013).

A nearshore area of sandwaves is identified from the ECC geophysical survey (GEOxyz, 2022) where the content of fine sediment (fine sand, very fine sand, silts and clays) reaches 31.9%, as determined from sediment grab sample ECC_58. These sandwaves extend for a distance of around 2.5 km along the alignment of the ECC where water depths are around 17 m (relative to mean sea level, MSL). This location

is considered to be the realistic worst-case for potential development of sediment plumes, being the location with the highest content of fines.

Table 5 summarises the anticipated proportion of sediment types within a single hopper load after dredging this section of sandwaves. Notably, there is expected to be a 0% gravel content at this location.

Table 5. Contribution of sediment types from sandwave clearance along a nearshore section of the ECC

Sediment type		Relative proportion (%)	Sediment volume (m ³)	Mass (kg)
Coarse	Gravel	0.00	0	0
	Medium / coarse sand	68.10	12,485	23,846,350
Fine	Very fine / fine sand	22.70	4,162	7,948,783
	Silt / clay	9.20	1,687	3,221,533

This dredging cycle is expected to be repeated six times along this section of the ECC to achieve the full planned width 30 m of sandwave clearance.

3.3.2. Environmental conditions

The environmental conditions at the representative spoil disposal site are established from a location to the south which remains within the same area of sandwaves and the ECC boundary (i.e., retaining sandwave clearance material within an area of adjacent sandwaves). Water depths at this location are estimated to be around 17 m (relative to MSL). Given that the draught of the loaded TSHD is around 12 m (Table 2), then the distance for spoil to fall from the open hopper doors to reach the local seabed depth of 17 m is expected to be around a further 5 m.

Tidal flows have the potential to deflect the falling spoil which may slightly reduce the height and increase the spread and deposition area of the spoil mound compared to deposition during a period of slack water. The maximum depth-average flow speed is estimated to be around 1 m/s on spring tides with a typical flow speed of around 0.5 m/s.

When the dredger reaches the target disposal site then the vessel is expected to slow to discharge the loaded hopper whilst turning to return to the dredging site. This operation will also serve to distribute the spoil over a slightly wider area compared to a stationary period of disposal.

3.3.3. Representative spoil mound

STFATE predicts the area of deposition and height of the spoil mound once all the material reaches the seabed and based on the prescribed inputs. Subsequent tidal winnowing of the spoil mound is not

accounted for, noting coarse sediments are unlikely to be subjected to high transport rates whereas fine sediments are likely to be rapidly moved on. Figure 3 presents the deposition footprint of the spoil mound from sandwave clearance for a nearshore section along the ECC.

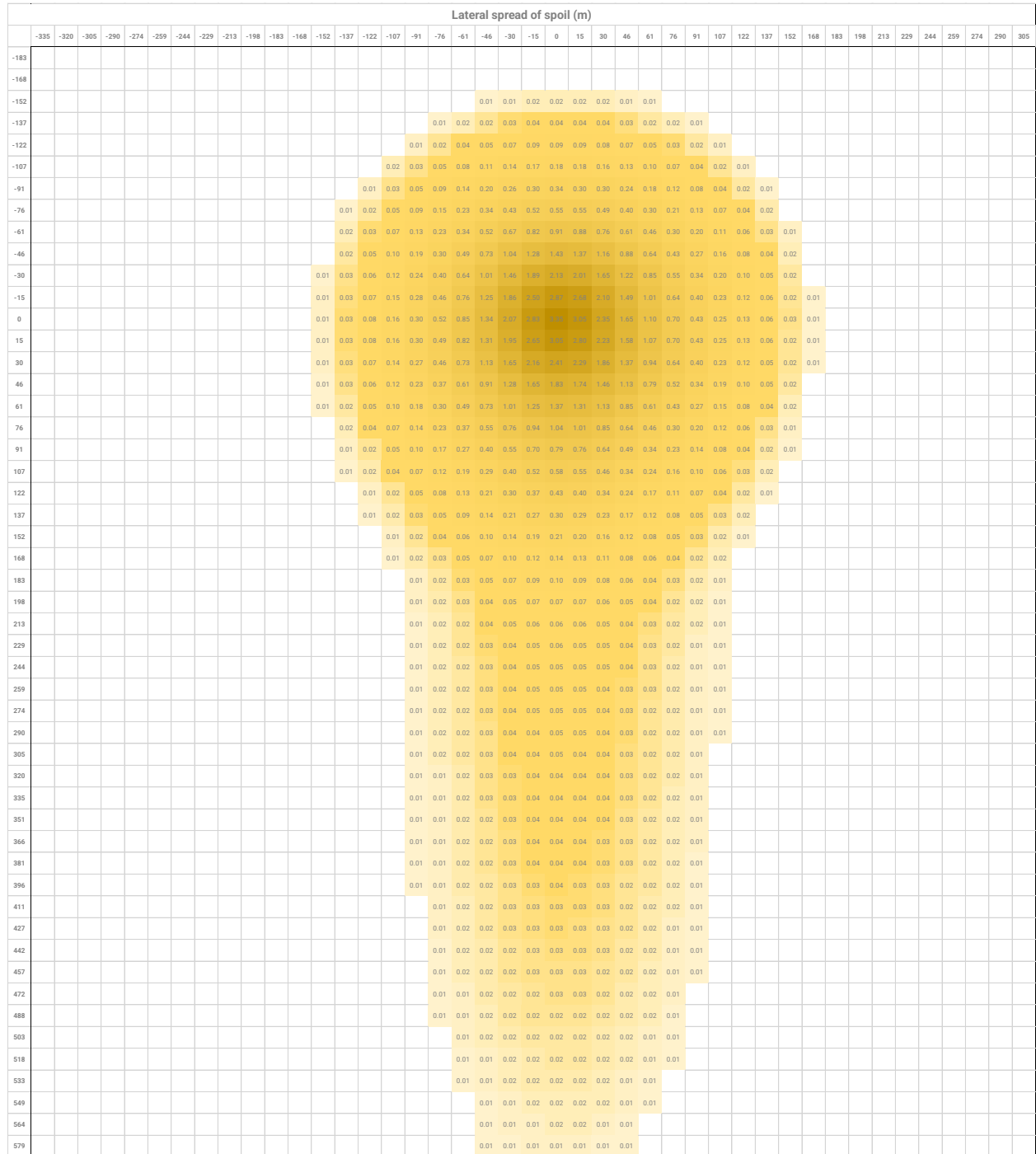


Figure 3. Predicted spoil mound height and extent for nearshore ECC sandwave clearance

In this scenario, the dredger is moving from west to east with a nominal cross flow from north to south. The southerly cross-flow leads to wider deposition of the fine sediments, notably the silts extend up to 573 m from the centre of the spoil mound which is estimated to have a maximum height of 3.35 m and comprises the majority of the coarser sediment (medium sand). This spoil mound is higher than the spoil

mound related to sandwave clearance in the array area, notably because the local water depth in the nearshore is much shallower and the relative contribution from coarser sediments is larger.

Table 6 provides a summary of the coverage area of the spoil mound for different heights above the seabed. The wider areas covered with heights up to 0.01 m are considered to be formed mainly of fine sediments.

Table 6. Estimated area and height of spoil mound from nearshore ECC sandwave clearance

Height of mound above seabed (m)	Area covered (km ²)
< 0.01	0.013
0.01 to 0.05	0.082
0.05 to 0.10	0.017
0.10 to 0.50	0.021
0.50 to 1.00	0.021
> 1.00	0.013
Total	0.166

If a subsequent disposal event from this operation fully overlapped with a prior spoil mound, then the depth of deposition (net height of small mound) can be estimated as additive. Alternatively, if the footprint of a subsequent disposal was separate then the area involved would be additive. A partial overlap would result in a proportional contribution of additional depth and area involved.

3.4. Seabed levelling – array area

3.4.1. Sediment volumes

The realistic worst case (i.e., largest sediment volume) for seabed levelling relates to the jacket with suction bucket foundation option for the 100 * 15 MW WTG option, along with additional levelling for OSP. The volume of sediment to be removed for a single WTG is estimated to be 4,450 m³ and 9,800 m³ for each OSP.

A bulking factor of 1.25 has been assumed for present purposes which is mid-range of 1.15 to 1.35 for sand/gravel/clay mixtures (Bray, Bates, & Land, 1996) which are common across the array area for sites not covered by sandwaves. In addition, the overspill loss is estimated to 18%. On this basis, seabed levelling around five WTG equates to around a single hopper load.

Seabed levelling around WTG-65, -58, -50, -95 and -94 in the south-west of the array area coincides with the location identified to have the largest contribution of fine sediments (grab sample OWF_76, (GEOxyz, 2022)). Table 7 summarises the anticipated proportion of sediment types within a single hopper load after dredging this location.

Table 7. Contribution of sediment types from seabed levelling around WTG_65 to 94

	Sediment type	Relative proportion (%)	Sediment volume (m ³)	Mass (kg)
Coarse	Gravel	39.20	7,152	13,660,396
	Medium / coarse sand	24.70	4,507	8,607,444
Fine	Very fine / fine sand	28.80	5,255	10,036,210
	Silt / clay	7.20	1,314	2,509,052

3.4.2. Environmental conditions

The environmental conditions at the representative spoil disposal site are established from a location close to the eastern boundary which remains within the same type of sediment classification. Water depths at this location are estimated to be around 26 m (relative to MSL). Given the draught of the loaded TSHD is around 12 m (Table 2) then the distance for spoil to fall from the open hopper doors to reach the local seabed depth is expected to be around a further 14 m.

Tidal flows have the potential to deflect the falling spoil which may slightly reduce the height and increase the spread and deposition area of the spoil mound compared to deposition during a period of slack water. The maximum depth-average flow speed is estimated to be around 1 m/s on spring tides with a typical flow speed of around 0.5 m/s.

When the dredger reaches the target disposal site then the vessel is expected to slow to discharge the loaded hopper whilst turning to return to the dredging site. This operation will also serve to distribute the spoil over a slightly wider area compared to a stationary period of disposal.

3.4.3. Representative spoil mound

STFATE predicts the area of deposition and height of the spoil mound once all the material reaches the seabed and based on the prescribed inputs. Subsequent tidal winnowing of the spoil mound is not accounted for, noting coarse sediments are unlikely to be subjected to high transport rates whereas fine sediments are likely to be rapidly moved on.

Figure 4 presents the deposition footprint of the spoil mound produced from seabed levelling at WTG-65 to 94.

m from the centre of the spoil mound which is estimated to have a maximum height of 1.25 m and comprises the majority of coarse sediment.

Table 8 provides a summary of the area of coverage for the spoil mound for different heights above the seabed. The wider areas covered with heights up to 0.01 m are considered to be formed mainly of the finer sediments.

Table 8. Area of coverage of spoil mound from seabed levelling around WTG-65 to 94

Height of mound above seabed (m)	Area covered (km ²)
< 0.01	0.032
0.02 to 0.05	0.304
0.05 to 0.10	0.039
0.10 to 0.50	0.038
0.50 to 1.00	0.025
> 1.00	0.002
Total	0.440

If a subsequent disposal event from this operation fully overlapped with a prior spoil mound, then the depth of deposition (net height of small mound) can be estimated as additive. Alternatively, if the footprint of a subsequent disposal was separate then the area involved would be additive. A partial overlap would result in a proportional contribution of additional depth and area involved.

4. Summary

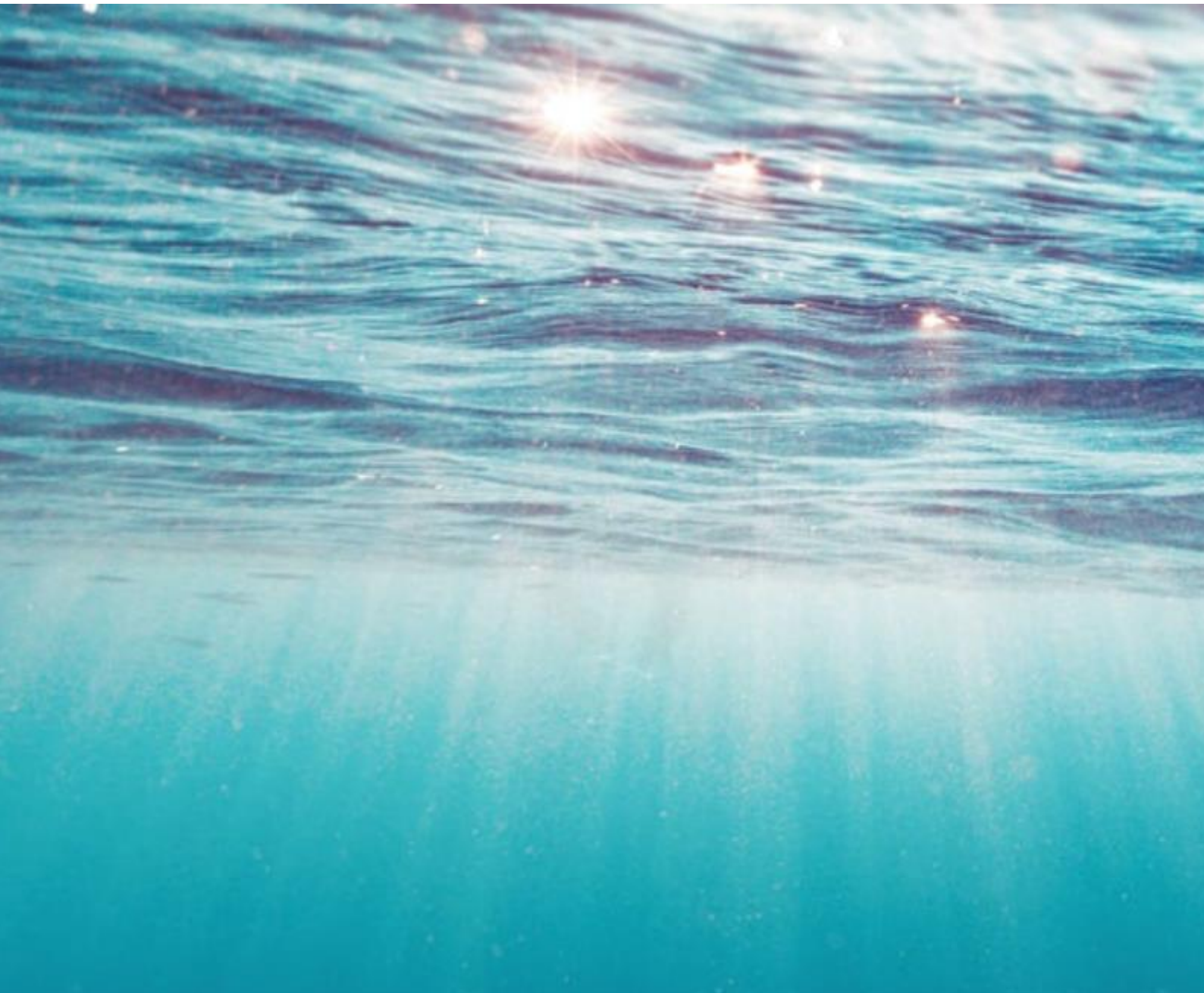
Representative spoil mounds produced from the disposal of dredged arisings from sandwave clearance and seabed levelling are investigated based on a jumbo-sized TSHD with an assumed capacity of around 22,000 m³. A larger or smaller TSHD would produce a proportionally different scale of a spoil mound.

Based on the 22,000 m³ hopper capacity, comparable sized spoil mounds are formed at each location despite local conditions of sediment type and water depth being site specific. All locations can be considered relatively shallow, with the convective descent being quick in each case. Slight differences occur between in the maximum height of spoil mounds which relate to variations in the proportion of coarse sediments and local water depths.

Given the similarity between representative spoil mounds the expectation is that the addition of further spoil mounds to complete all dredging activities would produce a similar scale per mound. This finding allows the individual dimensions of a spoil mound to be scaled up by simple addition, to account for the full total of disposals, if required.

5. References

- Bray, R. N., Bates, A. D., & Land, J. M. (1996). *Dredging: A Handbook for Engineers 2nd Edition*.
- Enviros. (2022). *Outer Dowsing Offshore Wind Farm Geophysical UHRS and Light Geotechnical Survey, East Anglia, Offshore UK. ENV21-21042-GTR4-02_Rev.01*.
- GEOxyz. (2022). *Benthic Ecology ECC Area Results Report (Vol. 2). UK4855H-824-RR-02. Revision 1*.
- GEOxyz. (2022). *Benthic Ecology OWF Area Results Report (Vol. 1). UK4855H-824-RR-01*.
- MetOceanWorks. (2023). *Marine Physical Processes Numerical Modelling. GoBe_C00003_R01_Marine_Physical_Processes_Modelling*.
- Miedema, D. S. (2013). *Dredging Processes. The loading process of a Trailing Suction Hopper Dredge*. TUDelft.
- PNNL. (2006). *Preliminary Assessment of Potential Impacts to Dungeness Crabs from Disposal of Dredged Materials from the Columbia River. Contract DE-AC05-76RL01830*.
- Tyler-Walter, H., Tillin, H. M., d'Avack, E. A., Perry, F., & Stamp, T. (2018). *Marine Evidence-based Sensitivity Assessment (MarESA) – A Guide. Marine Life Information Network (MarLIN). Marine Biological Association of the UK, Plymouth, pp. 91*.
- USACE. (1995). *Development and verification of numerical models for predicting the initial fate of dredged material disposed in open water. Report 2. Theoretical developments and verification results. Final Report. Dredging Research Program. Technical Report DRP-93-1*.



www.CooperMarineAdvisors.co.uk